METABOLIC REMODELING AND GROWTH REGULATION OF *MYCOBACTERIUM TUBERCULOSIS* AT ACIDIC PH

By

Jacob J. Baker

A DISSERTATION

Submitted to
Michigan State University
in partial fulfillment of the requirements
for the degree of

Microbiology and Molecular Genetics – Doctor of Philosophy

2017

ABSTRACT

METABOLIC REMODELING AND GROWTH REGULATION OF *MYCOBACTERIUM TUBERCULOSIS* AT ACIDIC PH

By

Jacob J. Baker

Mycobacterium tuberculosis (Mtb), the leading cause of infectious disease death worldwide, remains a global health threat. The success of Mtb as a pathogen can be attributed to its ability to sense and adapt to the host environment. Understanding the mechanisms of Mtb adaptation to the host environment has the potential to inform the development of novel and effective tuberculosis treatments. An important aspect of Mtb adaptation is its ability to regulate growth rate, as slow growing and growth arrested Mtb has been shown to exhibit increased phenotypic tolerance to killing by the immune system or antibiotics.

In response to the important host cue of acidic pH, I have observed that Mtb exhibits carbon source specific growth arrest. While the majority of carbon sources were unable to promote growth at acidic pH in minimal medium, carbon sources associated with the anaplerotic node and with the host relevant nutrient cholesterol were permissive for Mtb growth. Transcriptional profiling of Mtb at acidic pH demonstrated that Mtb induces genes involved in anaplerotic metabolism, lipid synthesis, and redox homeostasis. Furthermore, deletion of the two-component regulatory system *phoPR* that is induced at acidic pH led to enhanced growth at acidic pH, suggesting that slow growth is an aspect of Mtb adaptation to acidic pH. By performing growth curves and metabolic profiling of wild type Mtb as well as mutants lacking specific enzymes of the anaplerotic node, I have also sought to characterize the mechanisms of metabolic remodeling that occur at acidic pH and their role in growth regulation. Finally, through the isolation of mutants with enhanced growth at acidic pH, I have demonstrated that growth arrest at acidic pH is a regulated process in Mtb necessary for phenotypic tolerance.

TABLE OF CONTENTS

LIST OF TABLES

LIST OF FIGURES

KEY TO ABBREVIATIONS

3-NP 3-nitropropionate

bp ..... Base pairs

CFU ..... Colony forming units

CMFDA ..... 5-chloromethylfluorescein diacetate

CPM ..... Counts per minute

DAT ..... Diacyltrehalose

LC/MS ..... Liquid chromatography/mass spectrometry

Mtb ..... Mycobacterium tuberculosis

OADC ..... Oleic acid, albumin, dextrose, catalase

PAT ..... Polyacyltrehalose

PEP ..... Phosphoenolpyruvate

SDS ..... Sodium dodecyl sulfate

SL ..... Sulfolipid

TAG ..... Triacylglycerol

TLC ..... Thin Layer Chromatography

WT ..... Wild type

CHAPTER 1 - Acid Fasting: Restriction of metabolism and growth at acidic pH in *Mycobacterium tuberculosis*.

Introduction

Mycobacterium tuberculosis (Mtb) persists as a major disease of humans, infecting one third of the global population, causing active disease in 10.4 million people annually, and causing 1.8 million deaths (1). The success of Mtb as a human pathogen depends on its ability to sense and adapt to the environment and stresses encountered during infection (2), including changes in pH (3), metal ion concentration (4), oxygen tension (5), and reactive oxygen species and nitrogen intermediates (6,7). Targeting these adaptation pathways of Mtb may identify new ways to treat Mtb infection.

A growing body of research supports the proposal that adaptation to acidic pH is important to Mtb pathogenesis. Vandal *et al.* (3,8,9) identified several mutants susceptible to acid *in vitro*, and these mutants exhibited reduced virulence during infection. The virulence defect of these mutants supports the notion that Mtb acid resistance is required *in vivo*. One of the genes identified in that work, encoding for the serine protease MarP, has been further studied in the context of the *Mycobacterium marinum*/zebrafish infection model, and has been shown to be required for *M. marinum* survival within the phagolysosome, a highly acidic environment (10). Additionally, the importance of pH adaptation in Mtb is evident by examining its transcriptional response during infection: Rohde *et al.* (11) observed the induction of 68 Mtb genes two hours after infection; when acidification of the phagosome is blocked with the vacuolar ATPase inhibitor concanamycin A, 30 of these genes are no longer induced. Such transcriptional adaptation to acidic pH also appears to be important to Mtb pathogenesis. For example, the acid-induced *phoPR* regulon is required for Mtb virulence (12). In fact, an attenuated vaccine strain of Mtb with deletions in *phoPR* and *fadE26* showed comparable safety to the BCG

vaccine in phase I clinical trials (13,14). Notably, the *phoPR* mutant is not killed under acidic conditions (15,16), suggesting that at acidic pH Mtb undergoes adaptations beyond those simply promoting acid tolerance.

Mtb regulates many genes involved in metabolic adaptation in response to acidic pH, including induction of genes involved in lipid synthesis and anaplerosis (11,15,17), suggesting that this is an important aspect of acid adaptation in Mtb. Additionally, several studies have also observed slowed growth of Mtb in response to acidic pH (15,17,18). This pH-dependent adaptation is unique from that of closely related non-pathogenic *Mycobacterium* strains (18), suggesting that it represents a specific adaptation rather than a physiological limitation. Indeed, the intracellular pH of Mtb remains neutral even when exposed to conditions as acidic as pH 4.5 (8,19), revealing that slowed growth of Mtb is not due to a loss in cytoplasmic pH homeostasis. This chapter discusses the interrelated mechanisms of metabolic adaptation and slow growth in Mtb, considering each broadly in the context of Mtb stress response. The shared role of slow growth and metabolic remodeling in acid adaptation will be discussed, addressing aspects shared with general stress adaptation as well as aspects unique to pH adaptation. Finally, in light of the growth and metabolic adaptations of Mtb to acidic pH, the merits of describing acidic pH as both an environmental stress as well as an environmental cue will be discussed.

Metabolic restriction under environmental stress in Mtb

During infection, the metabolic requirements of Mtb differ from those encountered *in vitro*, as evidenced by the number of central carbon metabolism enzymes that are required specifically *in vivo*. Although dispensable for growth in nutrient rich medium *in vitro*, phosphoenolpyruvate carboxykinase (encoded by *pckA*) (20,21) lipoamide dehydrogenase (encoded by *lpdC*) (22), dihydrolipoamide acyltransferase (encoded by *dlaT*) (23), the E1 subunit of α-ketoglutarate dehydrogenase (encoded by *hoas) (24),* and the bifunctional methylisocitrate/isocitrate lyase

(encoded by *icl*) (25) have all been shown to be required for full virulence during infection. Further characterization of these enzymes has helped uncover the metabolic environments encountered during infection that lead to their role in pathogenesis. For example, *pckA* was shown to be required for gluconeogenic carbon flow when grown on fatty acids, a somewhat surprising finding given that Mtb contains genes that are annotated as encoding malic enzyme (*mez*), pyruvate carboxylase (*pca*), and pyruvate phosphate dikinase (*ppdK*); suggesting that despite these alternate routes of metabolism, Mtb specifically requires *pckA* for gluconeogenesis during infection (20). Additionally, *icl* was shown to be required for the metabolism of propionyl-CoA generated from the catabolism of cholesterol, methyl-branched fatty acids, and odd chain fatty acids (26-28), carbon sources utilized during Mtb growth *in vivo* (29-32). Further study has shown that the source of toxicity when Mtb is grown on propionate or C-3 producing carbon sources is due to the accumulation of two methylcitrate cycle intermediates, methylcitrate and methylisocitrate (33,34). Furthermore, providing alternate routes for propionyl-CoA metabolism through the vitamin B12 dependent methylmalonyl-CoA pathway (35) or by increasing methyl-branched lipid synthesis reduced the growth defect of the *icl* mutant (33,36), as did simply blocking propionyl-CoA entry into the methylcitrate cycle (34). As can be seen from these examples, probing the *in vivo* requirements for metabolic enzymes and pathways has provided a better understanding of the metabolic constraints incurred by the host environment.

Understanding Mtb metabolism during infection has also been probed by culturing Mtb *in vitro* in media with host mimicking environments or stresses and measuring the adaptive metabolic response. The findings observed in this approach have complemented the studies of *in vivo* essentiality, and, in the case of isocitrate lyase, expanded the observed functions of this enzyme in promoting Mtb survival. Under conditions of *in vitro* hypoxia, Mtb uses the reductive TCA cycle to maintain membrane potential in a process that leads to succinate accumulation in the medium (37,38). The glyoxylate shunt also appears to be an important metabolic adaptation

to hypoxia, as Eoh and Rhee (38) observed that the *icl* mutant has reduced succinate secretion and survival under hypoxia, defects that can be restored by the addition of the reductive TCA precursor aspartic acid (38). This critical role for *icl* contrasts with the previous observation by Watanabe *et al.*, who reported no defect in succinate secretion in the *icl* mutant (37), although differences exist in the media used, Middlebrook 7H9/10 medium versus Dubos medium for the Eoh and Watanabe studies, respectively. This hypoxia-induced metabolic remodeling appears to be dependent on the absence of oxygen as an electron acceptor, because addition of the alternate electron acceptor nitrate limits succinate secretion by Mtb (38). Thus, increased metabolism via the reductive TCA cycle, and specifically the enzyme *icl*, are implicated in Mtb's metabolic adaptation to hypoxic environments. It remains to be seen what role this metabolic pathway plays during Mtb adaptation *in vivo*.

Interestingly, the *icl*-dependent accumulation of reductive TCA intermediates was also observed in response to the unrelated stress of antibiotic treatment. Treatment of Mtb with rifampin, streptomycin, or isoniazid, antibiotics with distinct mechanisms of killing, led to a similar accumulation of the reductive TCA cycle intermediates malate, fumarate, and succinate, and decrease in the oxidative TCA cycle intermediate α-ketoglutarate in a dose dependent manner (39). These metabolic changes were shown to be absent in the *icl* mutant, and notably the *icl* mutant was shown to be more sensitive to killing by each of the antibiotics (39). Utilization of the reductive TCA cycle and glyoxylate shunt in adaptation to two unique stresses, hypoxia and antibiotic treatment, suggests that Mtb may employ a shared adaptive program to mitigate metabolic stress. Further support for this hypothesis comes from Mtb grown in a carbon source limited chemostat at a slow growth rate. In this carbon-limited state, metabolic flux analysis suggests that Mtb increases metabolic flux through the glyoxylate shunt as well as increasing anaplerotic oxidation of pyruvate to malate or oxaloacetate (40). This finding again implicates the glyoxylate shunt in metabolic adaptation to stress, in this case to nutrient limitation. While the reason for the observed convergence of metabolic stress responses is somewhat puzzling,

insight into its potential purpose comes from earlier work done by Fischer and Sauer studying the metabolism of *E. coli* (41). Slow growing, glucose limited *E. coli* in continuous culture completely oxidized glucose via a metabolic cycle that they named the PEP-glyoxylate cycle that requires flux through the glyoxylate shunt. Notably, this cycle was active in an NADPH-overproducing mutant of *E. coli*, which led the authors to speculate that the purpose of this PEP-glyoxylate cycle was to decouple central carbon catabolism from NADPH production that occurs through the oxidative TCA cycle. By extension, it is tempting to speculate that the glyoxylate shunt could be performing a similarly vital role in Mtb adaptation to stress, allowing catabolism to continue without the production of reduced cofactors via the irreversible oxidative decarboxylation of the TCA cycle.

Mtb growth arrest models

Since its identification over 100 years ago, Mtb has been recognized as a slow growing pathogen capable of surviving long periods of growth arrest, with early research demonstrating that viable Mtb could be recovered from sealed cultures even after incubating at 37ºC for 30 years (42). More recent experiments have observed the doubling time of Mtb to vary substantially based on its environment, ranging from 20 hours during logarithmic growth *in vitro* to 70 days during mouse infection (43-45). The resilience of Mtb during infection and antibiotic treatment is thought to stem in part from this ability to slow and arrest growth (44,46), and as such characterizing the environments that induce slow growth is of particular interest. *In vitro* conditions that slow and arrest Mtb growth include hypoxia (47,48), nitric oxide (49), low iron (50), nutrient starvation (51), phosphate limitation (52), and combined stress models (53).

One well-studied model for Mtb growth arrest is hypoxia, which can be characterized using the Wayne model (54), a method of gradual oxygen depletion that results in a uniform nonreplicating culture. In this model, Mtb replication ceases at 1% dissolved oxygen, a state

associated with continued cell elongation, increased expression of glycine dehydrogenase, and maintenance of ATP concentrations. At 0.06% dissolved oxygen, cell elongation ceases and oxygen consumption slows even further, although ATP concentration is maintained even after 400 hours in culture (54). In this nonreplicative state, the viable count of bacilli decreases with a half life of 11 days, although it is not clear whether this is due to cell death or to the formation of unculturable bacteria (55). Similarly to hypoxia, Mtb exposed to low levels of nitric oxide also arrests growth amidst inhibition of respiration (49). In both hypoxia and nitric oxide induced growth arrest, the ability of Mtb to survive and recover is dependent on the two-component regulatory system DosRST that senses and responds to both oxygen and nitric oxide. The DosRST regulon is induced during both hypoxia and nitric oxide stress, and is necessary to maintain ATP levels and redox homeostasis in these growth arrested states (49). The importance of DosRST signaling in adaptation to hypoxic growth arrest can be attributed in part to the role of the DosR-regulated triacylglycerol synthase (encoded by *tgs*). Baek *et al.* (50) showed that Mtb lacking *tgs* continued to replicate under conditions of hypoxia, and they proposed a model by which Mtb limits growth by redirecting carbon flux away from the oxidative TCA cycle through the synthesis of triacylglycerol. Baek *et al.* (50) also showed that *tgs* acted to reduce Mtb growth in both low iron and low pH environments, although neither of these environments were completely growth arresting for the bacteria.

One of the oldest models of Mtb growth arrest is nutrient starvation. Loebel *et al.* (51), among others, observed that Mtb, unlike other species of bacteria, survives long periods of nutrient starvation in normoxia that is associated with decreased oxygen consumption. More recently, it was shown that during starvation, Mtb requires ATP synthase, the enzyme isocitrate lyase, and, unlike in the Wayne model, cellular respiration to maintain viability and ATP homeostasis. Also unique from the Wayne model of growth arrest, nutrient starvation led to a ~5-fold decrease in ATP concentration, although Mtb maintained this new concentration of ATP during 20 days of starvation (56,57).

In each of these growth arrest models, Mtb exhibits markedly improved tolerance to several chemically distinct antibiotics (50,54,56,58), supporting the hypothesis that growth rate is an important determinant of drug efficacy during treatment of tuberculosis. This observation has implications for the effective treatment of Mtb, because the long course of antibiotic treatment required for sterilization is, in part, a consequence of Mtb phenotypic drug tolerance during infection. Indeed, *in vivo* Mtb drug tolerance has been shown to be linked to host-derived stresses such as nitric oxide and pH that are known to slow Mtb growth *in vitro* (59). One approach to confront this drug tolerance is to impair the ability of Mtb to properly adapt to or maintain growth arrest. This approach appears to hold promise, as the mutation of *tgs* that resulted in increased replication in hypoxia and low iron conditions also led to increased susceptibility to isoniazid, ethambutol, streptomycin, and ciprofloxacin both *in vitro* as well as in macrophage and mouse infection models (50). Additionally, recently described inhibitors of DosRST, required for hypoxic adaptation, also decreased antibiotic tolerance to isoniazid in Mtb cultured in hypoxia (60).

Slow growth and metabolic restriction at acidic pH

As has been discussed for other environmental stresses encountered by Mtb during infection, Mtb slows its growth at acidic pH (15,17,18). In rich medium, Mtb exhibits slow growth at acidic pH, with complete growth arrest occurring at pH 5.0 (17). Piddington *et al*. (18) observed that Mtb arrests growth in the defined Sauton's medium (containing glycerol, glucose, and albumin) at pH 6.0 and low Mg^{+2} levels (10 μM), whereas at higher Mg^{+2} levels (100 μM) Mtb exhibits reduced growth compared to pH 7.0. This acid and low Mg^{+2} dependent growth arrest is unique from that of closely related non-pathogenic strains of mycobacterium, suggesting that it represents a specific adaptation rather than a physiological limitation. Indeed, the intracellular pH of Mtb remains neutral even when exposed to conditions as acidic as pH 4.5 (8,19),

revealing that slowed growth of Mtb is not due to a loss in pH homeostasis. In the minimal medium MMAT (61), Mtb begins to slow growth at pH 6.4 and arrests growth by pH 5.7 in a variety of carbon sources (15). MMAT contains 83 μM Mg^{+2}, intermediate to the Mg^{+2} concentrations used by Piddington *et al.* (18). Notably, in MMAT Mtb can grow at pH 5.7 when supplied with acetate, oxaloacetate, pyruvate, or cholesterol, carbon sources that fuel the anaplerotic node (62) of metabolism. Notably, acetate, oxaloacetate, and pyruvate are catabolic products of cholesterol, a primary carbon source for intracellular Mtb (30), and metabolic flux analysis of intracellular Mtb predicts that the bacterium catabolizes both acetate and 3-carbon substrates during infection (63). This carbon source dependent growth arrest at acidic pH suggests a metabolic remodeling of the accessible pathways for carbon metabolism compared to neutral pH.

To further understand the mechanisms of Mtb growth restriction at acidic pH, a logical step is to consider its extensive transcriptional response, and central to this response is the PhoPR regulon. The PhoPR regulon is controlled by a two-component system consisting of the sensor kinase PhoR and the response regulator PhoP (64). PhoPR regulates expression of about 4% of the Mtb genome, including genes involved in lipid metabolism and general metabolism (64-66). At acidic pH, induction of the PhoPR regulon leads to increased synthesis of sulfolipid, di-, and polyacyltrehaloses (15,17,64,66,67), representing a significant shift in anabolic metabolism at acidic pH.

Mtb also induces several genes encoding proteins involved in redox homeostasis at acidic pH, including thioredoxins, alkyl hydroperoxidase reductases, and the regulatory protein WhiB3. WhiB3 has previously been shown to regulate the synthesis of lipids such as sulfolipid, poly- and diacyltrehalose, and phthiocerol dimycocerosate (PDIM). This WhiB3-regulated lipid synthesis acts as a reductive sink necessary to maintain redox homeostasis (68). Why Mtb induces genes involved in redox homeostasis at acidic pH is not completely clear, but one clue comes from the remodeling of the electron transport chain. At acidic pH, genes encoding type-I

NADH dehydrogenase and *c*-type cytochrome oxidases are repressed transcriptionally, whereas those encoding type-II dehydrogenase and *bd*-type cytochrome oxidases are induced. This change in respiration machinery constitutes a shift from proton-translocating to non-proton-translocating components. Whether this shift is in response to an increased extracellular proton concentration or is responsible for changes in Mtb redox poise remains to be investigated.

At acidic pH, the expression of genes encoding the anaplerotic enzymes isocitrate lyase (*icl*), malic enzyme (*mez*), and phosphoenolpyruvate carboxykinase (*pckA*) are induced, reminiscent of the necessity of anaplerotic metabolism in adaptation to hypoxia, antibiotic stress, and starvation as discussed previously. In hypoxia, an important role of these anaplerotic reactions is the maintenance of redox homeostasis. In a similar manner, Mtb in pH 5.7 growth arrest exhibits a more reduced intracellular environment that Mtb at neutral pH (15), suggesting that the anaplerotic node may have a role in maintaining redox homeostasis at acidic pH as well.

Despite the induction of the PhoPR regulon at acidic pH, mutation of the genes encoding PhoPR does not lead to bacterial death at acidic pH. In rich medium titrated to pH 4.5, deletion of PhoPR was shown to cause a 3-fold reduction in growth, suggesting that Mtb requires PhoPR for optimal adaptation to acidic pH in a nutrient rich environment (16). However, in minimal medium buffered to pH 5.7 and supplemented with a carbon source permissive for growth, the *phoPR* mutant actually exhibits enhanced growth compared to wild type Mtb (15), demonstrating that at least in some acidic conditions PhoPR is dispensable for Mtb growth.

Acid Adaptive Fasting

Common themes and important distinctions exist between the growth regulation and metabolic adaptation of Mtb to acidic pH and the other environmental stresses discussed. Similar to other growth arrest models like hypoxia or nitric oxide, acidic pH growth arrest does

seem to involve perturbations in redox homeostasis as evidenced by measurement of intracellular redox poise as well as the transcriptional response of Mtb. Unlike hypoxia or nitric oxide, neither oxygen limitation nor a direct inhibitor of respiration can easily account for the redox imbalance; however, the shift in electron transport chain machinery from proton pumping to non-proton pumping could represent a response to a so far unexplored restriction in Mtb respiration at acidic pH. Unlike the starvation model of growth arrest, ample carbon source is available for Mtb catabolism during acidic pH growth arrest. Furthermore, while the *dosRST* mutant has impaired survival in hypoxia, deletion of *phoPR*, the two-component system activated at acidic pH, does not impair acid tolerance under growth arresting conditions. Given these differences, understanding the mechanisms of acidic pH growth arrest may provide new insights into the constraints of Mtb growth *in vivo*.

It is worth noting that unlike hypoxic growth arrest, where mutation leading to increased replication is detrimental to Mtb survival, the increased replication of the *phoPR* mutant does not reduce viability (15,16). This difference raises the possibility that some portion of growth regulation at acidic pH is not due simply to physiological constraints incurred by acid stress, but rather represents an adaptive process of Mtb. In this interpretation, the growth arrest observed at acidic pH is not starvation, an inability to utilize fuel for energy production and growth, but rather fasting, an active process of avoiding energy production for growth. This conjecture assumes that factors necessary to maintain acid tolerance such as MarP are intact (9,10); however, when acid tolerance is intact the metabolic and growth restriction of Mtb at acidic pH may be better understood as a response to an environmental cue. Adaptation in response to acidic pH could prepare Mtb for the concomitant stresses encountered with acidic pH during infection, and as such it is tempting to speculate that Mtb has evolved to use the acidic pH of the phagolysosome as a cue for the forthcoming antimicrobial environment of the macrophage.

To address the open questions posed above, I have carried out a series of studies to investigate Mtb metabolic and growth adaptation to acidic pH. In chapter 2, I investigate the role

of growth regulation in Mtb acid adaptation, identifying a role of available carbon sources and *phoPR* in Mtb growth regulation at acidic pH. Furthermore, I characterize changes in redox homeostasis, lipid synthesis, and transcriptional adaptation that occur at acidic pH. The transcriptional profiling performed in chapter 2 implicated the anaplerotic node of metabolism in Mtb metabolic remodeling at acidic pH. In chapter 3, I seek to characterize this metabolic remodeling by probing the growth and metabolic profiles of two deletion mutants that encode enzymes of the anaplerotic node. In chapter 4, I seek to characterize the physiology of growth arrest at acidic pH and to test the hypothesis that growth arrest at acidic pH is a genetically regulated process. In chapter 5, I discuss the implications of these studies in our understanding of Mtb acid adaptation.

CHAPTER 2 - Slow growth of *Mycobacterium tuberculosis* at acidic pH is regulated by *phoPR* and host-associated carbon sources

Jacob J. Baker, Benjamin K. Johnson and Robert B. Abramovitch

Published in Molecular Microbiology, 2014 October; Volume 94(1), pages 56-69.

I would like to acknowledge the contributions of Benjamin K. Johnson to this chapter. Dr. Johnson performed the RNA-seq data analysis presented in this chapter and provided manuscript feedback and editing.

Summary

During pathogenesis, *Mycobacterium tuberculosis* (Mtb) colonizes environments, such as the macrophage or necrotic granuloma, that are acidic and rich in cholesterol and fatty acids. The goal of this study was to examine how acidic pH and available carbon sources interact to regulate Mtb physiology. Here we report that Mtb growth at acidic pH requires host-associated carbon sources that function at the intersection of glycolysis and the TCA cycle, such as pyruvate, acetate, oxaloacetate and cholesterol. In contrast, for other tested carbon sources, Mtb fully arrests its growth at acidic pH and establishes a state of non-replicating persistence. Growth-arrested Mtb is resuscitated by the addition of pyruvate suggesting that growth arrest is due to a pH-dependent checkpoint on metabolism. Additionally, we demonstrate that the *phoPR* two-component regulatory system is required to slow Mtb growth at acidic pH and functions to maintain redox homeostasis. Transcriptional profiling and functional metabolic studies demonstrate that signals from acidic pH and carbon source are integrated to remodel pathways associated with anaplerotic central metabolism, lipid anabolism and the regeneration of oxidized cofactors. Because *phoPR* is required for Mtb virulence in animals, we suggest that pH-driven adaptation may be critical to Mtb pathogenesis.

Introduction

Mycobacterium tuberculosis (Mtb) is a slow growing bacterial pathogen. During growth *in vitro,* in macrophages, or in mice, Mtb has measured doubling times ranging from ~20 hours to 70 days (43-45). Under low oxygen, Mtb enters a non-replicating persistent state where the pathogen arrests growth but remains viable. Slow or arrested growth is thought to play an important role in the establishment of chronic infections and drug resistance. Understanding how Mtb regulates its growth rate in response to environmental cues encountered during infection, including acidic pH and carbon source availability, should provide insight into the physiology that makes Mtb a successful and difficult to treat pathogen.

Mtb growth and gene expression are strongly regulated by environmental pH (3,8,9,17,18). In rich medium, the bacterium slows its growth below pH 6.4 and arrests its growth at ~pH 5.0 (17). Following one day of exposure to an acidic environment at pH 4.5, Mtb maintains an intracellular pH of ~7.4, demonstrating that Mtb effectively buffers its cytoplasm and that changes in growth rate are not solely associated with cytoplasmic acidification (9). Mutation of the gene encoding the Rv3671c membrane protein causes a loss of cytoplasmic pH-homeostasis and results in strong attenuation of virulence during mouse infection, supporting the idea that Mtb encounters environments *in vivo* where acidic pH-dependent adaptations are essential for pathogenesis (9).

Transcriptional profiling studies of Mtb in response to acidic pH *in vitro* and in macrophages demonstrate widespread changes in gene expression (11,69). The phagosomal acidic pH regulon (11) exhibits significant overlap with the *phoPR* two-component regulatory system regulon (64,65), suggesting that *phoPR* may play a role in pH-driven adaptation. For example, the acid and phagosome regulated locus, *aprABC,* is strongly induced by acidic pH, requires *phoP* for its expression, and its promoter is strongly bound by the PhoP response regulator (17,70). *phoPR* mutants are highly attenuated during mouse and guinea pig infections (12,71),

further supporting the hypothesis that pH-driven adaptation plays an important role during the course of infection.

Several PhoPR-regulated, acidic-pH induced genes are associated with carbon metabolism. For example, the *pks2, pks3,* and *pks4* genes are associated with the production of cell envelope lipids sulfolipid, diacyl- and polyacyltrehalose (DAT and PAT) (64,67), and the *aprABC* locus is associated with the control of triacylglycerol (TAG) accumulation and regulation of genes of central carbon and propionate metabolism (17). While all the carbon sources available to Mtb *in vivo* are not specifically known, the requirement for isocitrate lyase (encoded by *icl*) during infection suggests that Mtb metabolizes acetyl-CoA derived from long chain fatty acids via the glyoxylate shunt (25) or propionyl-CoA derived from cholesterol via the methylcitrate cycle (33,35,72). Several lines of evidence suggest that cholesterol is an important carbon source during infection. For example, in macrophages, Mtb metabolizes cholesterol, and likely other lipids available on low-density lipoprotein, as carbon sources (30,73); cholesterol and TAG are abundant lipids in the caseum of the human Mtb granuloma (74); and, several genes involved in cholesterol catabolism are essential for *in vivo* survival (30,75). Mtb has also been shown to acquire and metabolize macrophage derived fatty acids (36) . The catabolism of cholesterol and fatty acids is predicted to produce acetyl-CoA, propionyl-CoA, pyruvate, and glycerol (31), suggesting Mtb physiology may be regulated by these host-associated carbon sources.

Both the macrophage phagosome and the caseum of a necrotic granuloma can be acidic environments (76); therefore, it is possible that Mtb integrates environmental signals from acidic pH and carbon nutrient availability to modulate its growth and metabolism. Indeed, Baek and colleagues have shown that a TAG synthase mutant (*tgs1*) has enhanced growth at acidic pH as compared to the wild type (WT) strain, genetically linking acidic pH, carbon metabolism, and growth rate (50). In this study, we explore the hypothesis that acidic pH and available carbon sources interact to regulate Mtb growth and physiology.

Results

Mtb exhibits carbon source specific growth arrest at acidic pH

Mtb has been shown to slow its growth at acidic pH in a variety of rich and minimal media (9,17,18,50). To confirm these observations, Mtb strain CDC1551 was grown in 7H9 (OADC) medium buffered at pH 7.0 or pH 5.7 using 100 mM MOPS or MES, respectively. Following 9 days of incubation at pH 5.7, Mtb exhibited a 4-fold reduction in growth relative to Mtb grown at pH 7.0 (Appendix Figure 1A). We hypothesized that changes in carbon metabolism may be associated with pH-dependent slowed growth. 7H9 (OADC) medium contains a variety of potential carbon sources including glycerol, glucose, oleic acid, albumin, amino acids and Tween-80. In order to isolate the role of specific carbon sources, we investigated the growth of Mtb at pH 7.0 and 5.7 in a defined, buffered minimal medium (36). We first tested glucose and glycerol as carbon sources and observed that Mtb fully arrests its growth at pH 5.7 in the presence of these carbon sources alone or combined (Appendix Figure 1B-C). In glycerol-amended medium, Mtb begins to exhibit slowed growth at pH 6.4, consistent with previous observations in rich medium (17).

Given the observation of growth arrest in medium supplemented with glycolytic carbon sources, Mtb growth was examined in the presence of a variety of carbon sources associated with central metabolism (Figure 2.1A, Appendix Figure 2). For these experiments, Mtb cultures were grown in rich medium, pelleted and then seeded at an initial density of OD 0.05 in standing, vented flasks containing 8 mL of buffered minimal medium and a single carbon source. Cultures were incubated for nine days and growth was measured at three-day intervals. As a control, to determine the effect of residual extracellular or intracellular carbon sources, cultures were also seeded in medium without the addition of a carbon source. In this “No Carbon” control, very little growth was observed at pH 7.0 and no growth was observed at pH 5.7 (Figure 2.1A, Appendix Figure 2), supporting the notion that growth above this baseline is

promoted by metabolism of the specified carbon source. For the carbon sources that supported growth at pH 7.0, it was observed that at pH 5.7, some carbon sources restricted growth while others permitted growth (Figure 2.1A, Appendix Figure 2). Notably, carbon sources that feed central metabolism at the intersection of glycolysis and the TCA cycle permitted growth at acidic pH, including phosphoenolpyruvate (PEP), pyruvate, oxaloacetate, and acetate (Figure 2.1A). Pyruvate was the preferred carbon source at pH 5.7, with similar growth relative to pH 7.0 (Figure 2.1B). In a long-term 36-day growth experiment, Mtb cultured in 10 mM glycerol at pH 7.0 reaches stationary phase, while at pH 5.7 the culture remains growth-arrested, showing that the 9-day trends extend to stationary phase and that differing total biomasses are achieved. In contrast, cultures incubated in 10 mM pyruvate at acidic and neutral pH over 36 days reach a similar optical density at stationary phase (Appendix Figure 3A). Mtb cholesterol catabolism is predicted to generate pyruvate, acetyl-CoA and propionyl-CoA and, indeed, cholesterol also permitted modest growth at acidic pH (Figure 2.1A, Appendix Figure 2). Together, these data demonstrate that the ability of Mtb to grow at acidic pH is carbon source-specific. The growth permissive carbon sources all feed central metabolism at a switch point in metabolism known as the PEP-pyruvate-oxaloacetate node or anaplerotic node (62). Therefore, our findings suggest that metabolic flexibility afforded by carbon sources feeding the anaplerotic node may play a role in promoting growth in acidic environments (Figure 2.1C).

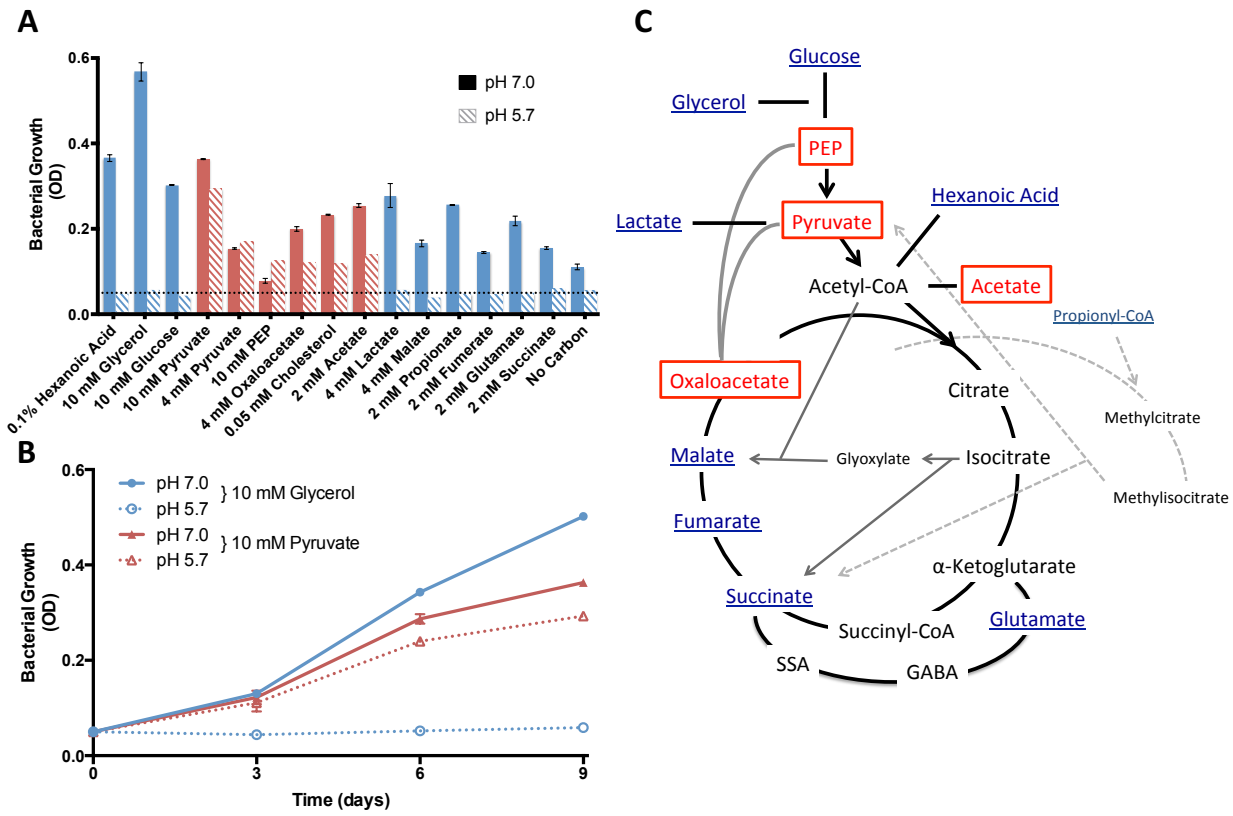

Figure 2.1. Mtb exhibits carbon source specific growth arrest at acidic pH. A. Mtb growth on various carbon sources at both neutral and acidic pH. Cultures were seeded at a starting density of 0.05 OD_{600} (horizontal dotted line) and growth was measured every three days for 9 days. The growth curves are presented in Appendix Figure 2 and the day 9 endpoint data are summarized in this panel. Carbon sources are designated as either permissive (red bars) or restrictive (blue bars) for growth at acidic pH, as compared to the growth baseline in the "No Carbon" control. Only PEP, pyruvate, oxaloacetate, acetate and cholesterol promoted growth at acidic pH. B. Growth curves showing glycerol arrests growth and pyruvate promotes growth of Mtb at acidic pH. C. Model showing the position within central carbon metabolism of carbon sources permissive (boxed) and restricted (underlined) for growth at acidic pH. The panel is modified from Tian *et al.* (77). Error bars represent the standard deviation and the data are representative of two independent experiments.

pH-driven, carbon-source dependent growth arrest is species specific

During pathogenesis, Mtb will encounter environments with acidic pH and restricted carbon sources; therefore, we hypothesized that the pH-dependent growth arrest phenotype may have evolved as a pathogenesis-specific adaptation. Previously, Piddington and colleagues (18) observed that Mtb grown in pH 6.0 Sauton's medium (where glycerol is the primary carbon source) exhibits strongly restricted growth at acidic pH, as compared to a modest decrease in growth with the non-pathogenic, environmental species *Mycobacterium smegmatis*. To determine if pH- and carbon source-specific growth arrest is an evolved pathogenesis trait, the growth of the non-pathogenic species *M. smegmatis* was examined in a variety of single carbon sources at acidic and neutral pH. In contrast to Mtb, the growth of *M. smegmatis* was not slowed at pH 5.7 on any of the tested carbon sources, except glycerol and malate, where there was an ~30% reduction in growth (Appendix Figure 4A). The lack of carbon source-specific growth arrest at acidic pH in *M. smegmatis* supports an evolutionary model whereby this physiology may function to promote pathogenesis in animals.

Given that differences exist in the physiology and virulence of different Mtb strains (78), we examined if the growth arrest phenotype observed in CDC1551 was conserved in other Mtb strains. The Mtb strains CDC1551, H37Rv, HN878, and Erdman were all grown at pH 7.0 and pH 5.7 in the presence of either glycerol or pyruvate. Consistent with CDC1551, all of the strains grew well on glycerol at pH 7.0, but were arrested for growth at pH 5.7 (Appendix Figure 4B). Pyruvate as a single carbon source allowed growth at both pH 7.0 and pH 5.7 for each strain, albeit with differences in the magnitude of growth (Appendix Figure 4B). This finding supports that the carbon source specific growth arrest observed in CDC1551 is qualitatively consistent with other Mtb strains.

Intracellular pH homeostasis and viability are maintained during growth arrest

To investigate the physiology of pH-dependent growth arrest, we examined the effect of growth arrest on intracellular pH homeostasis and viability. Previously, in rich medium at acidic pH, it has been shown that Mtb maintains intracellular pH homeostasis (9). However, it is possible that in minimal medium, Mtb is impaired in maintaining pH homeostasis. To determine if pH-dependent growth arrest was associated with a loss of pH homeostasis, intracellular pH was quantified using an assay employing the pH sensitive fluorescent dye CMFDA (79). Mtb grown in minimal medium with glycerol or pyruvate at pH 5.7 exhibited a slight acidification of the cytoplasm as compared to growth at pH 7.0 (Figure 2.2A). However, at pH 5.7, there was no significant difference between the cytoplasmic pH of Mtb under growth restrictive or permissive conditions. Therefore, Mtb is capable of maintaining pH homeostasis at pH 5.7 in both glycerol and pyruvate, and intracellular pH is not associated with differential growth.

To determine if growth-arrested cells were viable, colony-forming units (CFU) were counted for Mtb grown in minimal medium, at pH 7.0 or 5.7, with glycerol or pyruvate as a sole carbon source. No significant reduction in bacterial viability was observed in Mtb cultured at pH 5.7 with glycerol over the 9-day time course, showing that growth-arrested Mtb maintains its viability in the absence of growth (Figure 2.2B). Thus, growth arrest is not due to glycerol-mediated toxicity and cell death.

Pyruvate resuscitates growth-arrested Mtb

The viability of growth-arrested Mtb raised the possibility that the bacteria may be resuscitated with a growth permissive carbon source. To test this hypothesis, following 9 days of growth arrest on glycerol at pH 5.7, 10 mM pyruvate was added to the culture. Remarkably, pyruvate resuscitated growth-arrested Mtb (Figure 2.2C), even in the continued presence of 10 mM glycerol in the medium, demonstrating bacterial viability and the growth permissive effect of pyruvate is dominant over the growth restrictive effect of glycerol.

To further explore the growth permissive activity of pyruvate, Mtb growth in 10 mM glycerol at pH 5.7 was examined with increasing amounts of pyruvate (from 1 mM to 10 mM). At pH 5.7, pyruvate relieved glycerol-dependent growth arrest in a concentration dependent manner (Figure 2.2D). Mtb grown with 10 mM of both pyruvate and glycerol, showed improved growth as compared to 10 mM pyruvate alone, suggesting the addition of pyruvate enables the co-metabolism of glycerol. Together, these findings demonstrate that Mtb integrates environmental pH and available carbon source to control its growth. Indeed, Mtb appears to establish a state of non-replicating persistence under acidic pH with glycerol and can be resuscitated in the presence of pyruvate.

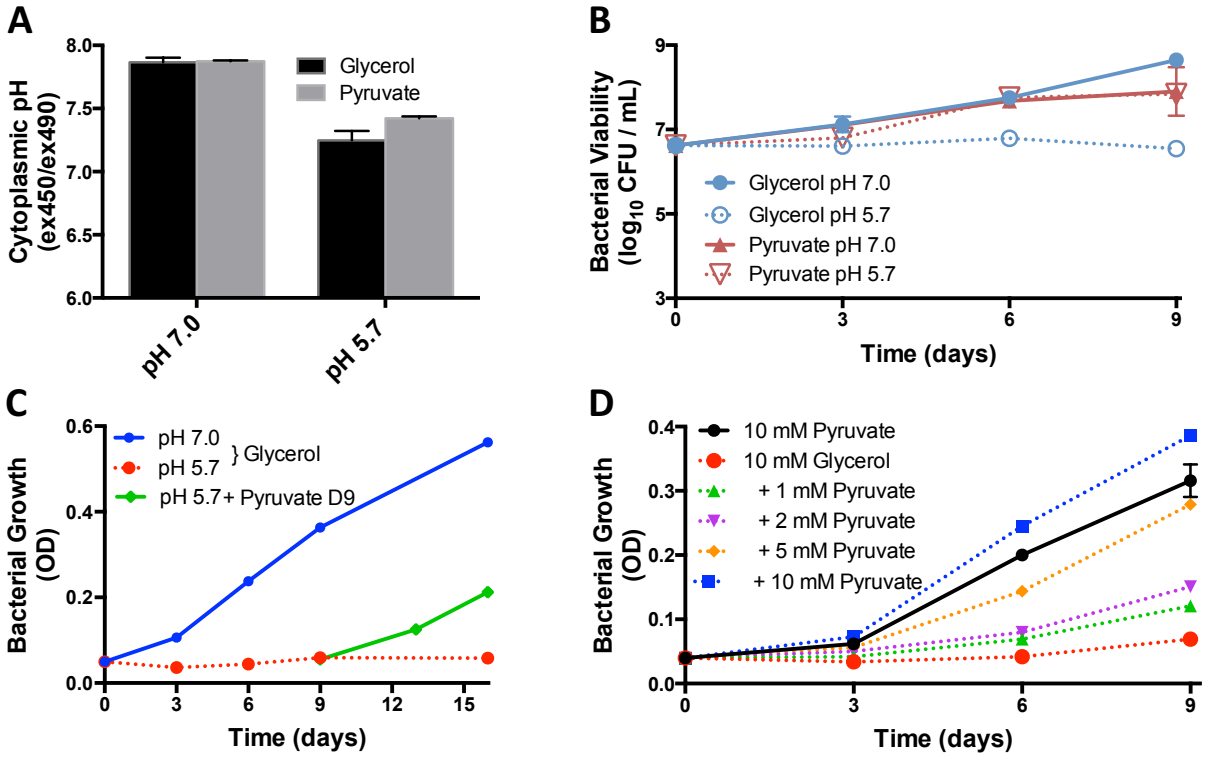

Figure 2.2. Growth-arrested Mtb is resuscitated with pyruvate. A. Mtb can maintain its cytoplasmic pH homeostasis in response to both glycerol and pyruvate at pH 7.0 and pH 5.7. B. Mtb remains viable during acidic pH growth arrest as measured by colony forming units (CFU). This finding suggests that Mtb enters a state of non-replicating persistence driven by acidic pH and carbon source. C. Following 9 days of growth arrest in minimal medium with 10 mM glycerol at pH 5.7, addition of 10 mM pyruvate resuscitates Mtb growth (green line). Therefore, Mtb growth arrest at acidic pH is reversible and non-lethal. D. Pyruvate promotes Mtb growth in 10 mM glycerol in a concentration dependent manner. Error bars represent the standard deviation and the data are representative of three individual experiments.

phoP *is required to slow growth in response to acidic pH*

Mtb begins to slow its growth in minimal medium with glycerol at pH 6.4, the same pH threshold at which the *phoPR* regulon is induced by acidic pH (17). The *phoPR* regulon is strongly induced at pH 5.7 and differentially regulates genes associated with carbon and lipid metabolism (17,64,65). Therefore, we hypothesized that *phoPR* may play a role in carbon-source dependent growth arrest. To explore this hypothesis, we examined the response of a CDC1551 *phoP* transposon mutant (*phoP*::Tn, (17)), a *phoPR* deletion mutant and the complemented mutant (*ΔphoPR* and *ΔphoPR* comp (80)) during growth on single carbon sources at acidic pH. Unexpectedly, at pH 7.0, the *ΔphoPR* mutant exhibited impaired growth on glycerol and pyruvate as single carbon sources as compared to the WT and complemented *ΔphoPR* mutant (Figure 2.3A and 2.3C). Therefore, *phoPR* is required for growth in medium with glycerol or pyruvate as single carbon sources at neutral pH. At pH 5.7, the *phoP* mutants maintained arrested growth on glycerol (Figure 2.3B); however, the *phoP* mutants exhibited significantly enhanced growth on pyruvate as compared to wild type Mtb (Figure 2.3D). The enhanced growth on pyruvate at pH 5.7 was complemented in the *ΔphoPR* mutant. The ability of the *phoP* mutants to grow better on pyruvate at acidic pH than at neutral pH is an important observation for several reasons. This finding demonstrates that acidic pH, in a *phoP*-independent manner, remodels Mtb physiology to allow growth on pyruvate, and makes available physiological pathways that are inaccessible at neutral pH. It is also notable that following these adaptations, the *ΔphoPR* mutant exhibits faster growth on pyruvate at pH 5.7 than the WT in any other tested growth condition. This finding shows that *phoPR* functions to slow growth at acidic pH and, thus, explains why reduced growth and induction of the *phoPR* regulon are so closely associated (17).

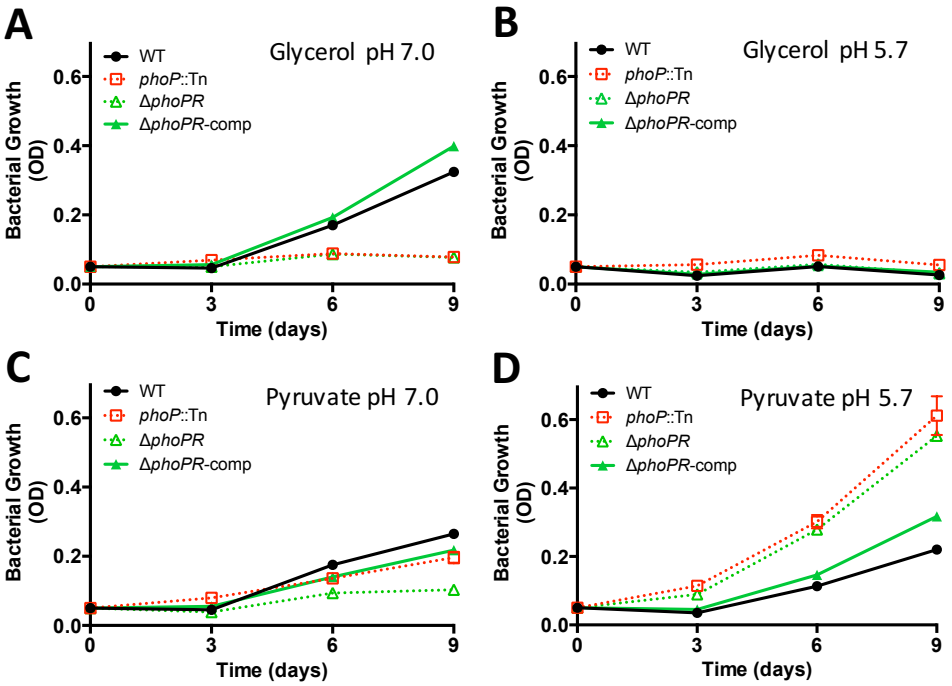

Figure 2.3. *phoPR* is required to slow Mtb growth at acidic pH. Growth of WT, *phoP*::Tn mutant, Δ*phoPR* mutant, and Δ*phoPR* complemented strains in minimal medium containing 10 mM glycerol at pH 7.0 (A), 10 mM glycerol at pH 5.7 (B), 10 mM pyruvate at pH 7.0 (C), and 10 mM pyruvate at pH 5.7 (D) as a single carbon source. Note that at neutral pH the strains lacking *phoP* have reduced growth on pyruvate and glycerol as compared to the WT or complemented strains. At pH 5.7, strains lacking *phoP* have enhanced growth on pyruvate, as compared to the WT and complemented strains. Error bars represent the standard deviation and the data are representative of three biological replicates.

Acidic pH, carbon source and* phoP *modulate redox homeostasis

The involvement of *phoPR* in the control of growth in response to changes in pH and carbon metabolism suggests that genes of the *phoPR* regulon play a role in modulating growth. Several genes in the *phoPR* regulon, including *pks2, pks3, pks4,* and *aprA* have been proposed to control redox homeostasis in Mtb (17,68). In this model, under conditions that cause an accumulation of reduced cofactors, such as NADH or NADPH, Mtb synthesizes long chain fatty acids using the NADPH consuming fatty acid synthase 1 enzyme (encoded by *fas*) to replenish pools of oxidized cofactors (68,81). Long chain fatty acids can then be used for the generation of storage lipids such as TAG and *phoP*-dependent cell envelope-associated lipids such as sulfolipid. Given this model, we hypothesized that changes in cytoplasmic redox homeostasis may be associated with pH-, carbon source- and *phoP*-dependent growth arrest.

To characterize the role of redox homeostasis in growth arrest, we examined cytoplasmic redox potential using an Mtb strain expressing a redox sensitive GFP (roGFP). roGFP exhibits ratiometric changes in the excitation wavelength based on the redox state of its disulfide bonds and thus provides a measure of cytoplasmic redox potential (82,83). roGFP has recently been shown to function in Mtb as a reporter of cytoplasmic redox potential (84). At pH 5.7, glycerol as a sole carbon source resulted in a decreased roGFP ratio (Figure 2.4A-B, *i.e.* a more reduced intracellular environment) showing that acidic pH in the presence of glycerol causes enhanced thiol reduction and a reduced cytoplasmic potential. For the growth-arrested *phoP:*:Tn mutant in minimal medium with glycerol at pH 7.0, we observed a reduced cytoplasmic potential that was equal to that of WT Mtb on glycerol at pH 5.7 (Figure 2.4B). This finding demonstrates that *phoP* is required to maintain redox homeostasis during growth on glycerol and that growth arrest is associated with reductive stress. The *phoP*::Tn mutant grown with glycerol at acidic pH exhibits an even more strongly reduced cytoplasm (Figure 2.4B) demonstrating that PhoP functions to counteract acidic pH-associated reductive stress.

Glycerol-mediated growth arrest at acidic pH is associated with a reduced cytoplasmic potential; therefore, we hypothesized that pyruvate may alleviate acid-mediated reductive stress. When Mtb is grown in pyruvate alone, or glycerol and pyruvate, the redox potential of the cytoplasm remains unchanged at pH 7.0 and 5.7 (Figure 2.4A), demonstrating that Mtb does not experience pH-dependent metabolic stress in the presence of pyruvate. Notably, the *phoP::*Tn mutant grown on pyruvate as a single carbon source exhibits slow growth at neutral pH and enhanced growth at acidic pH; however, the redox potential in both cases was similar to that of growth-arrested Mtb grown on glycerol at pH 5.7. Therefore, we conclude that a reduced cytoplasmic potential is associated with growth arrest on specific carbon sources, but reductive stress, in the absence of *phoP*, is not sufficient to cause growth arrest. To determine if growth arrest was associated with a shortage of oxidized cofactors, we examined NAD^+/NADH and $NADP^+$/NADPH ratios and observed a significant increase in the NAD^+/NADH ratio at acidic pH in both 10 mM glycerol or pyruvate and no change in the $NADP^+$/NADPH ratio (Appendix Figure 5). These observations demonstrate that Mtb can maintain a cellular pool of oxidized NAD under conditions of pH-induced reductive stress and that the reduced cytoplasmic potential may be driven by a cytoplasmic redox buffer, such as mycothiol or thioredoxin.

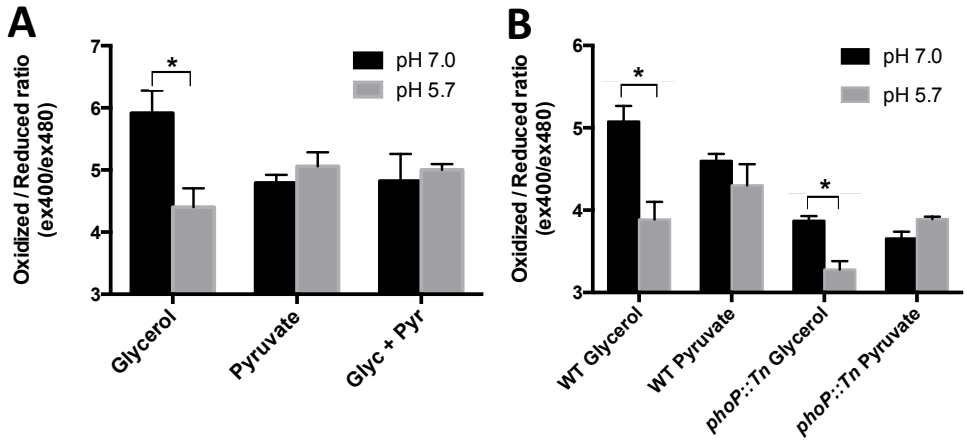

Figure 2.4. Acidic pH, carbon source and *phoP* modulate redox homeostasis. Intracellular redox state was measured using a redox sensitive disulfide bond-containing GFP (roGFP) by calculating the ratio of fluorescence emission intensity from 400 nm and 480 nm excitation. A lower ratio indicates a more reduced roGFP while a higher ratio indicates a more oxidized roGFP. A. WT Mtb growing on glycerol exhibits a more reduced cytoplasm at acidic pH. However, when pyruvate is present, Mtb does not exhibit a shift in cytoplasmic redox potential. B. The *phoP*::Tn mutant exhibits a more reduced cytoplasm, as compared to the wild type, at pH 7.0 when grown on both glycerol and pyruvate. At pH 5.7, the *phoP* mutant exhibits an even more reduced cytoplasm in glycerol, while maintaining it redox potential in pyruvate. Error bars indicate the standard deviation of three biological replicates each calculated from the average of three technical replicates. The data are representative of two individual experiments. *$p<0.05$ using a student's t-test.

Acidic pH causes transcriptional remodeling of pathways associated with anaplerosis, lipid anabolism, and oxidation of redox cofactors.

To explore the mechanisms by which acidic pH remodels Mtb physiology, we undertook RNAseq-based transcriptional profiling studies. Mtb transcripts were examined following 3 days incubation in minimal medium under four conditions: glycerol pH 7.0, glycerol pH 5.7, pyruvate pH 7.0 and pyruvate pH 5.7. At pH 7.0, only modest transcriptional changes are associated with growth on glycerol or pyruvate, with 63 genes significantly induced (up >1.5 fold, $p< 0.05$) and 17 genes significantly repressed in pyruvate as compared to glycerol (Appendix Figure 6A. This finding demonstrates limited transcriptional remodeling in response to these carbon sources, perhaps reflecting unrestricted metabolism between glycerol and pyruvate at neutral pH. At acidic pH, substantial transcriptional remodeling is observed in both glycerol and pyruvate, with hundreds of genes exhibiting significant differential regulation (Appendix Figure 6B-C). In contrast to pH 7.0, a direct comparison of transcriptional profiles between pyruvate and glycerol at pH 5.7, revealed 275 and 445 genes with differentially induced or repressed expression, respectively (Appendix Figure 6D). Overall, these findings support the proposal that acidic pH and carbon source, together, promote substantial remodeling of Mtb physiology.

Previous attempts to characterize pH-regulated genes have been complicated by the association of acidic pH with a strong downregulation of growth and induction of the stress response, thus making it difficult to separate the genes that are specifically responding to pH, from those associated with a shift in growth and stress status (17,69). Comparisons of the RNA-seq profiles identified genes with pH-dependent, carbon source-independent differential expression, with 185 acid-induced genes (Figure 2.5A, Appendix Figure 7A) and 134 acid-repressed genes (Figure 2.5B, Appendix Figure 7B). These genes represent the Mtb pH-dependent regulon that is independent of growth status. The induced genes are highly represented in pathways associated with carbon metabolism and redox homeostasis. For example, many genes of the *phoPR* regulon (17,64,65) are strongly induced by acidic pH in

both glycerol and pyruvate: *pks2-mmpL8* locus, *pks3-mmpL10* locus, malate dehydrogenase (*mez*) and NADH dehydrogenase (*ndh)*. Additionally, several genes without evidence of *phoP*-dependent regulation are induced by acidic pH in both glycerol and pyruvate, including fatty acid synthase (*fas*), PDIM synthesis (*ppsA-ppsE*), pyruvate phosphate dikinase (*ppdK)*, and thioredoxin reductase (*trxB*). These acid regulated genes are associated with the regulation of Mtb carbon metabolism, lipid anabolism, and replenishment of oxidized cofactors and are consistent with a model where acidic pH remodels carbon metabolism to produce lipids and oxidize redox cofactors (Appendix Figure 8).

An additional goal of performing these transcriptional studies was to identify the mechanisms by which pyruvate remodels physiology at acidic pH. Transcriptional profiles consistent with pyruvate- and acidic pH-specialized expression are predicted to exhibit i) differential expression in pyruvate at pH 5.7 as compared to pH 7.0 (Appendix Figure 6C) and ii) differential expression in pyruvate as compared to glycerol at pH 5.7 (Appendix Figures 6D, 7A-B). For example, genes that are induced in pyruvate and glycerol at pH 5.7, but exhibit enhanced induction in pyruvate exhibit pyruvate- and pH-specialized induction. We identified 16 genes with this profile (Figure 2.5C and Appendix Figure 7A). Genes exhibiting pyruvate and pH-specialized induction were also identified that are stable in glycerol at pH 5.7 (31 genes) and that are repressed in glycerol at pH 5.7 (13 genes), for a total of 60 genes that are induced in a pyruvate- and pH-specialized manner (Figure 2.5C, Appendix Figure 7A). Using a similar analysis, we identified 75 genes that are repressed in a pyruvate- and pH-specialized manner (Figure 2.5D and Appendix Figure 7B). Genes were also regulated in a glycerol- and pH-specialized manner, with 46 genes and 26 genes showing enhanced induction or repression in glycerol at acidic pH, respectively (Appendix Figure 7AB).

The transcriptional profiling data provide additional support for the hypothesis that Mtb promotes metabolism around the anaplerotic node at acidic pH (Figure 2.1A, Appendix Figure 2). Many of the genes that are most strongly induced in a pyruvate- and pH-specialized manner

are associated with the anaplerotic node, including phosphoenolpyruvate carboxykinase (*pckA*) and isocitrate lyase (*icl1,* Figure 2.5C, Appendix Figure 7C*)*. *pckA* links the TCA cycle to glycolysis via the reversible metabolism of oxaloacetate to PEP and *icl1* acts as a bypass of an oxidative branch of the TCA cycle via the glyoxylate shunt. *pckA* and *icl1* exhibit induction by pyruvate at pH 7.0 and further induction by acidic pH in both glycerol and pyruvate, with the result of 2-fold and 4-fold induction in pyruvate as compared to glycerol at pH 5.7, respectively. These findings are fully consistent with our growth studies and reinforce the proposal that acidic pH and pyruvate promote metabolism around the PEP-pyruvate-oxaloacetate node. The observation of *icl1* induction at acidic pH is also consistent with prior observations under different pH stress conditions (11,69). Icl also functions as a methylisocitrate lyase that is required for the methylcitrate cycle and Mtb growth on single carbon sources such as acetate and propionate (33). Therefore, it is interesting that the methyl citrate cycle is strongly repressed in a pH- and pyruvate specialized manner, with genes encoding methyl citrate synthase (*prpC*) and methylcitrate dehydratase (*prpD*) both being downregulated ~29 fold in pyruvate compared to glycerol at pH 5.7. This strong difference is the result of *prpCD* being induced by acidic pH in glycerol, but repressed in pyruvate (Figure 2.5D). The divergent regulation of the methyl citrate cycle further supports the pH-dependent modulation of central carbon metabolism and may have consequences for the metabolism of cholesterol during pathogenesis.

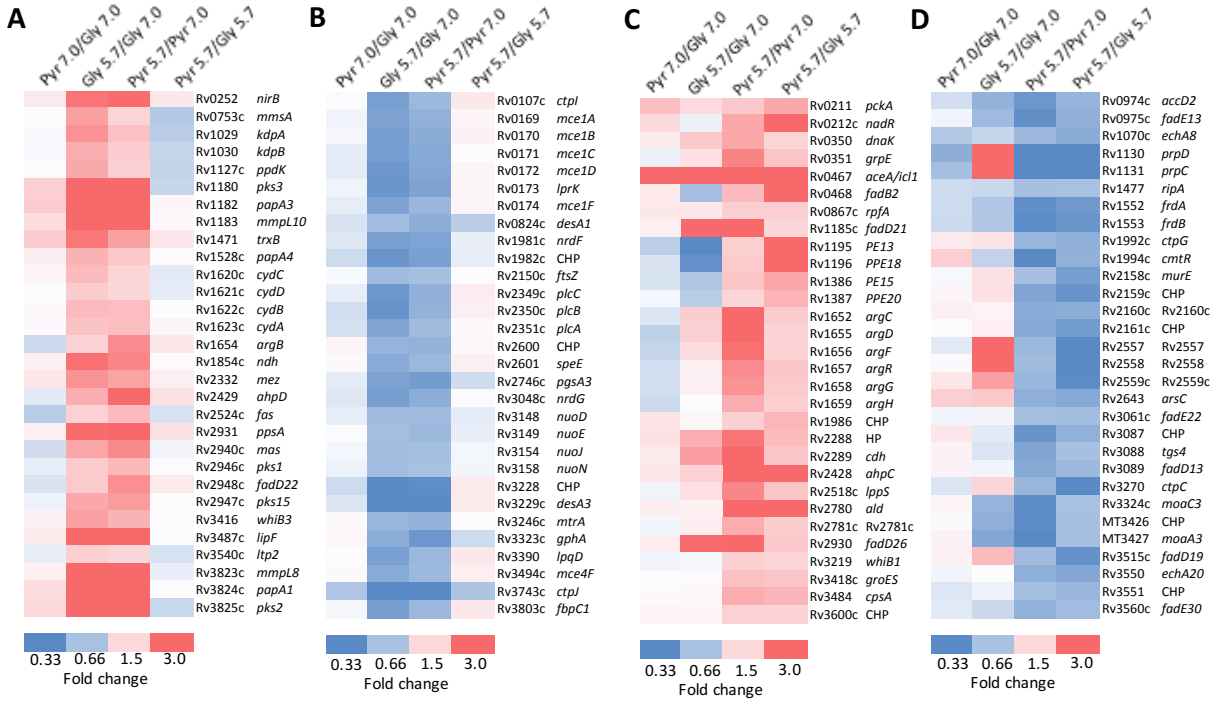

Figure 2.5. Genes that are induced or repressed by acidic pH in a carbon source independent and dependent manner. A. Selection of 30 genes (out of 185 total) that are induced by acidic pH in both glycerol and pyruvate without a significant difference in the induction. B. Selection of 30 genes (out of 134 total) that are repressed by acidic pH in both glycerol and pyruvate without difference in the induction. C. Selection of 30 genes (out of 60 total) that are induced at pH 5.7 in pyruvate and the induction is significantly greater in pyruvate as compared to glycerol. D. Selection of 30 genes (out of 75 total) that are repressed at pH 5.7 in pyruvate and the repression is significantly greater in pyruvate as compared to glycerol. CHP, conserved hypothetical protein; HP hypothetical protein.

Acidic pH remodels Mtb lipid and central carbon metabolism

The transcriptional profiling data identified widespread induction of genes associated with lipid metabolism. For example, in both glycerol and pyruvate at pH 5.7, the *mmpL8-pks2* operon (Rv3823c-Rv3825c) is strongly induced (Figure 2.5A). This operon has been shown to control the synthesis of sulfolipid (85) in a *phoPR*-dependent manner (64,67). Therefore, it is predicted that sulfolipid should accumulate at acidic pH. To test this prediction, Mtb was grown in minimal medium amended with 10 mM pyruvate buffered at pH 7.0 and pH 5.7. The culture was incubated for 3 days, to enable the cultures to become pH-adapted, and the lipids were then radiolabeled with a trace amount of ^{14}C acetate. As predicted, in wild type Mtb, sulfolipids were induced ~ 3 fold at pH 5.7 as compared to pH 7.0 (Figure 2.6A, Appendix Figure 9AC). The Δ*phoPR* mutant did not accumulate sulfolipids and this phenotype was complemented (Figure 2.6A, Appendix Figure 9C). Therefore, acidic pH remodels lipid metabolism by stimulating PhoPR and promoting the accumulation of sulfolipid.

One proposed role for the synthesis of *phoPR*-dependent lipids is to consume reductants and relieve reductive stress (68,81). This model is supported by our roGFP studies (Figure 2.4B), where the *phoP::*Tn mutant has a more reduced cytoplasm. Based on the reductive stress model, it is predicted that the Δ*phoPR* mutant may accumulate other long chain fatty acids to compensate for the loss of *phoPR*-dependent lipids. Indeed, enhanced PDIM accumulation has previously been observed in the *phoP::*Tn mutant (17) and, conversely, a loss of PDIM causes an accumulation of sulfolipid (86). When grown on pyruvate, relatively low levels of radiolabelled PDIM are observed in all of the tested strains or conditions (Appendix Figure 9B); however, TAG accumulation is induced ~3 fold in WT Mtb at pH 5.7 and ~6 fold in the *phoPR* mutant (Figure 2.6B, Appendix Figure 9C). Therefore, Mtb accumulates both TAG and sulfolipid at acidic pH, and in the absence of *phoPR* and sulfolipid, compensates by increasing the accumulation of TAG.

Our data support the notion that environmental pH acts as a checkpoint on Mtb metabolism and that acidic pH restricts some metabolic pathways while making new pathways available to the bacterium. Indeed, the *phoPR* mutant exhibits restricted growth on pyruvate at pH 7.0 and substantially enhanced growth at pH 5.7 (Figure 2.3), strongly supporting that acidic pH makes new metabolic avenues available to the pathogen. We hypothesized that the glyoxylate shunt or methylcitrate cycle may be promoted at acidic pH, based on the strong induction of *icl1* at acidic pH (Figure 2.5C) and the requirement of carbon sources that fuel the anaplerotic node for growth at acidic pH (Figure 2.1A). To test this hypothesis, the effect of the isocitrate lyase inhibitor 3-nitropropionic acid (3-NP, (87)) was tested on Mtb grown on pyruvate at pH 7.0 and 5.7. In wild type Mtb, a significant ~30% reduction of growth was observed at acidic pH in the presence of 3-NP (Figure 2.6C, Appendix Figure 10). No change in growth was observed at neutral pH, suggesting that *icl* is required in a pH-dependent manner. In the Δ*phoPR* mutant, we observed a similar 40% decrease in growth caused by the addition of 3-NP. Notably, almost all of the enhanced growth observed in the Δ*phoPR* mutant at acidic pH is inhibited by 3-NP (Figure 2.6C). Therefore, acidic pH, in a *phoP*-independent manner, promotes metabolism through a 3-NP sensitive pathway, such as the glyoxylate shunt or methylcitrate cycle.

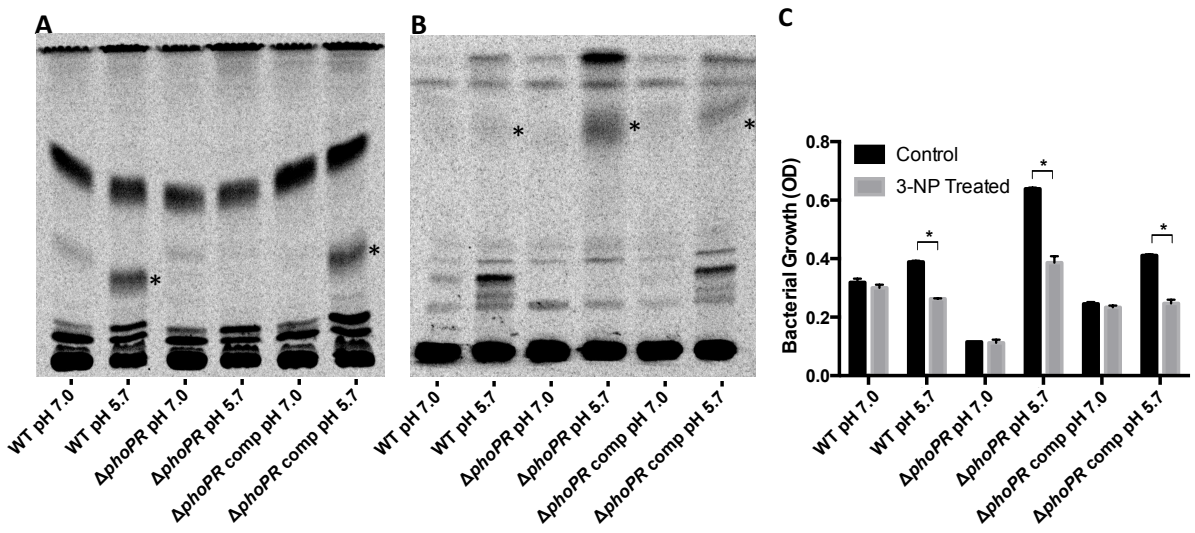

Figure 2.6. Acidic pH modulates accumulation of mycobacterial lipids and sensitivity to 3-NP. A. Accumulation of sulfolipid at acidic pH. For each strain, 20000 CPM of ^{14}C labeled lipids was spotted at the origin and the TLC was developed three times in chloroform:methanol:water (90:10:1 v/v/v). Sulfolipid is highlighted with the asterisk and accumulates in a pH- and *phoPR*-dependent manner. B. Accumulation of TAG in the *phoPR* mutant at acidic pH. For each strain, 20000 CPM of ^{14}C labeled lipids was spotted at the origin and the TLC was developed in hexane:diethyl ether:acetic acid (80:20:1 v/v/v). TAG is highlighted with the asterisk and accumulates in a pH- and *phoPR*-dependent manner. The data are representative of two independent biological replicates. C. 3-NP inhibits Mtb growth at acidic pH. The data presented are the end-point of culture growth following 9 days of incubation at acidic or neutral pH in the presence or absence of 0.1 mM 3-NP. Data showing the entire time-course are presented in Appendix Figure 10. Error bars represent the standard deviation and the data are representative of two biological replicates. *$p<0.005$ using a student's t-test.

Discussion

We have shown that acidic pH alone does not slow Mtb growth. When supplied an appropriate carbon source, such as pyruvate, or in the absence of *phoPR*, Mtb grows about as well, or better, at acidic pH as compared to neutral pH. This observation reveals that slow growth at acidic pH is regulated by available carbon sources and signal transduction-dependent transcriptional remodeling (Figure 2.7). Additional studies examining the mechanisms of slowed growth at acidic pH demonstrate that Mtb exhibits a reduced cytoplasm, promotes the synthesis of sulfolipid, and induces expression of genes associated with anaplerotic metabolism. Together, these findings support the proposal that Mtb can link pH and available carbon sources as environmental cues to regulate its growth and metabolism. During infection, this physiological adaptation may enable Mtb to survive in microenvironments that are otherwise inhospitable for microbial colonization.

We have identified two distinct branches of pH-driven adaptation: a *phoPR*-dependent branch and *phoPR*-independent branch (Figure 2.7). The *phoPR*-dependent branch plays a role in maintaining redox homeostasis and slowing growth. In glycerol, acidic pH causes a reduced cytoplasmic potential that is associated with slowed growth and induction of the *phoPR* regulon. Notably, the Δ*phoPR* mutant grows poorly at pH 7.0 on glycerol or pyruvate, carbon sources that are permissive for growth of WT Mtb at neutral pH (Figure 2.3). This growth arrest is associated with a reduction of the cytoplasmic potential (Figure 2.4B), demonstrating that *phoPR* is required for redox homeostasis and growth on glycerol or pyruvate. A possible mechanism for *phoPR*-dependent maintenance of redox homeostasis is the production of methyl-branched lipids such as sulfolipid. Anabolism of these lipids would oxidize NADPH as well as reduce flux through the TCA cycle, thus decreasing the production of NADH. Consistent with this model, we observe that sulfolipid accumulates in a pH- and *phoPR*-dependent manner (Figure 2.6A). In the absence of *phoPR*, Mtb accumulates TAG, possibly to compensate for a loss of *phoPR*-dependent lipid anabolism (Figure 2.6B). Similarly, Singh and colleagues (68)

have also observed that a *whiB3* mutant, that is defective in synthesis of sulfolipid, experiences reductive stress and enhanced TAG accumulation. Thus, we propose that *phoPR* may cause slow growth at acidic pH by syphoning carbon towards lipid anabolism as part of its function to maintain redox homeostasis.

The response of the Δ*phoPR* mutant to acidic pH also supports a role for *phoPR*-independent mechanisms of pH-driven adaptation. The dramatic shifts in growth phenotypes of the Δ*phoPR* mutant in pyruvate at pH 5.7 (enhanced growth) as compared to pH 7.0 (restricted growth) support the idea that *phoPR*-independent remodeling of metabolism promotes growth at acidic pH on select carbon sources. This hypothesis is supported by the observations that at acidic pH: i) addition of 3-NP, an inhibitor of isocitrate lyase, decreases the enhanced growth observed in the Δ*phoPR* mutant (Figure 2.6C), ii) *icl1* and *pckA* expression is induced (Figure 2.5C), and iii) Mtb favors carbon sources feeding the anaplerotic node (Figure 2.1A). The inhibitory effect of 3-NP on the enhanced growth and induction of *icl1* expression supports that the glyoxylate shunt or methylcitrate cycle may be one of the induced metabolic pathways that become available to Mtb at acidic pH. Eoh and Rhee (33) have shown that, when Mtb is grown on glucose or propionate, disruption of *icl* causes decreased cytoplasmic pH, imbalanced NAD^+/NADH ratios and an altered membrane potential. Therefore, induction of *icl* at acidic pH may function to promote metabolism that maintains pH- and redox-homeostasis.

The presented growth, genetic and lipid metabolism studies support a model whereby carbon metabolism is remodeled by acidic pH. Transcriptional profiling experiments reveal that several key genes of central metabolism are induced by acidic pH. Most notably, *pckA* and *icl1* are strongly induced by both acidic pH and pyruvate. Muñoz-Elías and McKinney have suggested that *pckA* and *icl1,* which are both essential for growth in animals (20,25,26), may be required for virulence to promote metabolism via the PEP-glyoxylate cycle (88). The PEP-glyoxylate cycle has been observed in *E. coli* during slow growth on glucose limiting medium and enables the full oxidation of carbon sources that fuel the anaplerotic node (41), such as

pyruvate or acetyl-CoA. During Mtb infection, these carbon sources are physiologically relevant as they are the products of cholesterol or fatty acid catabolism. In this manner, the PEP-glyoxylate cycle may promote efficient energy producing catabolism, while keeping PEP, pyruvate, oxaloacetate and acetyl-CoA abundant and available for anabolism. Studies from others provide support for this model. For example, Beste and colleagues have shown using ^{13}C-metabolic flux analysis that during slow growth in a chemostat or growth in macrophages Mtb exhibits anaplerotic carbon flux through *pckA*- and *icl1*-dependent pathways (40,63). Additionally, both *pckA* and *icl1* are upregulated during two weeks of growth in macrophages (44) and 50 days of growth in mice (89,90), demonstrating this physiology is relevant in the context of pathogenesis and may be driven by the combined influence of environmental pH and available carbon sources in animals. Together, these data support a model where acidic pH: 1) induces *phoP*-dependent lipid anabolism to oxidize redox cofactors and slow growth by diverting carbon from central metabolism, and 2) drives Mtb physiology to adopt the PEP-glyoxylate cycle, to balance energy production and carbon utilization (Appendix Figure 8).

Redox homeostasis was found to play an important role in pH-driven adaptation. The reduced cytoplasmic potential observed at acidic pH (Figure 2.4) may be the result of decreased oxidative phosphorylation where acidic pH restricts the efficiency of proton-pumping enzymes in the electron transport chain. In this manner, growth at acidic pH has parallels with hypoxia-driven adaptation, where oxidative phosphorylation is limited due to decreased oxygen as a terminal electron acceptor (91). However, we observed limited pH-dependent changes in the concentration of NAD^+ or $NADP^+$ (Appendix Figure 5), demonstrating that Mtb has physiological mechanisms to regenerate oxidized co-factors. Transcriptional profiling experiments provide insights into potential mechanisms of pH-dependent redox homeostasis. Acidic pH, independent of carbon source, causes the induction of the *phoPR* regulon, fatty acid synthase (*fas),* PDIM, and *whiB3* genes that would promote lipid anabolism and oxidize NADPH (36,68). Several additional genes induced at acidic pH are predicted to be associated with replenishing

oxidized cofactors (Appendix Figure 8), including *ahpCD* (92), NADH dehydrogenase (*ndh,* (93)*)*, and thioredoxin reductase (*trxB,* (94)). Another mechanism of redox homeostasis is the use of thiols, including mycothiol (95), as reductive sinks. roGFP measures redox potential via a thiol-based mechanism providing direct evidence for increased thiol reduction at acidic pH or in the *phoP* mutant (Figure 2.4). The mycothiol redox couple oxidizes NADPH and therefore, in combination with mechanisms considered above, may be an important redox buffer at acidic pH. These findings suggest that promoting lipid anabolism and redox cofactor oxidation at acidic pH may be important transcriptional adaptations.

Carbon source specific growth arrest in response to acidic pH appears to be a pathogenesis associated and evolved trait in Mtb, as the non-pathogen *M. smegmatis* does not share this physiology (Appendix Figure 4). It is possible that, as part of pathogenesis, Mtb is integrating signals from environmental pH and available carbon sources to adapt to specific host microenvironments. Therefore, acidic pH may restrict Mtb from metabolizing specific carbon sources *in vivo*, and require carbon sources feeding the anaplerotic node, such as cholesterol, as a checkpoint for growth and pathogenesis. *phoP, pckA* and *icl1* are required for virulence in animals (12,20,25,26), suggesting that this pH-driven response is important during pathogenesis. *phoP* mutants are attenuated for virulence and one demonstrated mechanism for this attenuation is decreased ESAT-6 secretion (96). Notably, in primary human macrophages, deletion of genes required to synthesize *phoPR*-regulated lipids such as sulfolipid, diacyl- and polyacyltreholose (*e.g. pks2, pks3* and *pks4)*, results in a macrophage growth defect in the absence of PDIM (97), suggesting that PDIM synthesis may compensate as a reductive sink during macrophage infection and that *phoPR*-regulated, pH-inducible lipids such as sulfolipid play a role in pathogenesis. It is possible that the inability of the *phoP* mutant to modulate redox homeostasis or metabolically constrain Mtb growth in response to acidic pH may also account, in part, for the attenuation of the *phoP* mutant observed in macrophages and animals (12).

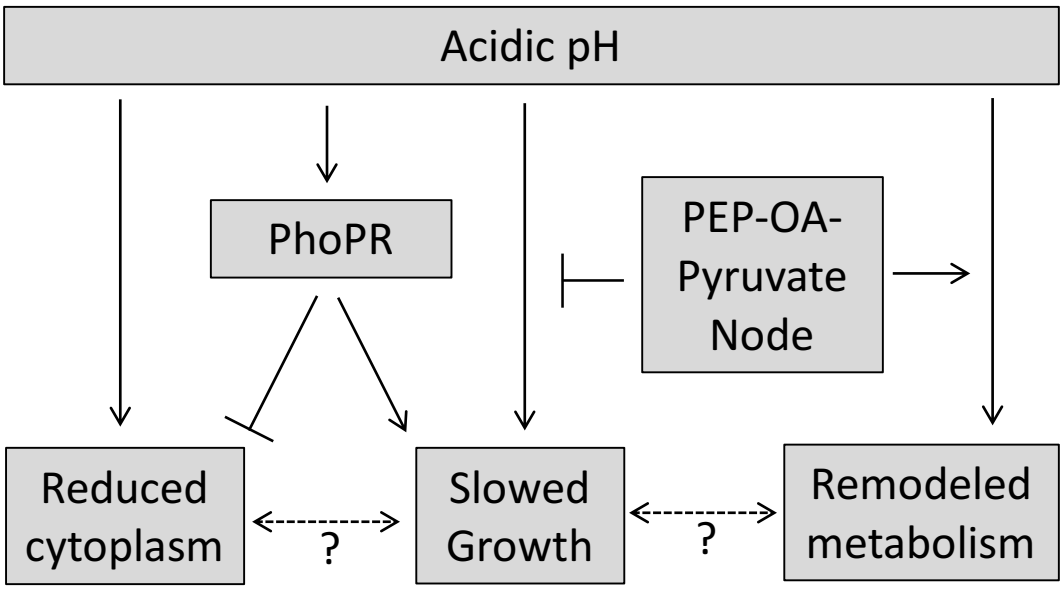

Figure 2.7. Schematic diagram summarizing the role of acidic pH in regulating growth and redox homeostasis. Acidic pH drives a reduction of the cytoplasmic potential and a slowing of Mtb growth. PhoPR functions to mitigate reductive stress and slow Mtb growth. This is possibly achieved by syphoning carbon away from the TCA cycle to promote oxidation of NADPH through lipid anabolism, such as acid inducible sulfolipid accumulation (Figure 2.6A). Addition of PEP-oxaloacetate-pyruvate node metabolites may promote growth by fueling the TCA cycle and remodeling central metabolism, including the induction of *pckA* and *icl1*.

Experimental Procedures

Bacterial strains and growth conditions.

All Mtb experiments, unless otherwise stated, were performed with Mtb strain CDC1551. The *phoP*::Tn and *ΔphoPR* mutants have been previously described (17,80). Cultures were maintained in 7H9 Middlebrook medium supplemented with 10% OADC and 0.05% Tween-80. All single carbon source experiments were performed in a defined minimal medium as described by Lee *et al.* (36): 1 g/L KH_2PO_4, 2.5 g/L Na_2PO_4, 0.5 g/L $(NH_4)_2SO_4$, 0.15 g/L asparagine, 10 mg/L $MgSO_4$, 50 mg/mL ferric ammonium citrate, 0.1 mg/L $ZnSO_4$, 0.5 mg $CaCl_2$, and 0.05% Tyloxapol. Medium was buffered using 100 mM MOPS (pH 6.6-7.0) or MES (pH 5.7-6.5) (18). Following 9 days of Mtb growth, the pH of the medium was tested and there were no significant changes to the pH, demonstrating the strong buffering is sufficient to counteract Mtb modulation of media pH. For 9-day growth experiments, Mtb was seeded in T-25 standing tissue culture flasks in 8 mL of minimal medium at an initial density of 0.05 OD_{600} and incubated at 37 ^{o}C and 500 µL samples were removed every 3 days for optical density measurements. The 36-day growth experiments were performed as described for the 9 days experiments, except that 250 µL of culture was removed for optical density measurements at each timepoint. Over the 36-day time course, pH was measured at each time point using pH strips sensitive to 0.3 pH units and no changes were observed. At the final day, the pH of the supernatants was measured using a pH meter, and only minimal (<0.2 units) changes in pH were observed (Appendix Figure 3B). 3-nitropropionic acid (3-NP) was used at 0.1 mM. Growth of *M. smegmatis* mc2155 was performed as described for Mtb.

Cytoplasmic pH measurement

Cytoplasmic pH was measured using the pH sensitive dye 5-chloromethylfluorescein diacetate (CMFDA) as described previously by Purdy *et al.* (79). Briefly, Mtb was inoculated into its

respective conditions at an original OD_{600} of 0.05. After three days, samples were collected, pelleted, and resuspended in 500 µl of the same minimal medium. 4 µl of 1 µg/mL CMFDA dye was added to each sample and incubated at 37°C for 2 hours. Samples were then washed twice, resuspended at OD_{600} 1.2 in the same medium, and transferred to a 96 well microplate. A standard curve was prepared using Mtb in buffered minimal medium treated with 10 µM nigericin. Fluorescent emission was measured at 520 nm after excitation at 450 nm and 490 nm.

Measuring intracellular redox poise.

The plasmid pVV-16 was modified to constitutively express a redox sensitive GFP roGFP-R12 (83). This construct was transformed into the CDC1551 background. Mtb was cultured in the indicated medium containing 10 mM of the carbon source at a starting OD_{600} of 0.3. For each experimental condition, CDC1551 containing an empty vector was also cultured to use as a control for background signal subtraction. On day 3, 200 µl of each treatment was transferred in triplicate to a 96 well microplate and fluorescence emission was read at 510 nm after excitation at 400 nm and 480 nm, measuring the relative abundance of the oxidized and reduced roGFP species, respectively.

RNA-seq transcriptional profiling and data analysis

Mtb cultures were grown at 37 ^{o}C in T-75 vented, standing tissue culture flasks in 40 ml of a defined minimal medium seeded an initial OD_{600} of 0.1. Four conditions were examined with two biological replicates: 1) 10 mM glycerol, pH 7.0, 2) 10 mM glycerol pH 5.7, 3) 10 mM pyruvate pH 7.0 and 4) 10 mM pyruvate pH 5.7. Following 3 days incubation, total bacterial RNA was stabilized and extracted as previously described (11). RNA quality and integrity were examined using an Agilent Bioanalyzer prior to subjecting samples to rRNA depletion using the Epicentre Ribo-Zero depletion kit. cDNA libraries were constructed using the Illumina TruSeq RNA library

preparation kit (v2), omitting the polyA selection step. After library quality control, sample libraries were pooled and sequenced in one lane of an Illumina HiSeq 2500 Rapid Run flow cell (v1) in 50 bp, single-end read format (SE50). After the sequencing run, reads were de-multiplexed and converted to FASTQ format using the Illumina bcl2fastq (v1.8.4) script. The reads in the raw data files were then subjected to trimming of low quality bases and removal of adapter sequences using Trimmomatic (v0.30) (98) with a 4 bp sliding window, cutting when the read quality dropped below 15 or read length was less than 36 bp. Trimmed reads were aligned to the Mtb CDC1551 genome (NCBI accession AE000516) using Bowtie (99) with the -S option to produce SAM files as output. SAM files produced by Bowtie were converted to BAM files and coverage depth was calculated using SAMtools (100) resulting in >98% coverage across the genome with an average of 172x coverage (ranging between 110x-211x depending on the sample). Aligned reads were then counted per gene feature in the Mtb CDC1551 genome using the HTSeq software suite. Data were normalized by estimating effective library sizes using robust regression within the DESeq package (101). Statistical analysis and differential gene expression was performed in RStudio (V0.97.551) by fitting a negative binomial model to each set of conditions and testing for differences utilizing the DESeq package. The Magnitude-Amplitude (MA) plots were generated by modifying a function in DESeq and plotting the average expression of differentially expressed genes from each set of conditions tested against the expression ratio. For each comparison (Appendix Figure 6A-D), differentially expressed genes were identified as genes with an average normalized count >100, differential gene expression >1.5 fold, and a p-value <0.05. Venn diagrams were generated using the Venny web tool (http://bioinfogp.cnb.csic.es/tools/venny/). Two biological replicates were performed for each sample and analysis using QualiMap (102) demonstrated excellent agreement between biological replicates with a Pearson's correlation coefficient of ~1. The transcriptional profiling data have been submitted to the NCBI GEO database (accession number: GSE52020). RNA-seq expression data for *pks2, icl1,* and *pckA* were confirmed using quantitative real-time PCR

and previously described methods (17). The acidic pH induction of *pks2* was confirmed to be carbon source independent, and acidic pH induction of *icl1* and *pckA* was confirmed to be enhanced in pyruvate (Appendix Figure 7C).

Analysis of mycobacterial lipids

For lipid analysis, bacterial cultures were grown as described above for the transcriptional profiling experiments. Two conditions were examined: 1) 10 mM pyruvate pH 7.0 and 2) 10 mM pyruvate pH 5.7. Following 3 days incubation, lipids were radiolabeled by adding 8 µCi of [1,2 ^{14}C] sodium acetate to each culture. The final concentration of acetate used for the labeling is 200 µM, a concentration 50-fold lower than the 10 mM pyruvate. Following 6 days of labeling, the bacteria were pelleted, washed in PBS and the lipids were extracted twice in 2:1 chloroform methanol and Folch washed. ^{14}C incorporation was determined by scintillation counting of the total extractable lipids. To analyze lipid species, 20 000 counts per minute (CPM) of the lipid sample was spotted at the origin of 100 cm^2 silica gel 60 aluminum sheets. To separate sulfolipid for quantification, the TLC was analyzed with the chloroform:methanol:water (90:10:1 v/v/v) solvent system (67). To separate TAG for quantification, the TLC was developed with hexane:diethyl ether:acetic acid (80:20:1, v/v/v) solvent system (17). To examine PDIM accumulation the TLC was developed in petroleum ether:acetone (98:2 v/v). Radiolabelled lipids were detected and quantified using a phosphor screen and a Storm Imager and ImageJ software (103). Radiolabelling experiments, lipid extractions and TLCs were repeated in two independent biological replicates with similar findings in both replicates.

Acknowledgements

We are grateful to the Remington laboratory for providing the roGFP gene, Christopher Colvin for technical assistance, the MSU RTSF for RNA-seq library preparation and sequencing, and Kathy Meek, Martha Mulks, Kyle Rohde and members of the Abramovitch lab for critical reading

of the manuscript. The High Performance Computing Cluster and iCER at Michigan State University provided computational support and resources. This research was supported by start-up funding from Michigan State University, AgBioResearch and a Career Development Grant from the Great Lakes Regional Center of Excellence (National Institute of Allergy and Infectious Disease Award U54 AI057153).

CHAPTER 3 - Anaplerotic remodeling of central carbon metabolism during acid adaptation in *Mycobacterium tuberculosis.*

Introduction

Survival of *Mycobacterium tuberculosis* (Mtb) during infection requires sensing and adapting to the diverse and adverse environments of the host. Growing evidence suggests that the mechanisms of Mtb adaptation during infection are unique from those required during *in vitro* culture. First, many genes dispensable for growth *in vitro* have been shown to be essential during infection (20,25). Similarly, past efforts that identified antimycobacterial drugs with potent *in vitro* activity have been unable to achieve *in vivo* efficacy possibly due to the distinct *in vivo* environment and the physiological state of Mtb in response to that environment (104). Thus, development of effective therapy for Mtb requires careful consideration of the environmental conditions encountered by Mtb during infection.

One of the earliest cues encountered during infection is the acidic pH of the macrophage phagosome. Mtb is capable of resisting acid stress, with Mtb maintaining viability in cultures as acidic as pH 4.5 (3,9). This ability to resist acid stress was shown to be impaired in a transposon mutant containing an insertion in Rv3671c (*marP*), encoding a membrane-associated protein (9). Notably, this mutant was severely attenuated during murine infection (9). Additionally, using a zebrafish-*Mycobacterium marinum* infection model, *marP* was shown to be specifically required to survive within the phagolysosome of the host (10), further supporting the hypothesis that the ability of Mtb to resist acid stress is required during infection. In addition to acid resistance, Mtb also responds transcriptionally to the low pH of the macrophage phagosome within 20 minutes after infection (11), and deletion of the acid-induced *phoPR* two component system leads to attenuation (13,64,71), emphasizing that how Mtb adapts to acidic pH is relevant to its pathogenesis.

We have previously identified that in response to acidic pH, Mtb exhibits carbon source specific growth arrest (15). Using minimal medium supplemented with single carbon sources, we observed that Mtb arrests growth at pH 5.7 when supplied most carbon sources. However, the carbon sources cholesterol, acetate, pyruvate, and oxaloacetate permit growth at pH 5.7. Cholesterol, predicted to be an important nutrient for Mtb during infection (30,31), generates acetyl-CoA, propionyl-CoA, and pyruvate during catabolisis (31), suggesting a link between cholesterol-related metabolism and growth at acidic pH.

The carbon sources that permit Mtb growth at acidic pH feed the anaplerotic node (62) of metabolism. The anaplerotic node is thought to be a key metabolic switch point in the regulation of anabolism, catabolism, and energy production (62), making proper function of this node important during metabolic adaptation. Transcriptional profiling of Mtb at acidic pH shows the induction of several genes involved in metabolism at the anaplerotic node, including those coding for phosphoenolpyruvate carboxykinase (*pckA*), isocitrate lyase (*icl1/2*), malic enzyme (*mez*), and pyruvate phosphate dikinase (*ppdk*) (15), suggesting that Mtb increases metabolism via the anaplerotic node at acidic pH. We hypothesize that proper function of the anaplerotic node is required for metabolic adaptation to acid pH. Consistent with this hypothesis, the isocitrate lyase inhibitor 3-NP reduces Mtb growth at acidic pH with pyruvate as the carbon source (15), suggesting that isocitrate lyase may be a component of anaplerotic adaptation at acidic pH.

In addition to inducing genes involved in the anaplerotic node, we also observed that Mtb induces a subset of genes specifically during acidic pH growth arrest (15). Notably, these genes were not induced at acidic pH when supplemented with the growth permissive carbon source pyruvate. Among these acidic pH growth arrest-induced genes were two genes involved in the methylcitrate cycle, encoding methylcitrate synthase and methylcitrate dehydratase (*prpC* and *prpD*, respectively). *prpCD* have been shown to be required for the metabolism of propionyl-CoA that is generated from the catabolism of cholesterol and odd and branched chain

fatty acids (105). Given the lack of an obvious propionyl-CoA source in the minimal medium conditions of acidic pH growth arrest, understanding the mechanisms of induction of *prpCD* at acidic pH could provide further insights into the metabolic state of Mtb at acidic pH.

Given that only carbon sources that feed the anaplerotic node can promote Mtb growth and that genes of the anaplerotic node were induced transcriptionally at acidic pH, in the current study we have investigated the role of the anaplerotic node in regulation of Mtb growth and metabolism at acidic pH. Additionally, I sought to further define mechanisms of *prpCD* regulation and their relevance to Mtb metabolism during acidic pH growth arrest. Through measurement of metabolites and lipid species, I have also sought to characterize the metabolic remodeling that occurs at acidic pH. Together, these approaches seek to identify and articulate the mechanisms of metabolic remodeling in response to the host-relevant cue of acidic pH.

Results

Role of anaplerotic metabolism in Mtb growth at acidic pH

Given the induction of genes of the anaplerotic node at acidic pH, as well as the ability of carbon sources of the anaplerotic node to promote growth at acidic pH, I hypothesized that genes regulating metabolism at the anaplerotic node play a role in Mtb growth regulation at acidic pH. To test this hypothesis, I examined the growth of two Mtb mutants with deletions of either *pckA* or *icl1/2*. Δ*pckA* and Δ*icl1/2* grew similarly to wild type (WT) Mtb in the rich medium 7H9+OADC buffered to pH 7.0 (Figure 3.1A-B). However, growth of both mutants was reduced compared to WT when the rich medium was buffered to pH 5.7, supporting the hypothesis that both *pckA* and *icl1/2* play a role in pH-dependent growth adaptations.

To better understand the underlying nature of the reduced growth observed at acidic pH, growth curves were also performed in defined minimal medium buffered at either pH 7.0 or pH 5.7. The Δ*pckA* mutant had reduced growth compared to WT Mtb on glycerol at pH 7.0 and maintained growth arrest at pH 5.7 (Figure 3.1). The mutant was also unable to grow on

pyruvate, acetate, or succinate at either neutral or acidic pH (Figure 3.1, 3.2A-C), with OD_{600} decreasing over the course of the experiment. This growth defect of the Δ*pckA* mutant on non-glycolytic carbon sources is consistent with what has been previously observed in unbuffered media in the H37Rv strain background, and has been linked to the inability of the mutant to achieve gluconeogenic carbon flux (20). To circumvent this limitation of the Δ*pckA* mutant, growth curves were repeated with the addition of glycerol to the culture media. Addition of glycerol was sufficient to restore growth of the Δ*pckA* mutant on pyruvate and acetate at both pH 7.0 and pH 5.7, (Figure 3.2D-E). Additionally, culture of the Δ*pckA* mutant in the presence of both glycerol and succinate restored the WT phenotype: growth at pH 7.0 and growth arrest at pH 5.7 (Figure 3.2F). These results suggest that, in addition to the growth defect previously observed in unbuffered medium (20), *pckA* is also required for growth on non-gluconeogenic carbon sources at acidic pH. When glycerol was supplemented to reverse this growth defect, no differences in growth between WT Mtb and the Δ*pckA* mutant were observed, suggesting that our ability to probe the role of *pckA* in pH-dependent growth adaptation through genetic deletion may be confounded by the general requirement of *pckA* for Mtb gluconeogenesis in minimal media.

Growth curves in minimal media were also performed with the Δ*icl1/2* mutant. The Δ*icl1/2* mutant exhibited slowed growth on pyruvate at both neutral and acidic pH compared to WT Mtb (Figures 3.1B, 3.3A-B); only increasing OD_{600} ~2-fold over the 12-day growth curve, suggesting that anaplerosis via isocitrate lyase is necessary for optimal growth in minimal medium on pyruvate. Growth of the Δ*icl1/2* mutant was absent with acetate as the single carbon source (Figure 3.3C), as has been observed previously given the requirement of isocitrate lyase for acetate assimilation (33). Unique to the Δ*pckA* mutant, supplementation of glycerol did not restore WT growth phenotypes in the Δ*icl1/2* mutant cultured in minimal medium with pyruvate or acetate (Figure 3.3D-E), suggesting that the slowed and absent growth observed in the Δ*icl1/2* mutant is not due to a deficiency in gluconeogenesis. Although reduced for growth with

glycerol as a single carbon source at pH 7.0, at pH 5.7 the Δ*icl1/2* mutant exhibited a ~2-fold increase in OD_{600} beginning after day 3 (Figures 3.1B), similar to the level of growth observed with pyruvate as a single carbon source. This small amount of growth in conditions typically restrictive for Mtb growth was significantly different from that observed for WT Mtb and was observed in four separate experiments, and we speculate that this small amount of growth may represent an inability of the Δ*icl1/2* mutant to maintain growth arrest at acidic pH. Together, these results indicate that isocitrate lyase is required for optimal growth in minimal medium on pyruvate, and at acidic pH achieves a comparable level of slow growth on both pyruvate and glycerol as single carbon sources.

Given the role of *icl1/2* in both the glyoxylate shunt and the methylcitrate cycle, we sought to clarify which of these activities was responsible for the growth phenotypes observed in minimal media. It has been shown previously that the supplementation of vitamin B12 allows for detoxification of propionyl-CoA via the methylmalonyl pathway (35), and that this supplementation is sufficient to restore growth defects caused by the toxic accumulation of methylcitrate cycle intermediates caused by a defective methylcitrate cycle (33,35). Growth of the Δ*icl1/2* mutant in minimal media containing glycerol or pyruvate was not changed with supplementation of vitamin B12 (Figure 3.4), suggesting that the observed growth phenotypes in the Δ*icl1/2* mutant are not due to methylcitrate toxicity and thus may be driven by a dependence of the glyoxylate shunt at acidic pH.

In summary, deletion of two enzymes of the anaplerotic node, *pckA* and *icl1/2*, revealed that proper function of the anaplerotic node is necessary for optimal growth of Mtb at acidic pH in rich medium. Furthermore, investigating the growth profiles of these mutants in minimal media has highlighted the importance of anaplerosis for growth in minimal media environments, as both mutants exhibited either slowed growth or growth defects at both neutral and acidic pH.

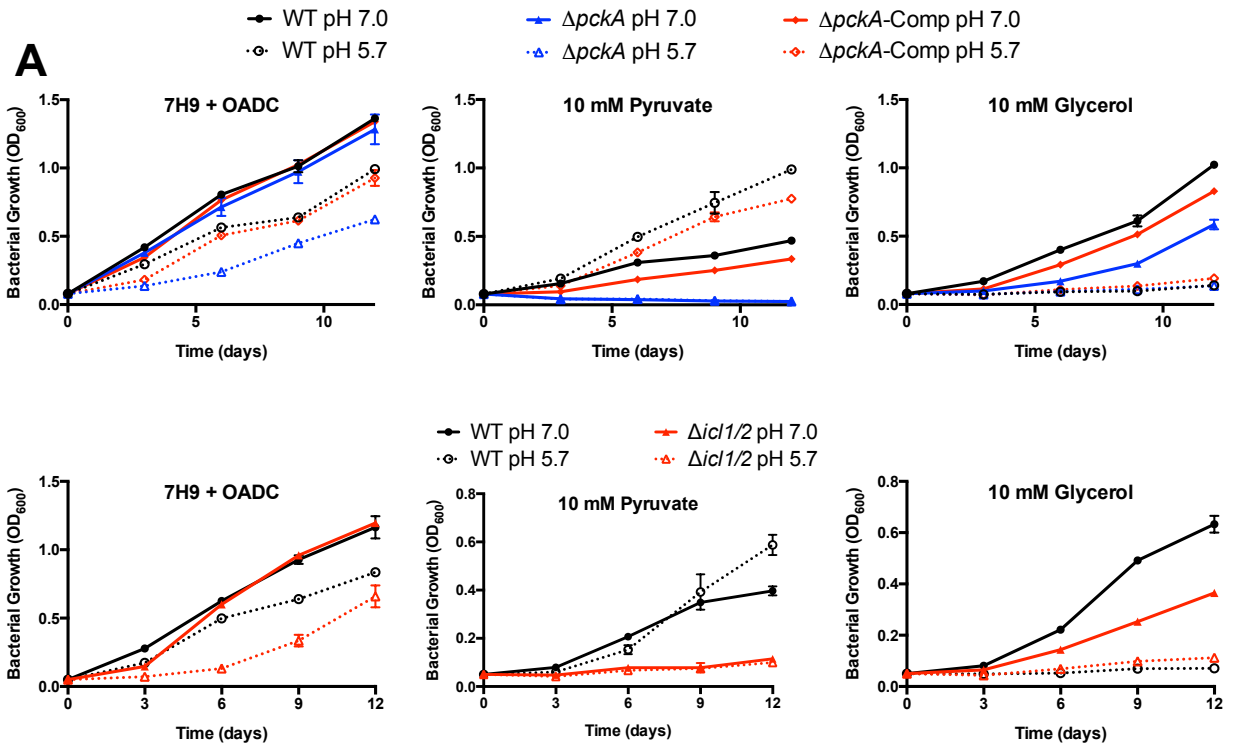

Figure 3.1. Δ*pckA* and Δ*icl1/2* mutants exhibit altered growth profiles at acidic pH and in minimal media.

A. Growth of CDC1551 WT, Δ*pckA*, and Δ*pckA* complemented (Δ*pckA*-Comp) strains in the rich medium 7H9 + OADC and in minimal medium containing either pyruvate or glycerol as a single carbon source, buffered to pH 7.0 or pH 5.7. The Δ*pckA* strain exhibits reduced growth at pH 5.7 in rich medium compared to the WT and complemented strains, and in minimal medium supplemented with pyruvate the OD of Δ*pckA* cultures decreases over time, consistent with bacterial lysis. Δ*pckA* growth on glycerol is reduced compared to the WT and complemented strains at pH 7.0, and is arrested for growth like the WT and complemented strains at pH 5.7.

B. Growth of Erdman WT and Δ*icl1/2* mutant strains in rich and minimal media buffered to pH 7.0 and pH 5.7. The Δ*icl1/2* strain exhibits reduced growth at pH 5.7 in rich medium compared to the WT. In minimal medium supplemented with pyruvate, growth is reduced at both pH 7.0 and pH 5.7 in the Δ*icl1/2* mutant.

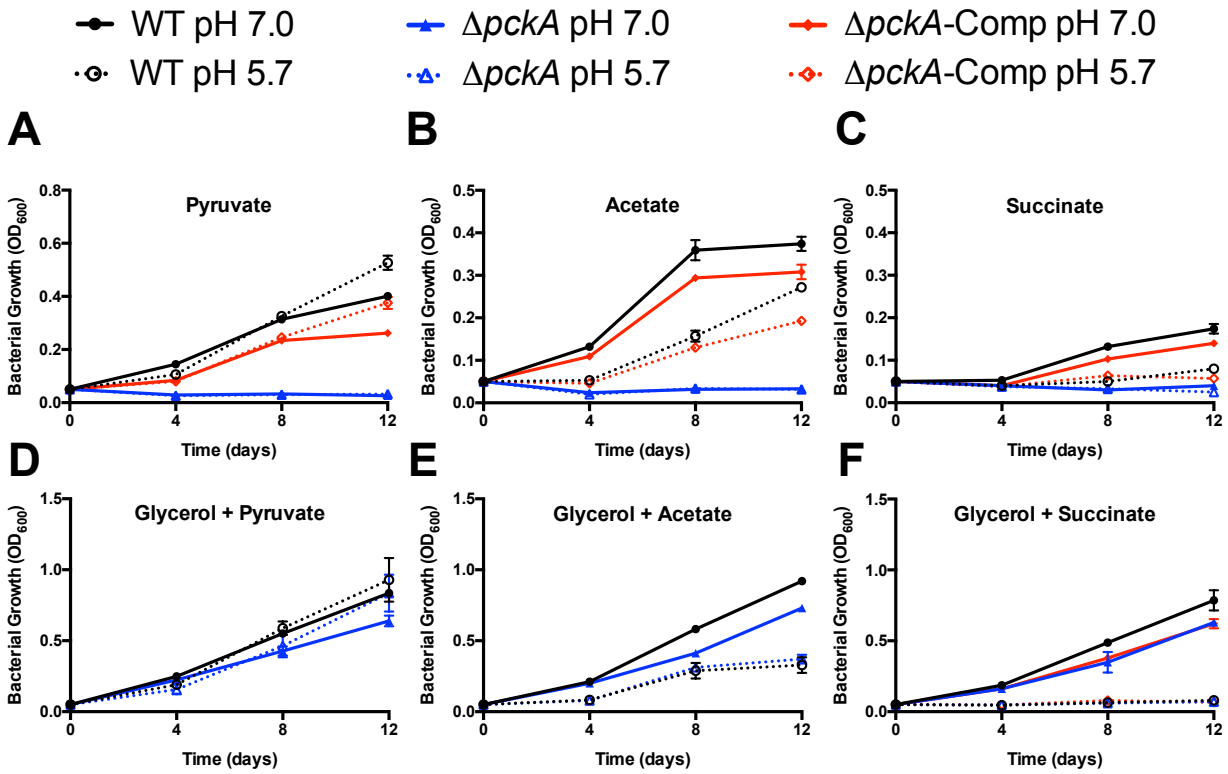

Figure 3.2. Wild type growth phenotypes are restored in the Δ*pckA* mutant with addition of glycerol. Growth of WT, Δ*pckA* mutant, and complemented strain *(*Δ*pckA*-Comp) was measured over time in minimal media supplemented with the indicated carbon sources. A-D) Δ*pckA* maintains growth arrest on glycerol at pH 5.7, but is deficient for growth on pyruvate, acetate, and succinate as indicated by a decrease in OD_{600} over time. E-G) Addition of glycerol as a second carbon source restores WT levels of growth in the Δ*pckA* mutant on acetate, pyruvate, and succinate.

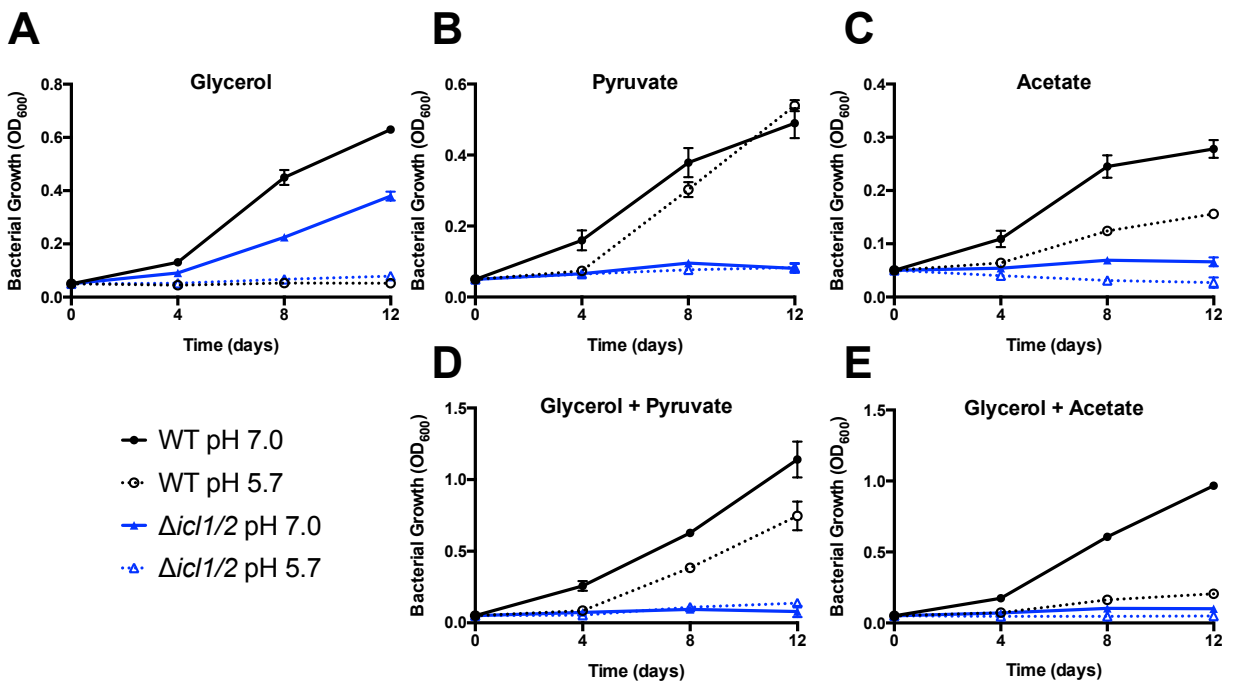

Figure 3.3. Growth defects of Δ*icl1/2* mutant are not restored with the addition of glycerol as a second carbon source. Growth of WT and Δ*icl1/2* mutant was measured over time in minimal media supplemented with the indicated carbon sources. A-B) Δ*icl1/2* achieves mild bacterial growth on both glycerol at pH 5.7 and pyruvate at pH 7.0 and pH 5.7. This low-level bacterial growth is increased compared to WT at pH 5.7 on glycerol and reduced compared to WT on pyruvate. C) The Δ*icl1/2* mutant is unable to grow with acetate as single carbon source. D-E) Addition of glycerol as a second carbon source does not restore growth of the Δ*icl1/2* mutant.

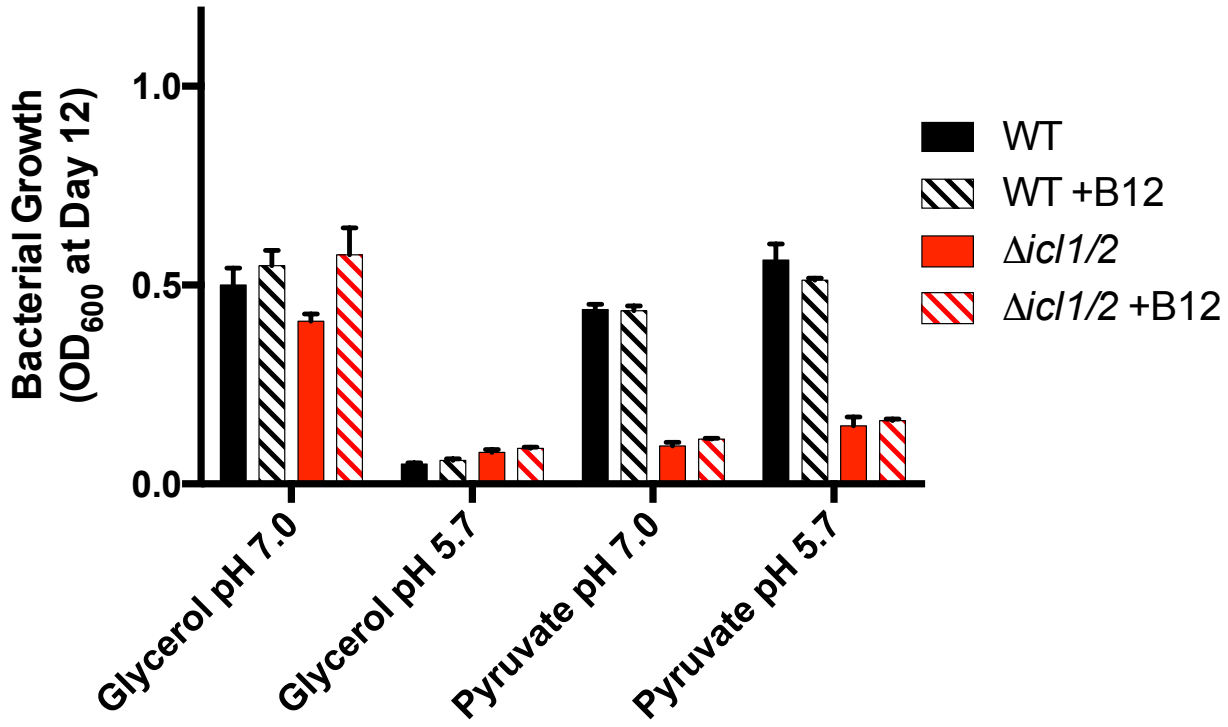

Figure 3.4. Growth of Δ*icl1/2* mutant at acidic pH is not affected by addition of vitamin B12. Summary data showing the OD_{600} measured on day 12 of growth curves performed in minimal media containing either glycerol or pyruvate as single carbon sources, buffered to pH 7.0 or pH 5.7, and with or without supplementation of vitamin B12. No difference in Mtb growth was observed with supplementation of vitamin B12.

Transcriptional induction of propionate metabolism during acidic pH growth arrest

Even though the absence of a vitamin B12 effect on growth suggests that *icl1/2* regulation of Mtb growth does not depend on the methylcitrate cycle, two of the genes induced specifically during acidic pH growth arrest were *prpC* and *prpD*, encoding the enzymes for the first two steps in the methylcitrate cycle. (15). *prpCD* have been characterized for their role in the detoxification of propionyl-CoA intermediates generated from the catabolism of cholesterol as well as branched- and odd-chain fatty acids (26,33-35). However, Mtb cultured at acidic pH in a defined minimal medium does not have an exogenous source of propionyl-CoA or these branched chain precursors. Induction of *prpCD* at acidic pH with glycerol as a single carbon source was verified by quantitative PCR (Figure 3.5A). I hypothesized that the observed *prpCD* induction is the result of increased endogenous production of propionyl-CoA during acidic pH growth arrest. Previous work has shown that supplementation of vitamin B12 is able to relieve the requirement for *prpCD*-mediated propionyl-CoA metabolism by opening the alternative methylmalonyl pathway (35). The supplementation of vitamin B12 reduced *prpCD* expression at both pH 7.0 and pH 5.7 (Figure 3.5B). Similarly, in the ∆*icl1/2* mutant that lacks methylisocitrate lyase activity, *prpCD* expression was increased ~2-fold at pH 5.7 compared to WT Mtb. Together, these results support the proposal that *prpCD* induction at acidic pH is linked to propionyl-CoA metabolism.

Because *prpCD* expression at acidic pH responds to changes in propionyl-CoA metabolism, I sought to identify the source of propionyl-CoA that could lead to *prpCD* induction. The rich medium 7H9+OADC may contain some propionyl-CoA sources from the supplemented albumin, so I first tested whether there was carryover of these carbon sources into the minimal medium culture. After washing Mtb cultures 3 times in minimal medium, *prpCD* was still induced at pH 5.7. Furthermore, Mtb grown from a frozen stock exclusively in minimal medium containing glycerol as a single carbon source still induced *prpCD* at pH 5.7. Together, these results suggest that the induction of *prpCD* is not due to an exogenous propionyl-CoA source.

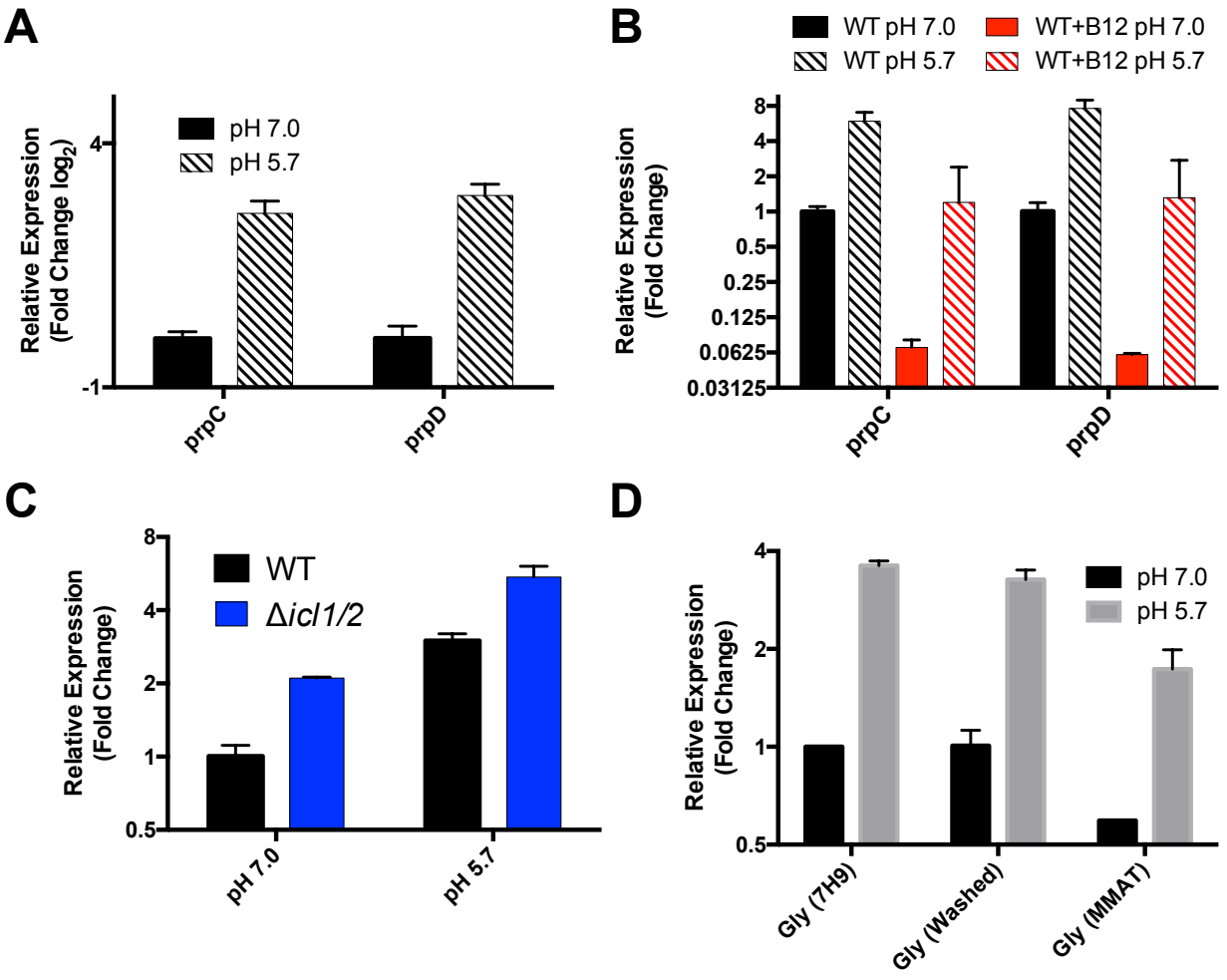

Figure 3.5. *prpCD* is induced at acidic pH and responds to alterations in propionyl-CoA metabolism. A) Quantitative real time PCR (qPCR) of *prpC* and *prpD* mRNA at pH 7.0 and pH 5.7 with glycerol as a single carbon source confirms that *prpCD* are induced during acidic pH growth arrest. B) *prpCD* expression at pH 7.0 and pH 5.7 is reduced with addition of vitamin B12. C) *prpC* expression at pH 7.0 and pH 5.7 is increased in the Δ*icl/12* mutant. D) *prpC* induction at pH 5.7 in minimal medium with glycerol as a single carbon is observed in Mtb that was maintained prior to the experiment in 7H9+OADC rich medium-(Gly [7H9]), in 7H9+OADC and washed 3 times in PBS + 0.05% Tween 80 (Gly [Washed]), and in Mtb cultured in minimal medium with glycerol as a single carbon source buffered to pH 7.0 (Gly [MMAT]).

Mtb cell envelope remodeling under acidic pH growth arrest modulates prpCD induction.

Given the absence of an exogenous propionyl-CoA source, I hypothesized that one source of propionate during pH 5.7 growth arrest could be the breakdown of Mtb cell envelope or storage lipids. To test this hypothesis, Mtb was cultured in the presence of ^{14}C-propionate or ^{14}C-acetate for 3 weeks in order to radiolabel Mtb lipids. This radiolabeled Mtb was then inoculated into minimal medium at pH 5.7 containing glycerol as a single carbon source and the relative abundance of lipid species was measured over time during pH 5.7 growth arrest. The total radioactivity of the samples decreased by less than 10% through the 12-day time course (Figure 3.6A); however, over the same time period the relative abundance of radiolabeled triacylglycerol (TAG) decreased to one-fourth of the initial concentration while the relative abundance of both trehalose dimycolate (TDM) and sulfolipid (SL) increased ~4-fold (Figure 3.6B-H). This result suggests that during pH 5.7 growth arrest, Mtb utilizes endogenous TAG to remodel its cell wall through the increased synthesis of both TDM and SL.

To test the hypothesis that lipid remodeling is a source of endogenous propionyl-CoA during pH 5.7 growth arrest, I sought to disrupt the ability of Mtb to remodel TAG to SL and TDM. The addition of the lipase inhibitor tetrahydrolipstatin (THL) to Mtb cultures blocked the remodeling of Mtb TAG to SL and TDM (Figure 3.7A-C). Interestingly, despite blocking lipid remodeling, treatment with THL increased *prpCD* expression during pH 5.7 growth arrest 3-fold compared to DMSO treated Mtb (Figure 3.7D). This result suggests that lipid remodeling of TAG to SL and TDM is not a source of *prpCD* induction at acidic pH; instead, the increase in *prpCD* induction with addition of THL suggests that lipid remodeling at acidic pH may act as a mechanism to relieve propionyl-CoA stress.

Given that endogenous lipid remodeling does not appear to be the source of *prpCD* induction at acidic pH, I sought to better understand the conditions leading to *prpCD* induction. Interestingly, although Mtb arrests growth at pH 5.7 with lactate as a single carbon source, induction of *prpCD* is not observed in Mtb cultured with lactate as a single carbon source

(Figure 3.7E). Furthermore, addition of glycerol as a second carbon source restores *prpCD* induction at pH 5.7 (Figure 5E). This observation suggests that *prpCD* induction during pH 5.7 growth arrest is glycerol-dependent rather than growth arrest dependent. The observation that *prpCD* induction at pH 5.7 does not appear to be a required for Mtb growth arrest is consistent with the previous finding that role of *icl1/2* in growth regulation appears to be independent of the methylcitrate cycle.

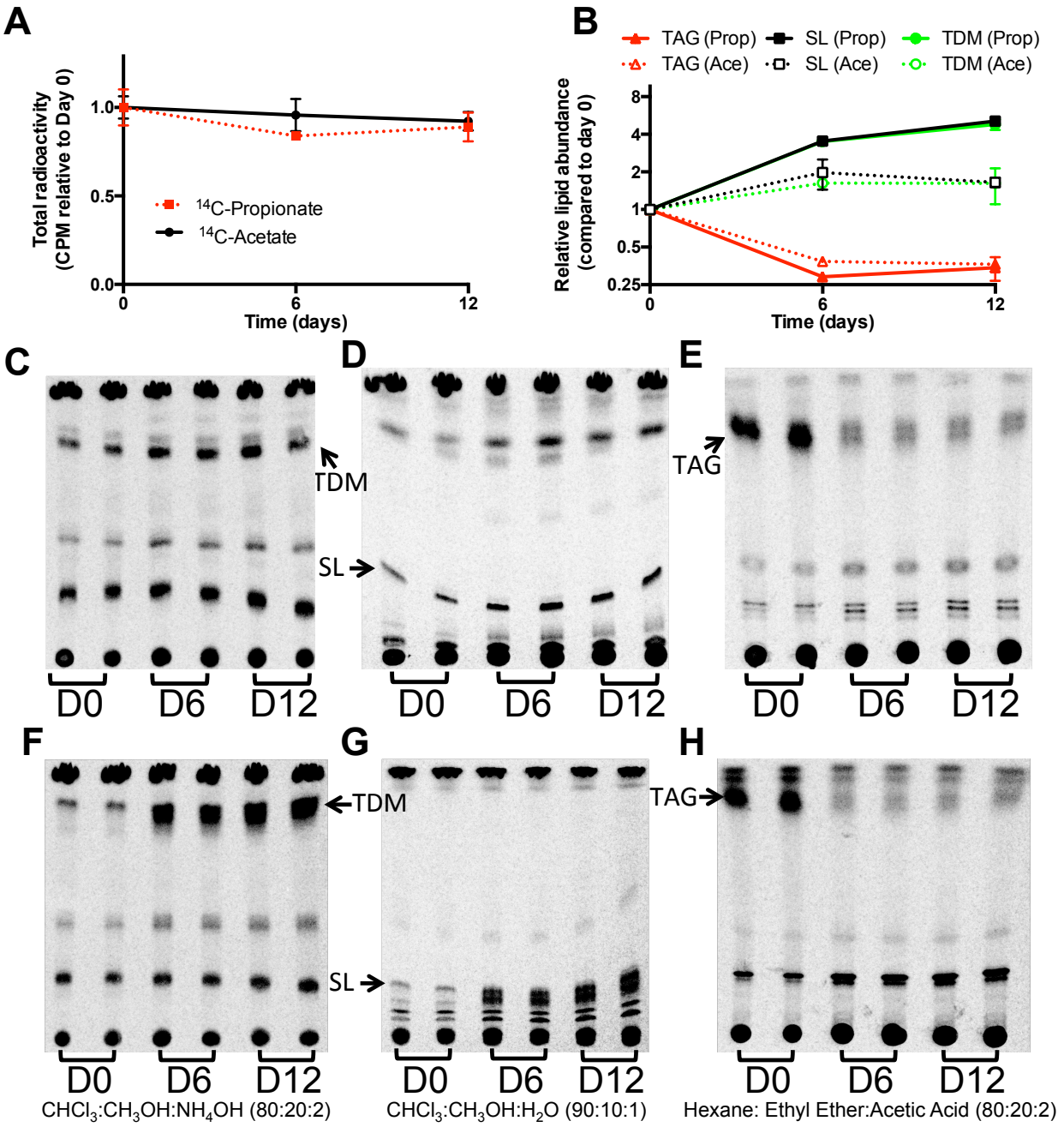

Figure 3.6. Mtb utilizes endogenous TAG for the synthesis of TDM and SL at acidic pH. Mtb was grown in the presence of ^{14}C-acetate or ^{14}C-propionate for 3 weeks prior to transferring to minimal medium containing glycerol as a single carbon source buffered to pH 5.7. A) Total radioactivity of Mtb whole cells over time. Over 12 days a ~10% reduction in radioactivity was observed. B) Relative lipid species abundance of triacylglycerol (TAG), sulfolipid (SL), and trehalose dimycolate (TDM) over time in Mtb labelled with ^{14}C-acetate (Ace) or ^{14}C-propionate (Prop). C-H) Thin Layer Chromatography (TLC) images showing relative abundance of TAG, SL and TDM at 0, 6, and 12 days after transfer of ^{14}C-acetate- (C-E) or ^{14}C-propionate- (F-H) labeled Mtb to acidic pH growth arrest (D0, D6, and D12, respectively).

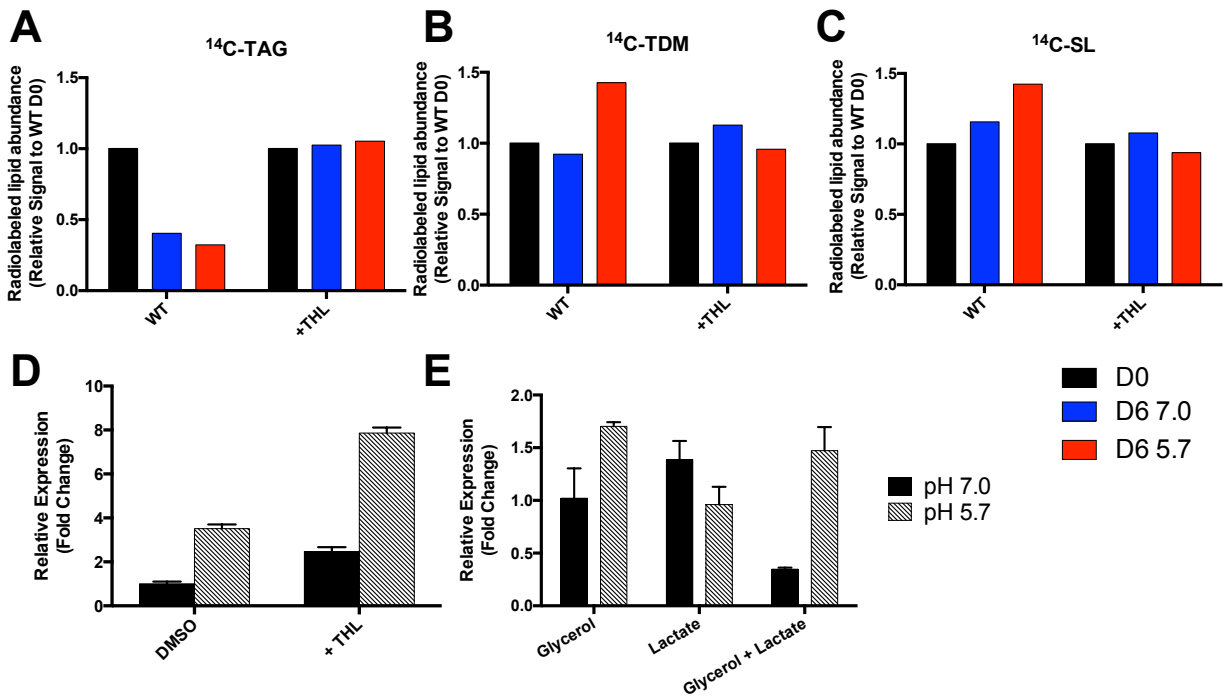

Figure 3.7. Inhibition of lipid remodeling at acidic pH increases *prpC* induction. A-C) Remodeling of radiolabeled TAG, TDM, and SL at day 0 (D0) and after incubation for 6 days at pH 7.0 or pH 5.7 (D6 7.0 or D6 5.7, respectively) in minimal medium with glycerol as a single carbon source with or without the addition of the lipase inhibitor tetrahydrolipstatin (WT or +THL, respectively). Addition of THL blocks the ability of Mtb to undergo lipid remodeling. D) Addition of THL increases *prpC* expression at pH 7.0 and pH 5.7. E) *prpC* is induced during Mtb growth arrest with glycerol or glycerol and lactate as the carbon source(s), but not with lactate as a single carbon source.

Mtb exhibits altered central carbon metabolism at acidic pH

Given the observed role of the anaplerotic node in acidic pH growth regulation as well as the carbon source-specific requirements for growth at acidic pH, I hypothesized that Mtb would exhibit metabolic remodeling at acidic pH that requires proper function of enzymes of the anaplerotic node. To test this hypothesis, metabolic profiling of 12 central carbon metabolism metabolites was performed. WT Mtb Erdman, Δ*icl1/2*, WT Mtb CDC1551, and Δ*pckA*, were grown on filters placed on agar plates containing minimal medium buffered to either pH 7.0 or pH 5.7 and supplemented with either glycerol or pyruvate as a single carbon source. Metabolites were extracted after 3 and 6 days of culture. Given the toxicity observed in the Δ*pckA* mutant when cultured with pyruvate as a single carbon source, glycerol and pyruvate were supplemented together for this mutant as well as its WT control. Quantification of relative metabolite concentrations was performed by LC/MS, and the data were analyzed for statistical significance using MANOVA followed by post hoc pairwise comparisons that were Bonferroni adjusted to correct for false discovery rate. Full metabolic profiling datasets and statistical analysis tables can be found in the appendix (Appendix Tables 1-8, Figures 1-2).

Decreased succinyl-CoA pools as a biomarker for slowed Mtb growth at acidic pH. Mtb cultured at pH 5.7 with glycerol as a single carbon source exhibits decreased pools of the oxidative TCA cycle intermediate succinyl-CoA (Figure 3.8). This decrease was present in both CDC1551 and Erdman WT strains (Appendix Figures 1-2). Interestingly, I observed that while succinyl-CoA concentration at pH 5.7 in the Δ*icl1/2* mutant is reduced at day 3 (when the mutant is growth arrested), by day 6 (when the mutant exhibits low-level growth on glycerol at pH 5.7) the succinyl-CoA pools were the same as those observed at pH 7.0 (Figure 3.8). These observations suggest that decreased succinyl-CoA may represent a biomarker for growth arrest at pH 5.7, and that isocitrate lyase may play a role in maintaining decreased succinyl-CoA levels at acidic pH.

Succinate secretion during acidic pH growth. The decreased succinyl-CoA pools observed during acid growth arresting conditions also occur at acidic pH with pyruvate as the carbon source, a growth permissive condition (Figure 3.9A). This observation suggests that the growth observed in pyruvate at pH 5.7 does not require maintaining succinyl-CoA levels, and that an alternative mechanism exists for Mtb growth on pyruvate at acidic pH. While metabolic profiling reveals that WT Mtb exhibits increased pools of phosphoenolpyruvate, acetyl-CoA, and α-ketoglutarate by day 6 (Figure 3.9A), each of these changes are absent at day 3 even though Mtb is already growing at this time point. However, it was observed that at both day 3 and day 6, Mtb does accumulate malate at acidic pH (Figure 3.9A). To further characterize Mtb metabolism at acidic pH, metabolite concentrations in culture supernatants were also measured. Interestingly, succinate accumulated >50-fold in the supernatant specifically in Mtb cultured at pH 5.7 with pyruvate as a single carbon source (Figure 3.9B). The secretion of succinate was still present in the Δ*icl1/2* mutant (Figure 3.9B), suggesting that Mtb does not require the glyoxylate shunt to secrete succinate.

Mtb also secretes succinate under conditions of hypoxia (37,38), and it has been hypothesized that succinate secretion allows Mtb to maintain membrane potential in the absence of respiration (37). This hypothesis is supported by the observation that under conditions of hypoxia the addition of nitrate as an alternate electron acceptor decreases succinate secretion and restores ATP levels and viability to near aerobic levels (38). To test whether nitrate acts as a similar modulator of respiration at acidic pH, succinate secretion and growth of Mtb was measured with or without addition of sodium nitrate. Interestingly, although having no effect on Mtb growth on pyruvate at pH 7.0, addition of nitrate at pH 5.7 decreased Mtb growth ~50% (Figure 3.10A). Succinate secretion by Mtb at pH 5.7 in the presence of nitrate was decreased ~40% (Figure 3.10B), although this likely is secondary to the decreased growth rate, as there are fewer bacteria contributing to secreted succinate pools. The ability of nitrate to modulate Mtb growth at acidic pH but not at neutral pH suggests that Mtb at acidic pH

exhibits altered respiration that is responsive to changes in available electron acceptors like nitrate. However, the inability of nitrate to modulate succinate secretion, as is observed under conditions of hypoxia, suggests that this altered respiration is unique from that encountered under conditions of hypoxia.

pckA as the mediator of increased gluconeogenesis in Mtb at acidic pH. Despite the Δ*pckA* mutant having no change in growth phenotypes compared to WT Mtb in the culture conditions where metabolic profiling was performed, significant differences in metabolite pools were observed specifically at acidic pH. Compared to WT Mtb, the Δ*pckA* mutant had increased intracellular concentrations of the TCA cycle intermediates citrate, succinate, and malate when cultured at pH 5.7 with glycerol or glycerol and pyruvate as the carbon sources (Figure 3.11A-B). The increased concentration of these metabolites was most notable at day 3, and returned toward WT levels by day 6 (Figure 3.11A-B). In Mtb cultured with both glycerol and pyruvate, a 4-fold increase in α-ketoglutarate was also observed (Figure 3.11A-B). Notably, no increase in citrate, succinate, or α-ketoglutarate was observed in the Δ*pckA* mutant compared to WT Mtb at neutral pH, and the increase in malate pools at pH 7.0 was less pronounced than at pH 5.7 (Appendix Figure 2). The increase in succinate, malate, and citrate specifically at acidic pH in the Δ*pckA* mutant demonstrates that Mtb uses *pckA* to prevent accumulation of these TCA cycle intermediates at acidic pH. Indeed, the Δ*pckA* mutant has a 2-fold increase in succinate secretion compared to WT Mtb (Figure 3.11C), perhaps secondary to this inability to reroute TCA cycle intermediates via the gluconeogenic reaction of *pckA*. However, the return of these TCA intermediates toward WT levels by day 6 suggests that Mtb can compensate metabolically for this overaccumulation. Together, these results support the hypothesis that at acidic pH Mtb utilizes *pckA* to increase gluconeogenic carbon flow.

Notably, in addition to the increased concentration of citrate at pH 5.7, the Δ*pckA* mutant does not have diminished succinyl-CoA pools at pH 5.7 compared to pH 7.0 at day 3 (Figure

3.11A-B). By day 6, succinyl-CoA pools in the Δ*pckA* mutant declined to WT levels (Figure 3.11A-B). This observation further supports the view that loss of *pckA* leads to a transient disruption of WT metabolic remodeling at acidic pH. However, both the return of metabolite levels toward WT concentrations in the Δ*pckA* mutant by day 6 and the shared growth phenotypes of the mutant and WT Mtb suggest that Mtb can compensate for deletion of *pckA* during metabolic adaptation at acidic pH.

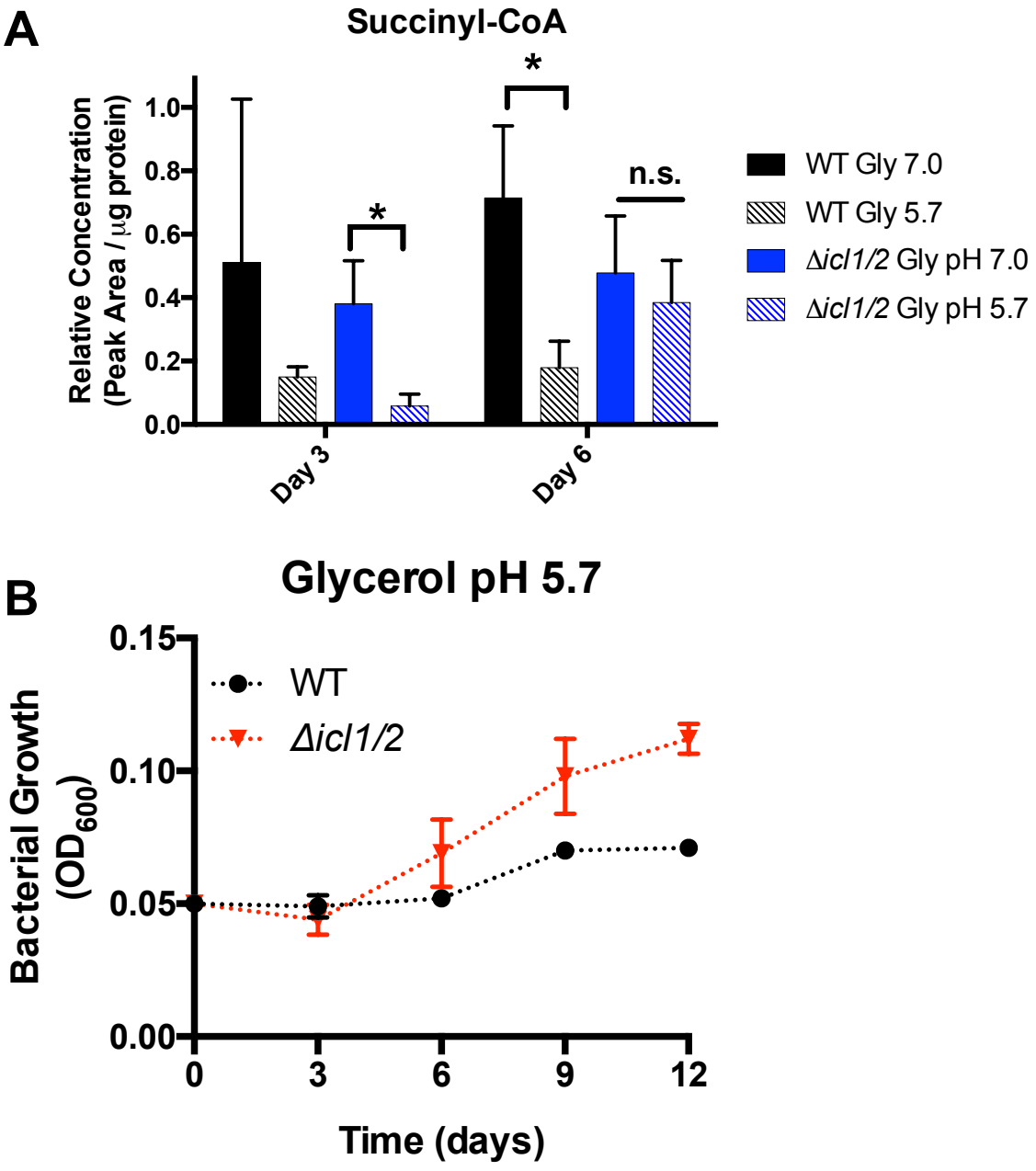

Figure 3.8. Decreased concentration of succinyl-CoA during growth arrest at acidic pH is *icl1/2* dependent. A) Relative concentration of succinyl-CoA in WT and Δ*icl1/2* mutant in minimal medium with glycerol as a single carbon source buffered to pH 7.0 or pH 5.7. Acidic pH is associated with reduced succinyl-CoA levels in WT Mtb. The Δ*icl1/2* mutant exhibited decreased succinyl-CoA levels at day 3, but by day 6 there was no difference in metabolite concentration between pH 7.0 and 5.7. B) This change in succinyl-CoA concentration at pH 5.7 with glycerol as a single carbon source in the Δ*icl1/2* mutant coincides with the observed switch from growth arrest to growth from day 3 to day 6.

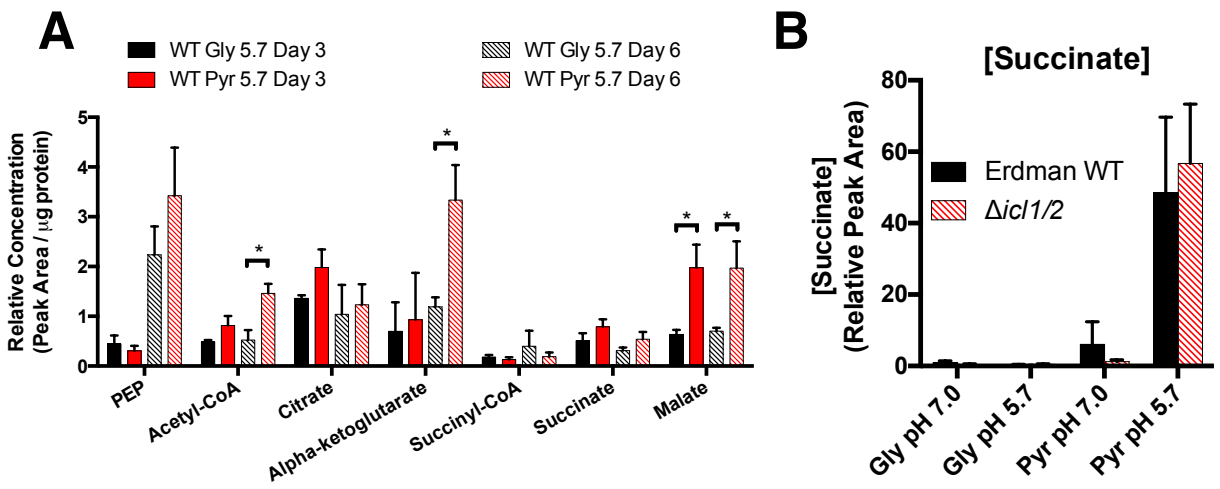

Figure 3.9. Changes in metabolic profile associated with growth at acidic pH. A) Relative concentration of selected central carbon metabolites at acidic pH with either glycerol (Gly) or pyruvate (Pyr) as the single carbon source. Mtb has increased concentrations of acetyl-CoA and α-ketoglutarate at day 6, and increased concentrations of malate on day 3 and day 6. B) Succinate concentration in supernatant after 3 days culture in minimal medium with glycerol (Gly) or pyruvate (Pyr) as single carbon sources buffered to pH 7.0 or pH 5.7. Mtb secretes succinate specifically at pH 5.7 with pyruvate as a single carbon source. Similar levels of succinate accumulation in the supernatant are observed in the Δ*icl1/2* mutant.

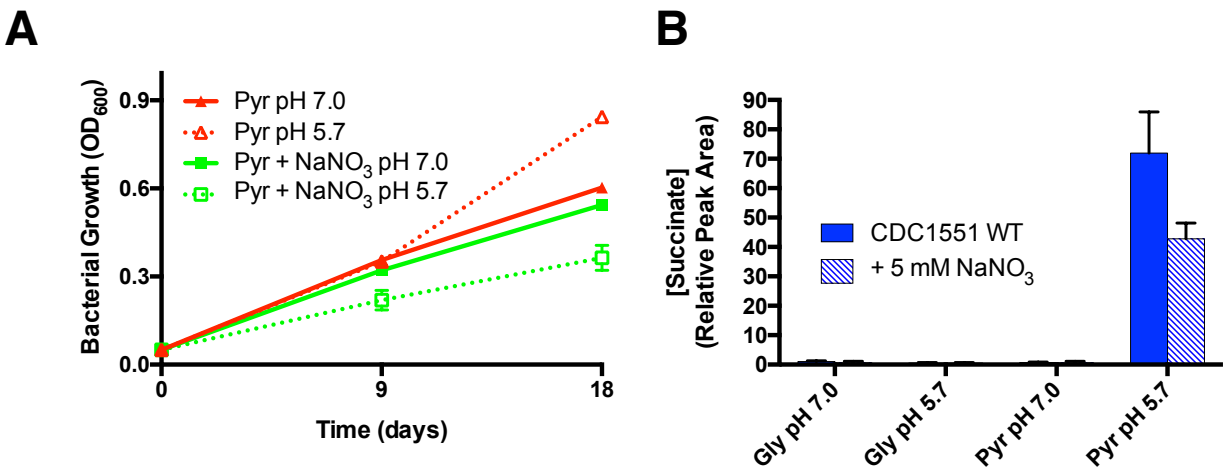

Figure 3.10. Nitrate decreases Mtb growth on pyruvate specifically at acidic pH but has little effect on succinate secretion. A) Growth of Mtb in minimal medium with pyruvate as a single carbon source buffered to pH 7.0 or pH 5.7 with or without 5 mM sodium nitrate ($NaNO_3$). Mtb growth at pH 7.0 is not affected by addition of nitrate, but at pH 5.7 addition of nitrate causes a ~50% inhibition of growth. B) Secretion of succinate is decreased ~40% with the addition of nitrate at pH 5.7 with pyruvate as a single carbon source, but this could be due to the decreased growth in this condition.

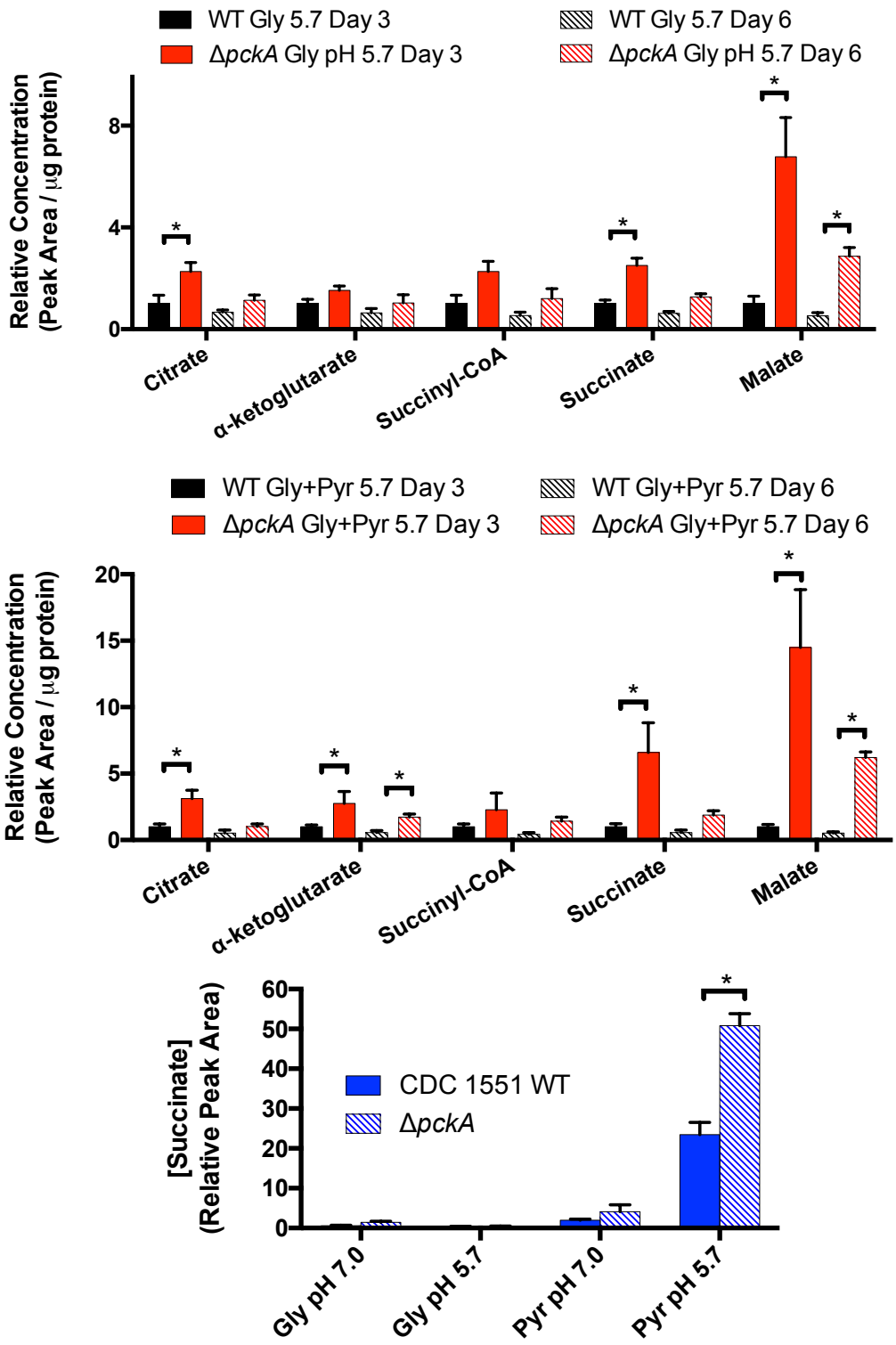

Figure 3.11. Metabolic profiling of the Δ*pckA* mutant reveals a role for *pckA* in gluconeogenesis at acidic pH. A-B) Concentration of TCA cycle intermediates in the Δ*pckA* mutant relative to WT Mtb at pH 5.7 with either glycerol (A) or glycerol and pyruvate (B) as the carbon source(s). C) Relative concentration of succinate secreted by WT and Δ*pckA* Mtb.

Discussion

Mtb exhibits metabolic plasticity in the face of changing environments. Mtb grown under conditions of hypoxia, where redox homeostasis would presumably be difficult to maintain due to the lack of oxygen available for respiration, recycles reduced cofactors via lipid synthesis (50) and increased flux through the reductive TCA cycle (37,38). With the addition of nitrate, Mtb adapts to another metabolic program during hypoxic culture in which nitrate respiration maintains homeostasis (38,106). To metabolize branched chain fatty acids and cholesterol, Mtb utilizes *prpCD* and *icl1/2* to prevent toxic accumulation of propionyl-CoA intermediates using the methylcitrate cycle (33,34,107). The supplementation of vitamin B12 opens yet another pathway for propionyl-CoA metabolism in Mtb, the methylmalonyl pathway (35). Even under conditions of starvation, Mtb can maintain membrane potential and a basal level of intracellular ATP (56). Notably, these metabolic adaptations in response to changing environments are crucial to Mtb pathogenesis. Although nonessential for growth *in vitro* in rich medium, several genes encoding for metabolic enzymes have been shown to be required for Mtb survival during infection, including *icl1/2* (25), *pckA* (20), *dlaT* (23), and *hoas* (24). Investigating the mechanisms of metabolic adaptation to environmental stress *in vitro* has helped elucidate the function of these genes during infection as well as explain the basis of their importance in Mtb pathogenesis.

In this study, I sought to characterize the metabolic adaptation of Mtb to the host cue of acidic pH. Deletion of two genes of the anaplerotic node, *pckA* and *icl1/2*, led to decreased growth at acidic pH but not neutral pH in rich medium, highlighting that Mtb requires anaplerotic metabolism specifically at acidic pH. In minimal media, the main growth phenotypes of both mutants appeared to be related to the inability to perform anaplerosis, as both mutants had difficulty growing in carbon sources other than glycerol, irrespective of pH. These minimal media growth defects of the mutants made it difficult to measure the role of the anaplerotic node specifically at acidic pH. In the case of *pckA*, the severe growth defect when grown on pyruvate confounded the ability to use mutants to study the role of gluconeogenic carbon flow in growth

regulation at acidic pH, as the addition of glycerol to prevent toxicity simultaneously provided a redundant source for gluconeogenic intermediates. Even still, the observed disadvantage that anaplerotic node deletion mutants have in minimal medium makes notable the inability of the Δ*icl1/2* mutant to maintain growth arrest at acidic pH.

The measurement of unlabeled metabolic intermediates performed here has its limitations, as the directionality and rate of carbon flux cannot be determined simply by looking at the concentrations of different metabolic intermediates. Indeed, the increase in concentration of a specific metabolite could arise from increased flux through a pathway just as easily as from a block in metabolism. The limitations of unlabeled metabolic profiling have been helped by combining this metabolic profiling with the use of mutant strains in known central carbon metabolism enzymes and transcriptional profiling. Using this approach, I have been able to demonstrate that Mtb does indeed undergo metabolic remodeling at acidic pH, and propose the following model of the mechanisms of this metabolic remodeling at acidic pH (Figure 3.12).

One of the key outcomes of metabolic remodeling at acidic pH that I observed was a decrease in succinyl-CoA levels, which I hypothesize is due to decreased metabolic flux through the oxidative TCA cycle. The oxidative TCA cycle is an energy generating pathway in the form of NADPH and ATP (81). Although other metabolic pathways can similarly generate energy, the oxidative TCA cycle is somewhat unique in that the process requires two steps of irreversible oxidative decarboxylation, from citrate to α-ketoglutarate to succinyl-CoA (Figure 3.12). High flux through these irreversible reactions requires that Mtb can incorporate the high-energy cofactors generated into other metabolic reactions. I hypothesize that under stressful conditions where metabolism may be restricted, avoiding flux through the oxidative TCA cycle may prevent Mtb from overaccumulating these intermediates and thus contribute to slowed growth. I observed that in the Δ*icl1/2* mutant, increased pools of succinyl-CoA coincided with the loss of growth arrest at acidic pH. Given this observation, I hypothesize that *icl1/2* plays an important role in regulating the flux through the oxidative TCA cycle to regulate Mtb growth (Figure 3.12A).

The identification of succinate secretion in growing Mtb at acidic pH is a puzzling observation (Figure 3.12B). In conditions of hypoxia, succinate secretion has been shown to be necessary to prevent succinate accumulation secondary to increased utilization of the glyoxylate shunt and reductive TCA cycle (37,38) for oxidized cofactor regeneration. The phenotype in hypoxia has been linked to decreased respiration in hypoxic environments, as the addition of nitrate as an alternative electron acceptor decreased succinate secretion (33). In Mtb growing at acidic pH, the reason for succinate secretion is less obvious. In this culture condition, oxygen is available to Mtb, making a complete halt in respiration at acidic pH non-intuitive. However, it was shown previously that at acidic pH Mtb induces transcriptionally type-II NADH dehydrogenase and *bd*-type cytochrome oxidase and represses expression of the type-I NADH dehydrogenase complex and *c*-type cytochrome oxidase (15). Why Mtb switches from a proton translocating to non-proton translocating electron transport chain is not well understood, but does suggest that changes in respiration may indeed be occurring at acidic pH. Furthermore, while the addition of nitrate as an alternative electron acceptor did not abolish succinate secretion as was observed under hypoxia, it did lead to an acidic pH-specific reduction in growth at acidic pH. Notably, the use of nitrate for respiration at acidic pH has been observed before, with Mtb in a hypoxic and acidic environment requiring nitrate respiration to maintain viability (106). The ability of an alternate electron acceptor to modulate Mtb growth at acidic pH suggests that changes in Mtb respiration could contribute to the metabolic remodeling observed at acidic pH. This possibility is worthy of further investigation.

The marked increase in TCA intermediates at acidic pH in the Δ*pckA* mutant suggests an increased requirement for *pckA*-dependent gluconeogenesis at acidic pH (Figure 3.12C). If, as I have proposed, Mtb shifts its metabolism away from the oxidative TCA cycle and toward the glyoxylate shunt at acidic pH, this shift would lead stoichiometrically to an increase in succinate-fumarate-malate intermediates as no carbon is lost through decarboxylation. In this setting, the gluconeogenic reaction of *pckA* allows for an alternate route of metabolism instead of moving

these metabolites back into the oxidative TCA cycle via citrate synthase (Figure 3.12C). Increased metabolism via *pckA* coupled with the increased use of the glyoxylate shunt, as is suggested by metabolic and transcriptional profiling, is reminiscent of the PEP-glyoxylate cycle previously characterized in *E. coli* grown in limited glucose culture (41). This PEP-glyoxylate cycle has been proposed to be a means of decoupling catabolism from NADPH production, an outcome that is necessary in situations where little biomass is synthesized (41). In Mtb at acidic pH, I speculate that one of two scenarios leads to a shift to this PEP-glyoxylate type metabolism. First, Mtb could require this decoupling to adapt to the changes in respiration that occur at acidic pH. Alternatively, in response to acidic pH, Mtb could actively remodel metabolism to slow growth, and the decoupling of catabolism from NADPH production provided by the PEP-glyoxylate cycle could aid in halting biosynthesis.

While initially assumed to be involved in production of propionyl-CoA at acidic pH, lipid remodeling at acidic pH instead appears to contribute to the metabolism of propionyl-CoA (Figure 3.13A). The metabolic coupling of propionyl-CoA metabolism to lipid synthesis at acidic pH is consistent with previous work showing lipid synthesis as a readily usable sink for propionyl-CoA incorporation (27,36,86). Unlike in this previous work, during acidic pH growth arrest the source of propionyl-CoA appears to be endogenous rather than exogenously supplied. The induction of *prpCD* during acidic pH growth arrest was shown to be dependent on glycerol being present in the media, suggesting that the induction of *prpCD* is secondary to metabolism of glycerol at acidic pH (Figure 3.13A). Glycerol metabolism leading to the production of propionyl-CoA has not been documented in the Mtb literature. However, the study of bacterium of the gut has identified three separate pathways for the production of propionyl-CoA (108). One of these pathways, the propanediol pathway, involves the conversion of methylgloxal to propionate (109). Given that methylglyoxal can accumulate in Mtb as a byproduct of dihydroxyacetone phosphate (DHAP) metabolism, particularly after inhibition of glycolysis (104), I speculate that *prpCD* induction at acidic pH could be secondary to production

of propionyl-CoA via this propanediol pathway (Figure 3.13B). However, whether Mtb contains enzymes capable of performing this metabolism is not known. Endogenous production of propionyl-CoA does not appear to be a necessary component of acidic pH growth arrest as growth arrested Mtb cultured in minimal medium with lactate does not induce *prpCD* at acidic pH; however, understanding this response could uncover additional aspects of Mtb metabolic remodeling that occurs during acidic pH growth arrest.

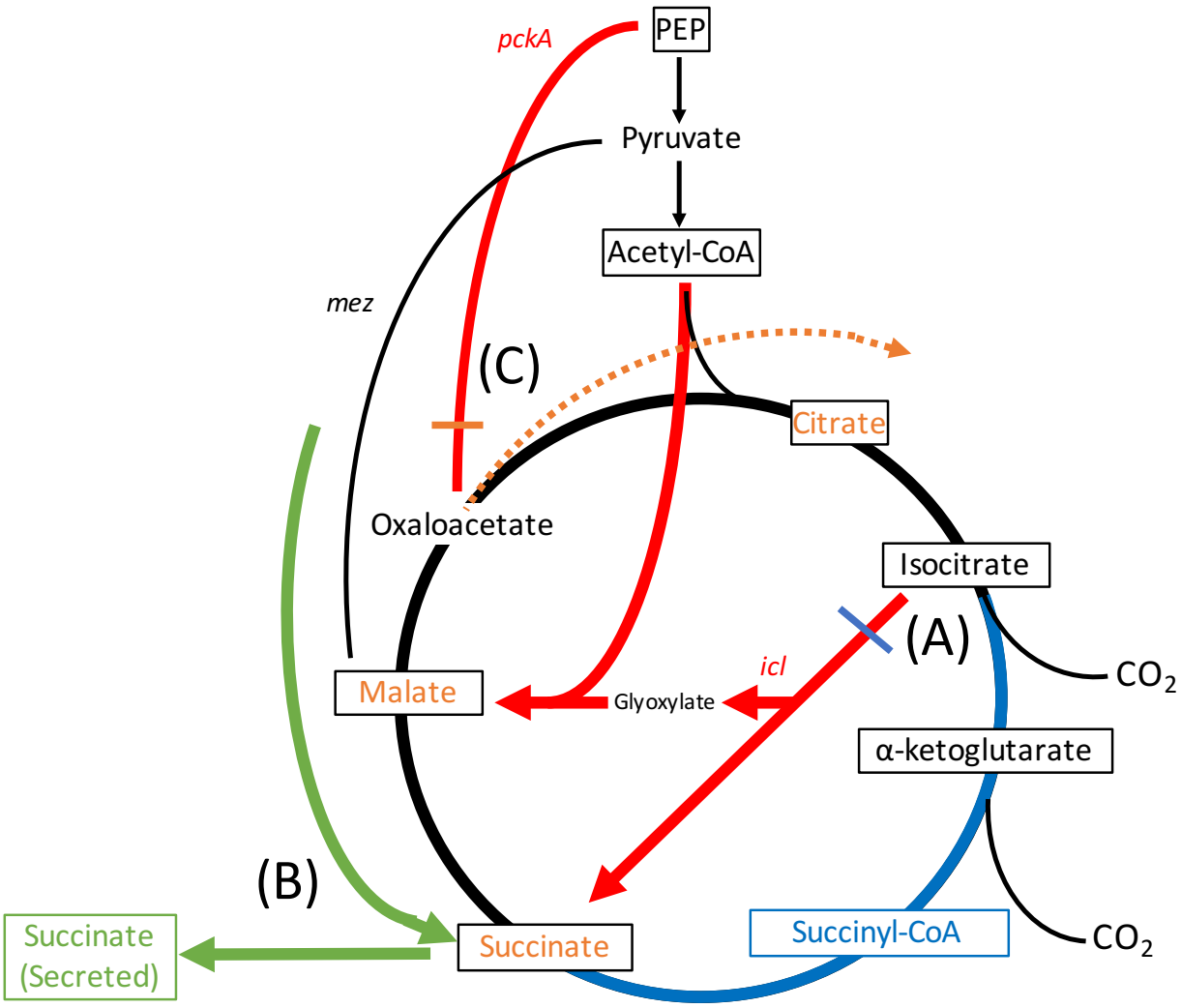

Figure 3.12. Speculative model of metabolic remodeling at acidic pH. A; blue) At acidic pH, the transcriptional induction of isocitrate lyase (*icl*) and decreased concentration of succinyl-CoA suggest that Mtb increases metabolic flux through the glyoxylate shunt and decreases flux through the oxidative TCA cycle. This remodeling limits production of NADPH and ATP via irreversible oxidative decarboxylation and additionally increases the production of reductive TCA cycle intermediates (succinate and malate). B; orange) The transcriptional induction of *pckA* at acidic pH, as well as the observed accumulation of succinate, malate, and citrate in the Δ*pckA* mutant at acidic pH suggests that Mtb utilizes the gluconeogenic reaction of *pckA* to divert the increased reductive TCA cycle intermediates away from citrate synthase. The decrease of these intermediates in the Δ*pckA* mutant to WT levels by day 6 suggests that Mtb can compensate metabolically for loss of *pckA*. C; green arrows) Growth at acidic pH is associated with secretion of succinate. The Δ*icl1/2* mutant still secretes succinate, suggesting that Mtb can utilize a route other than the glyoxylate shunt for succinate secretion.

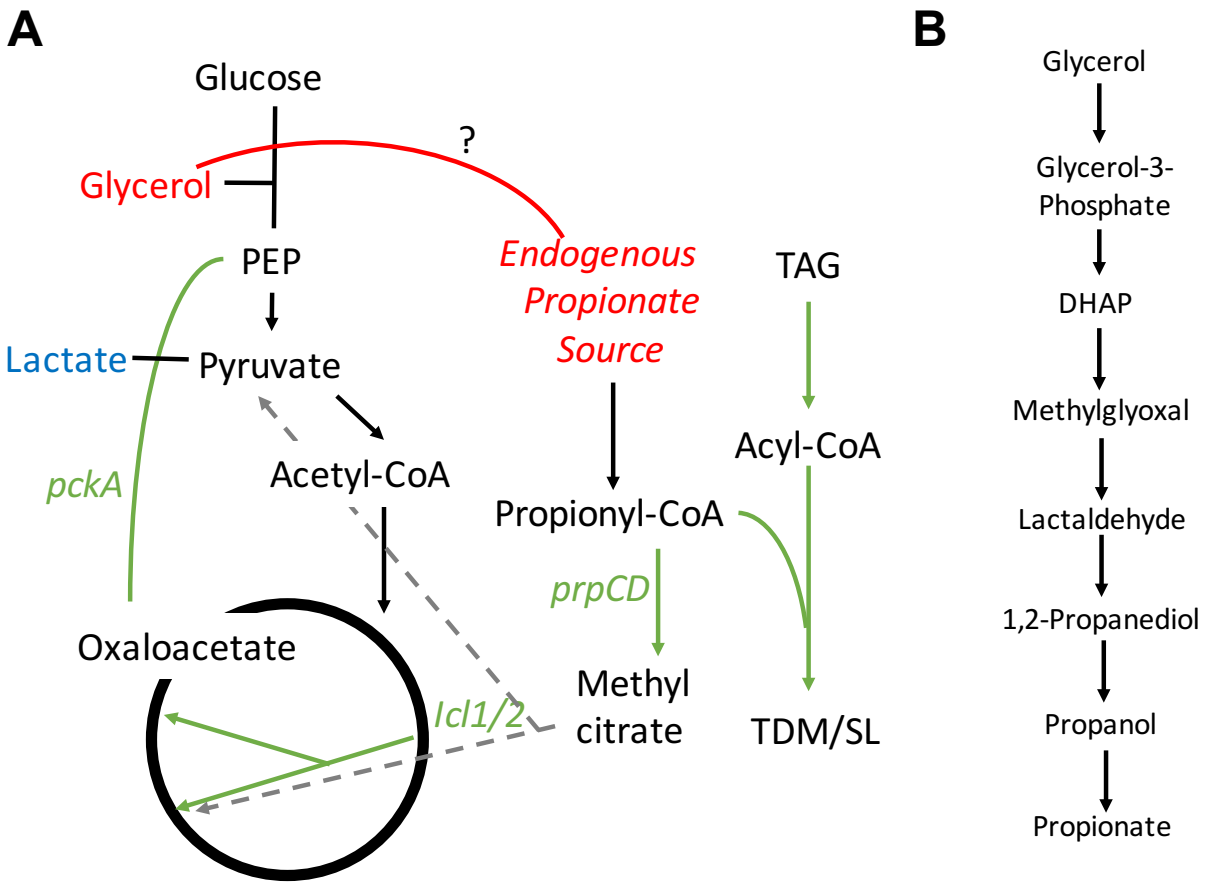

Figure 3.13. Speculative models for *prpCD* induction during acidic pH growth arrest. A) *prpCD* is induced during acidic pH growth arrest when glycerol is present in the medium, but not when lactate is the single carbon source. I speculate that the metabolism of glycerol may lead to *de novo* synthesis of propionyl-CoA. The increased expression of *prpCD* in the absence of Mtb lipid remodeling of triacylglycerol (TAG) to sulfolipid (SL) and trehalose dimycolate (TDM) suggests that Mtb uses lipid remodeling as a sink for propionyl-CoA. B) Speculative metabolic pathway for the generation of propionate from glycerol that has been observed in microbes found in the gut (109).

Materials and Methods

Bacterial strains and growth conditions

All Mtb experiments, unless otherwise stated, were performed with Mtb strain CDC1551. The Δ*pckA* mutant was generated by homologous recombination and verified by quantitative real time PCR. Complementation of the mutant was achieved by cloning the *pckA* gene as well as its native promoter (1000 bp upstream) into the integrative plasmid pMV306. The Δ*icl1/2* mutant and its WT control were a generous gift from John McKinney. Cultures were maintained in 7H9 Middlebrook medium supplemented with 10% OADC and 0.05% Tween-80. All single carbon source experiments were performed in a defined minimal medium as described by Lee *et al.* (36): 1 g/L KH_2PO_4, 2.5 g/L Na_2PO_4, 0.5 g/L $(NH4)_2SO_4$, 0.15 g/L asparagine, 10 mg/L $MgSO_4$, 50 mg/L ferric ammonium citrate, 0.1 mg/L $ZnSO_4$, 0.5 mg/L $CaCl_2$, and 0.05% Tyloxapol. Medium was buffered using 100 mM MOPS (pH 6.6–7.0) or MES (pH 5.7–6.5) (18). For growth experiments, Mtb was seeded in T-25 standing tissue culture flasks in 8 ml of minimal medium at an initial density of 0.05 OD_{600} and incubated at 37°C and 500 µl samples were removed at each time point for optical density measurements.

Metabolic profiling

For metabolic profiling studies, Mtb cultures were centrifuged, washed with 0.9% saline, and resuspended at a final OD_{600} of 2. 1 mL of washed Mtb was placed on a membrane filter via vacuum filtration and put on agar plates containing the indicated minimal medium (36). For extraction, Mtb laden filters were transferred to a 6-well plastic plate, frozen on dry ice, and quenched with 500 µL of methanol chilled on dry ice. 175 µL of water and 25 µL of the internal standard 100 µM succinic acid 2,2,3,3-d_4 were added to each sample, and bacteria were scraped off the membrane filters with a plastic loop and transferred to a 2 mL tube containing 1.2 mL chloroform. After a tube transfer to remove samples from the biosafety level 3 facility,

samples were vortexed at 4°C for 30 minutes, centrifuged for 5 minutes at 15,000 rpm, and the upper aqueous phase was transferred to a new tube. The aqueous phase was dried under liquid nitrogen and frozen at -80 °C until liquid chromatography/mass spectrometry (LC/MS) analysis. For protein quantification, the interphase of the sample was dried and resuspended by sonication in 20 mM Tris pH 8.0, 0.1 % sodium dodecyl sulfate (SDS), and 6M urea. For LC/MS analysis, samples were resuspended in 10 mM tributylamine (TBA), 10 mM acetic acid (AA), 97:3 water:methanol. Samples were applied to a C18 BEH-amide column and metabolites were separated using a 10 minute inlet method with the mobile phase starting at 99:1 10 mM TBA: 10 mM AA in 97:3 water:methanol and finishing at 100% methanol. Multiple reaction monitoring (MRM) channels were developed for each metabolite using known standards, and metabolites were identified by comparing monoisotopic mass and retention time to these standards.

RNA extraction and real time PCR

Mtb cultures were grown at 37°C in T-25 vented, standing tissue culture flasks in 8 mL of a defined minimal medium seeded at an initial OD_{600} of 0.25. After three days, total bacterial RNA was stabilized and extracted as previously described (11). Semi-quantitative real-time PCR was performed using previously described methods (17). Vitamin B12 was supplemented at 10 µg/mL and tetrahydrolipostatin (THL) was added at a concentration of 20 µM.

Analysis of mycobacterial lipids

For lipid remodeling experiments, bacterial cultures were grown in 7H9 +10% OADC with either 8 µCi of [1,2 ^{14}C] sodium acetate or [1-^{14}C] sodium propionate. Following 15 days of labeling, the bacteria were pelleted and resuspended in the minimal medium containing glycerol as a single carbon source buffered to either pH 7.0 or pH 5.7. At day 0, 6, and 12, two 1 mL aliquots were pelleted and fixed in 4% paraformaldehyde, and the remaining bacteria were pelleted, washed, and the lipids extracted as described previously (15). Total radioactivity and ^{14}C

incorporation were determined by scintillation counting of the fixed samples and the total extractable lipids, respectively. To analyze lipid species, 5,000 counts per minute (CPM) of the lipid sample was spotted at the origin of 100 cm^2 silica gel 60 aluminum sheets. To separate sulfolipid for quantification, the TLC was developed with a chloroform:methanol:water (90:10:1 v/v/v) solvent system (67). To separate TAG for quantification, the TLC was developed with a hexane:diethyl ether:acetic acid (80:20:1, v/v/v) solvent system (17). To examine PDIM accumulation the TLC was developed in petroleum ether:acetone (98:2 v/v). To examine TDM and TMM accumulation the TLC was developed in a chloroform:methanol:ammonium hydroxide (80:20:2 v/v/v) solvent system. Radiolabeled lipids were detected and quantified using a phosphor screen and a Typhoon Imager, and band density quantified using ImageQuant software (103). Radiolabeling experiments, lipid extractions and TLCs were repeated in at least two independent biological replicates with similar findings in both replicates.

Statistical methods

All growth curves were performed in biological duplicate and are representative of at least two independent experimental replicates. The error bars for all growth curves represent the standard deviation of a single experiment, although sometimes are too small to see given the consistency of measurement. For quantitative real time PCR of mRNA transcript levels, RNA was extracted in biological duplicate and quantitative PCR performed on each sample in technical triplicate. Data are representative of at least two independent experiments. Lipid profiling was performed in biological duplicate as can be seen from the TLC images, except for the experiments using THL, which were not performed in duplicate. For metabolic profiling, five biological replicates were extracted for each treatment, and statistical significance determined using a MANOVA followed by post-hoc pairwise comparisons Bonferroni adjusted for false discovery. Differences were considered significant at $p < 0.05$.

Acknowledgements

I would like to thank John McKinney for the generous gift of the Δ*icl1/2* mutant and matched wild type control strain used in this study. Also, I would like to acknowledge the MSU RTSF Mass Spectrometry Core Facility, including Dan Jones, Lijun Chen, and Anthony Schilmiller, as well as Martin Ogrodzinski and Anna Huff for assistance in developing methods for extraction and analysis of metabolites.

CHAPTER 4 – Growth arrest at acidic pH is a regulated process that promotes phenotypic tolerance.

Introduction

The success of *Mycobacterium tuberculosis* (Mtb) as a human pathogen and public health threat can be attributed in part to its ability to persist in adverse conditions through the cessation of growth. Upon infection of humans, Mtb survives long periods of slowed and arrested growth, remaining quiescent for decades before reemerging to cause disease (110). Even in active cases of tuberculosis, the long course of antibiotic treatment required to clear infection, 6 to 9 months (111), is understood to be necessary due to the phenotypic tolerance of Mtb subpopulations with reduced growth (112). The issue of phenotypic tolerance is exacerbated by the diversity of Mtb-containing lesions that develop during infection, implying that throughout infection Mtb populations exist in a variety of host environments permissive for varying degrees of growth (2). Even from sputum samples of infected patients, Mtb can be isolated that displays increased tolerance to front line Mtb antibiotics (113). Thus, efforts to understand how Mtb regulates persistence during infection are of relevance to the successful treatment of tuberculosis.

While the exact mechanisms responsible for growth arrest *in vivo* are not completely understood, several studies have investigated the response of Mtb to host-relevant stresses *in vitro*. In response to environmental conditions such as hypoxia or starvation, Mtb enters a state of non-replicating persistence (51,54). These *in vitro* persistent states are characterized by metabolic remodeling (37) and increased antibiotic tolerance (56). Similar observations of antibiotic tolerance have been made during Mtb growth arrest in response to nitric oxide (49), low iron (50), and in multiple stress models (53).

The relationship between non-replicating persistence and Mtb phenotypic tolerance makes inhibition of Mtb persistence an inviting therapeutic target. Indeed, deletion of the genes

encoding the two-component system necessary for adaptation to hypoxic non-replicating persistence, *dosRST*, leads to a defect in survival under hypoxia (114) as well as during infection (5,115,116). Furthermore, inhibitors of DosRST have also been shown to increase Mtb sensitivity to isoniazid during hypoxic culture (60), demonstrating that inhibiting the ability of Mtb to maintain non-replicating persistence reduces the phenotypic drug tolerance characteristic of these growth arrested states.

In addition to these models of Mtb growth arrest, we have previously studied the *in vitro* response of Mtb to the stress of acidic pH. The ability of Mtb to sense and adapt to the host-relevant cue of acidic pH is necessary for the pathogenesis of Mtb (3,17). In studying the response of Mtb to acidic pH, I observed that Mtb cultured at acidic pH exhibits carbon source specific growth arrest, with only carbon sources of the anaplerotic node, such as acetate, pyruvate, and oxaloacetate, promoting growth (15). When grown in the presence of other single carbon sources, such as glycerol, Mtb enters a growth arrested state, remaining viable and maintaining pH homeostasis (15). Given the importance of non-replicating persistence in Mtb pathogenesis, I sought to further characterize Mtb growth arrest in response to acidic pH, exploring the physiology and genetics behind this growth arrest as well as its role in antibiotic tolerance and pathogenesis.

Results

Growth arrest at acidic pH induces a metabolically active, non-replicating state in Mtb.

Previously, I have shown that Mtb cultured at pH 5.7 in minimal medium containing glycerol as a single carbon source is arrested for growth but maintains viability (15). A long-term viability assay was performed to verify that Mtb remains in a growth arrested state when cultured in these conditions. I observed that Mtb maintains viability in the absence of replication at pH 5.7 for the 39-day duration of the experiment (Figure 4.1A). I also measured ATP concentration during this viability assay, and observed that ATP concentration in Mtb cultured at

pH 5.7 in glycerol was ~1/4th of the concentration at pH 7.0 (Figure 4.1B) after 6 days of culture, albeit still ~5-fold higher than that of Mtb at either pH 7.0 or 5.7 after 26 days of culture, a time point that is assumed to be carbon limited relative to day 6. Together, these results suggest that Mtb cultured in minimal medium with glycerol as a single carbon source buffered to pH 5.7 is a viable, non-replicating state; a physiology that will hereafter be referred to as acid growth arrest.

To determine whether Mtb under acid growth arrest was still metabolically active, Mtb uptake of ^{14}C-glycerol was measured. Over time, Mtb accumulated ^{14}C-glycerol at pH 5.7, albeit at a rate ~70% lower than at pH 7.0 (Figure 4.2A). In a separate experiment, Mtb was adapted for 3 days to minimal medium with glycerol as a single carbon source at either pH 7.0 or pH 5.7 and washed immediately prior to the addition of radiolabeled carbon sources. In this case, no difference in radiolabel uptake was observed (Figure 4.2B), suggesting that the decreased uptake observed in Mtb under acid growth arrest is not due to changes in cell wall or membrane permeability. To determine whether the imported ^{14}C-glycerol is metabolized by Mtb under acid growth arrest, the incorporation of ^{14}C-glycerol into Mtb lipids was measured. While the level of lipid labeling observed in acid growth arrested Mtb was again reduced ~70% compared to pH 7.0 (Figure 4.2B), radiolabel incorporation into trehalose di- and monomycolate (TDM, TMM), triacylglycerol (TAG), and sulfolipid (SL) was observed in growth arrested Mtb (Figure 4.3C-E). Notably, unlike the observed accumulation of TAG during Mtb non-replicative persistence in response to hypoxia (50), TAG does not accumulate during acid growth arrest. Instead, a small increase in production of sulfolipid and TDM was observed at pH 5.7. The uptake of glycerol as well as its anabolic incorporation into Mtb lipids suggests that Mtb under acid growth arrest is metabolically active, and supports the view that acid growth arrest is a metabolically active, non-replicating state.

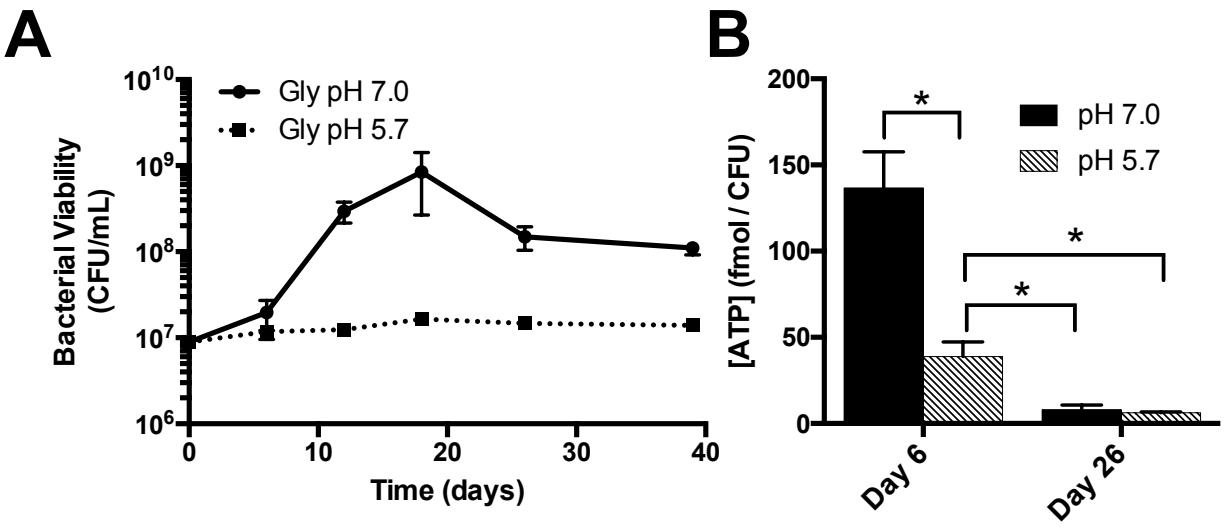

Figure 4.1. Mtb remains viable during acid growth arrest.
A. Mtb remains viable during culture in minimal medium buffered to pH 5.7 with glycerol as a single carbon source in the absence of growth.
B. The concentration of ATP in Mtb under acid growth arrest is reduced compared to pH 7.0, but still higher than that observed on Day 26 at pH 7.0 or pH 5.7. Error bars represent the standard deviation. *$p < 0.05$, using a Student's t-test.

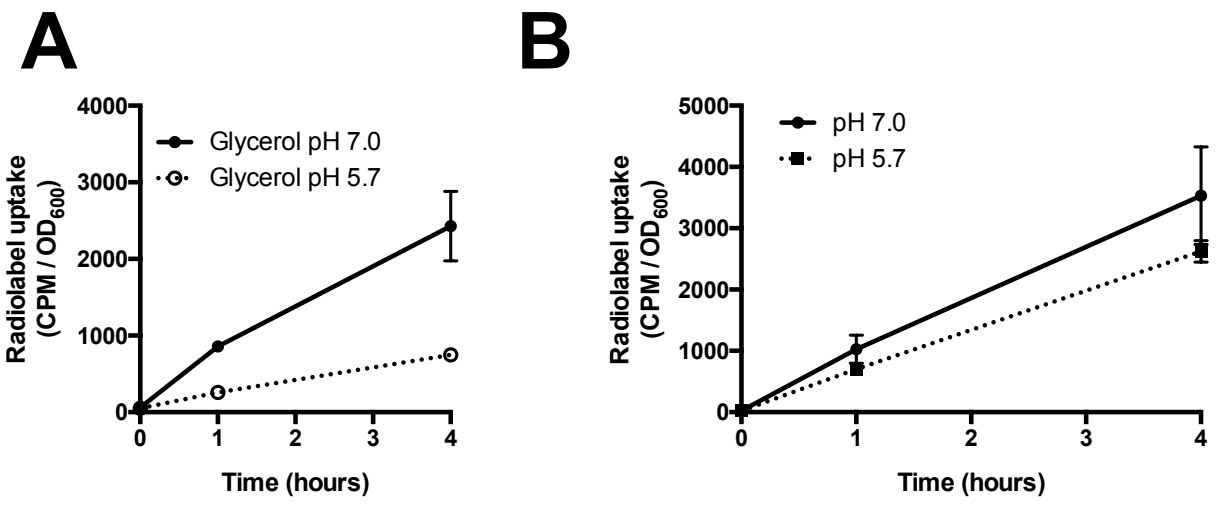

Figure 4.2. Mtb under acid growth arrest is metabolically active.
A. Mtb was incubated in minimal medium with glycerol as a single carbon source at pH 7.0 and pH 5.7 and the uptake of ^{14}C-glycerol was monitored over time. Mtb uptakes ^{14}C-glycerol during acid growth arrest, albeit at a reduced rate.
B. Uptake of ^{14}C-glycerol. Mtb cultures were conditioned to minimal medium with glycerol as a single carbon source for 3 days, pelleted, and resuspended in PBS + 0.05% Tween-80. Accumulation of ^{14}C-glyerol was measured over time, with no significant difference in accumulation observed based on two-way ANOVA (p=0.239). Error bars represent standard deviation.

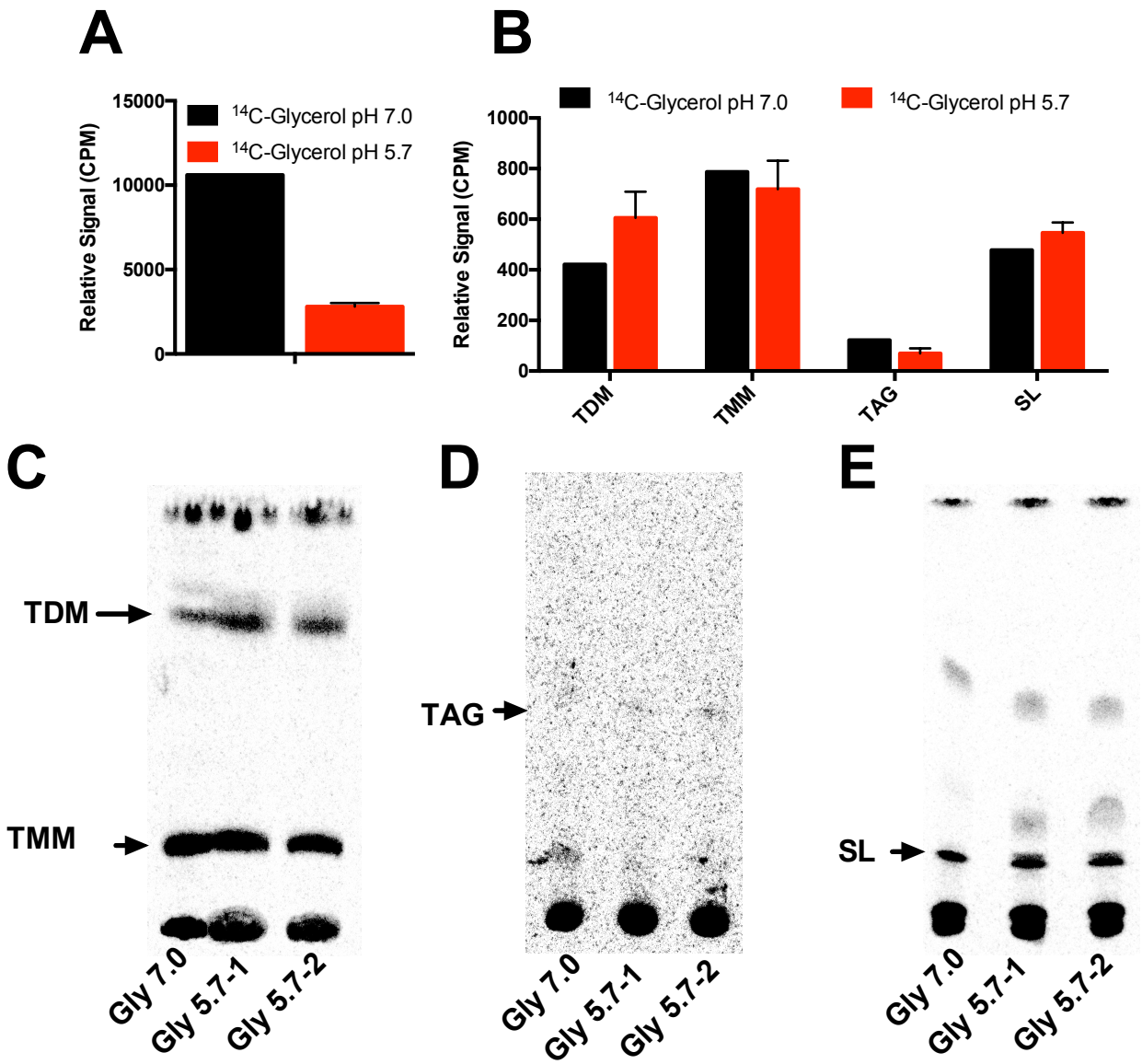

Figure 4.3. Mtb utilizes glycerol for anabolic metabolism during acid growth arrest.
A. Incorporation of ^{14}C-glycerol into Mtb lipids. Following 10 days of culture with ^{14}C-glycerol, lipids were extracted and total radioactivity of the samples was measured. Mtb cultured at pH 5.7 had reduced incorporation of ^{14}C in lipids, although this difference may be in part attributable to increased bacterial numbers over time at pH 7.0.
B. Relative radiolabeled lipid species abundance. Thin layer chromatography (TLC) was performed by spotting 10,000 CPM of ^{14}C-labelled lipids at the origin and developing the TLC in the necessary solvents for separation of trehalose di- and monomycolate (TDM, TMM), and sulfolipid (SL) as described in the methods. For each lipid species, bars indicate relative signal of each lipid species.
C-E. TLC images showing relative abundance of TDM and TMM (C), TAG (D), and SL (E) at pH 7.0 and pH 5.7. Very little ^{14}C-glycerol was incorporated into TAG.

Acid growth arrest is associated with increased antibiotic and SDS tolerance

A hallmark of metabolically active, non-replicating states is the development of phenotypic tolerance to antibiotics and stress (50,56,58,60). The sensitivity of Mtb to isoniazid, rifampin, and the detergent sodium dodecyl sulfate (SDS) was measured to test whether acid growth arrest was associated with phenotypic drug or stress tolerance. The concentration of drug necessary to kill 90% of Mtb (MBC_{90}) at pH 7.0 and pH 5.7 in both rich and minimal media was determined via spot plating of Mtb treated with different concentrations of drug for 6 days. (Table 4.1). The MBC_{90} of isoniazid, rifampin, and SDS was increased in Mtb under acid growth arrest compared to the other conditions tested, demonstrating that acid growth arrest does increase Mtb tolerance to these drugs. A role of acidic pH in promoting antibiotic tolerance by preventing cytosolic alkalinization has been proposed previously in *Mycobacterium smegmatis* (117). Indeed, Mtb grown in minimal medium with pyruvate as a single carbon source does exhibit a higher MBC_{90} to isoniazid at pH 5.7 compared to pH 7.0. However, the MBC_{90} increases even further in Mtb under acid growth arrest. These results indicate that Mtb exhibits phenotypic tolerance during acid growth arrest.

	Isoniazid (μM)	Rifampin (μM)	SDS (%)
7H9 +OADC pH 7.0	3.5	< 0.31	0.03
7H9 +OADC pH 5.7	1.6	< 0.31	0.03
Glycerol pH 7.0	1.6	< 0.31	0.03
***Glycerol pH 5.7**	**>10**	**1.6**	**0.2**
Pyruvate pH 7.0	10	< 0.31	0.06
Pyruvate pH 5.7	4	< 0.31	0.08

***Acid growth arrest**

Table 4.1. Minimum bactericidal concentration (MBC_{90}) of Isoniazid, Rifampin, and SDS in different culture conditions. MBC_{90} is defined as the concentration of drug necessary to reduce CFU by 90% after 6 days of exposure in the specified culture conditions. The culture conditions tested were rich medium (7H9 + OADC) and minimal medium containing glycerol or pyruvate as a single carbon source, buffered to pH 7.0 or pH 5.7. All culture conditions promote Mtb growth except glycerol as a single carbon source at pH 5.7, which is arrested for growth.

A genetic screen to identify mutants with enhanced acidic pH growth arrest

In other persistent states of Mtb, such as starvation (57) or hypoxia (47), cessation of growth is understood to be due to a physiological limitation, such as absence of a carbon source or a terminal electron acceptor. However, Mtb under acid growth arrest is provided both a metabolically utilized carbon source, glycerol, as well as a terminal electron acceptor, oxygen. I hypothesized that instead of representing a physiologic limitation, acid growth arrest is a regulated adaptation of Mtb. To test this hypothesis, a genetic screen was performed to identify mutants unable to arrest growth at acidic pH. A transposon mutant library containing >100,000 mutants was plated on agar plates containing minimal medium buffered to pH 5.7 and supplemented with 10 mM glycerol. Mutants with enhanced acid growth (*eag* mutants) formed colonies that were isolated. Isolated mutants were confirmed as *eag* mutants by measuring bacterial growth in minimal medium supplemented with 10 mM glycerol at pH 5.7 (Figure 4.4A-B). In total, 165 mutants were isolated from plates, of which 98 were confirmed as *eag* mutants. In addition to the transposon mutant screen, wild type *M. tuberculosis* was plated on the same acid growth arrest condition to screen for spontaneous *eag* mutants. Two spontaneous mutants were isolated, both exhibiting robust growth in minimal medium supplemented with glycerol at pH 5.7 (Figure 4.4C).

The transposon insertion site was determined for the confirmed *eag* mutants. For select transposon mutants, complementation was attempted via introduction of an integrative plasmid expressing the wild type version of the disrupted gene with its native promoter. This attempt at complementation did not restore the wild type growth arrest phenotype (Figure 4.5A), even though measurement of transcript levels revealed that the complementation constructs did restore mRNA levels of the disrupted genes to wild type levels (Figure 4.5B). The observation of genetic complementation without phenotypic complementation suggests that these disrupted genes were not responsible for the enhanced acid growth phenotype.

Given the isolation of spontaneous *eag* mutants, I hypothesized that the lack of complementation in the transposon *eag* mutants may be due to additional spontaneous mutations within the transposon library. To test this hypothesis, whole genome sequencing was performed on both the spontaneous mutants and select transposon mutants. Of the 6 *eag* mutants sequenced, 4 contained a missense mutation in the Mtb gene *PPE51* (*MT3221*, *Rv3136*), including both spontaneous *eag* mutants (Table 4.2). The presence of single nucleotide variants was confirmed by amplification and Sanger sequencing of the *MT3221* gene from each mutant as well as a wild type control. Overexpression of the S211R-encoding mutant allele of *MT3221* in wild type Mtb was sufficient to allow growth at acidic pH with glycerol as a single carbon source (Figure 4.6A), whereas overexpression of the wild type *MT3221* allele in the *eag* mutant background did not restore growth arrest (Figure 4.6B), revealing that the S211R-encoding mutation has a dominant effect on enhanced growth at acidic pH. Thus, the mutation in MT3221 giving rise to the S211R variant protein was shown to be sufficient for enhanced growth at acidic pH, demonstrating a genetic basis for acid growth arrest.

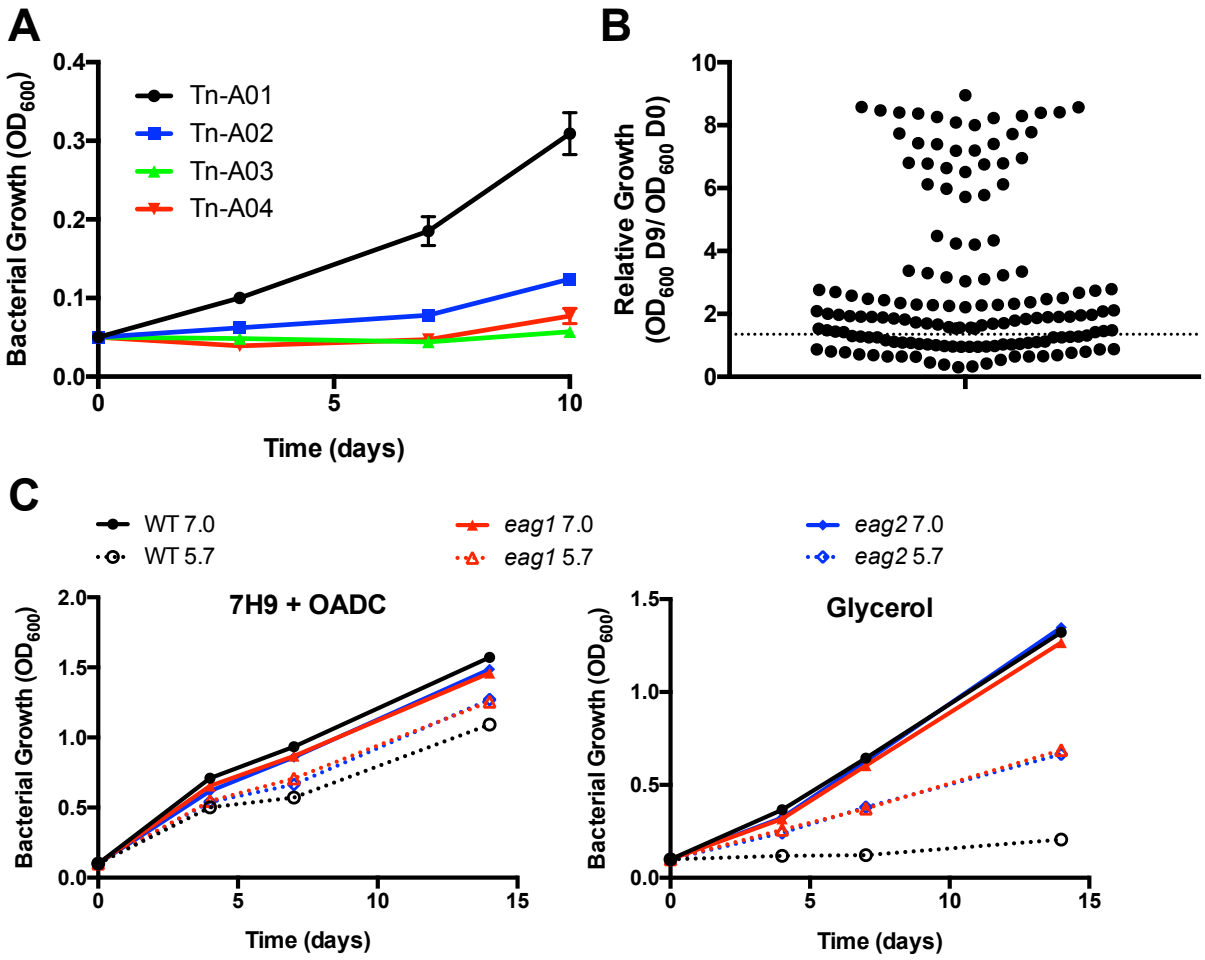

Figure 4.4. Genetic screen to identify mutants with enhanced growth at acidic pH. Mutants able to form colonies on agar plates buffered to pH 5.7 containing glycerol as a single carbon source were isolated and confirmed as enhanced acid growth (*eag*) mutants by measuring growth in liquid culture conditions of acid growth arrest.

A. Representative growth curve of four isolated mutants, two of which were confirmed as *eag* mutants.

B. Compiled growth phenotypes for all isolated mutants. Each dot represents an individual mutant, with the fold change in OD_{600} from day 0 to day 9 reported. The dotted line represents the fold change observed in the WT control.

C. Growth curves in rich medium (7H9+OADC) and in minimal medium with glycerol as a single carbon source with two spontaneous *eag* mutants. Notably, the enhanced growth of *eag* mutants is only observed at pH 5.7 and not at pH 7.0.

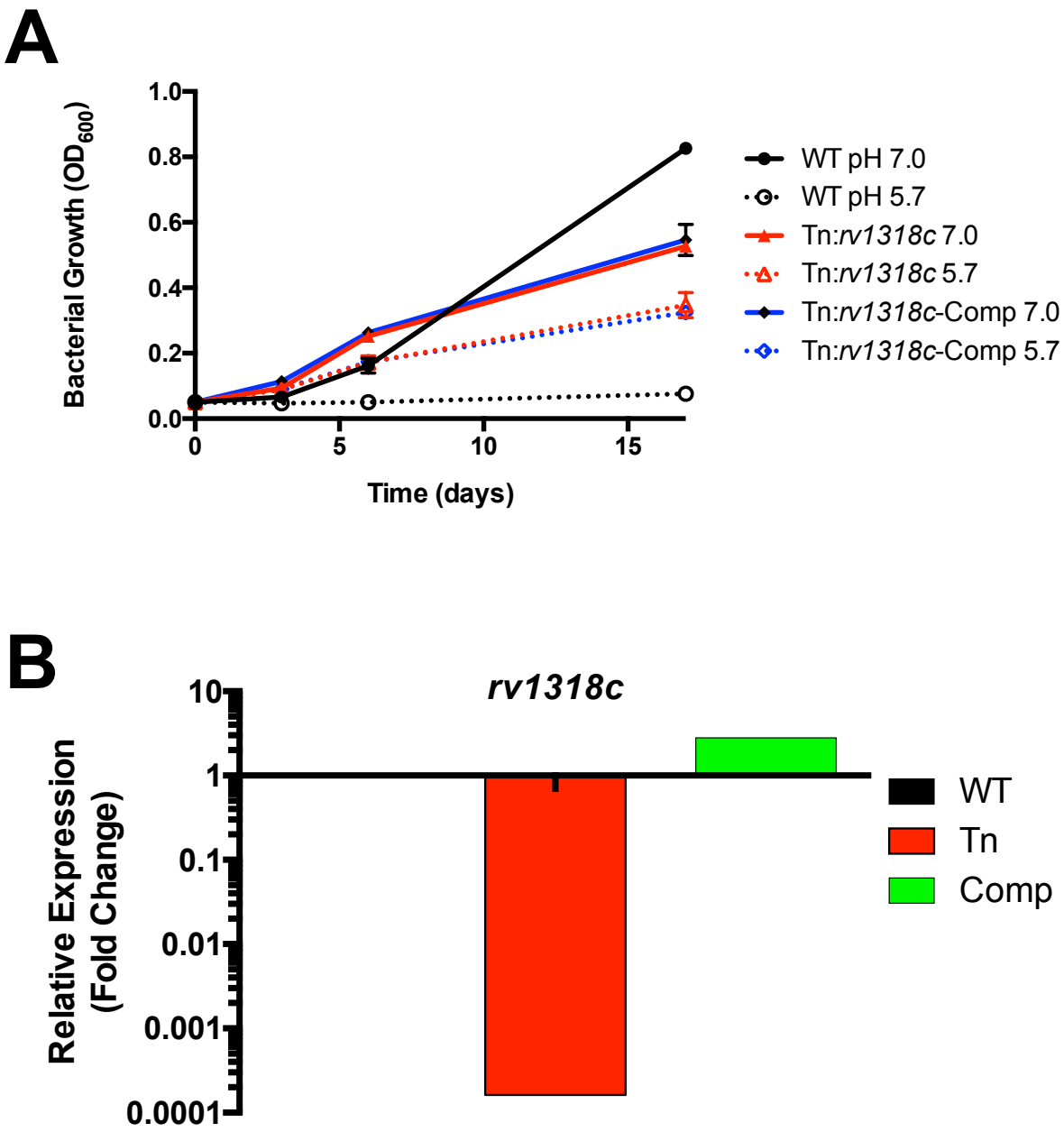

Figure 4.5. *eag* mutant genetic complementation of a transposon mutant does not restore growth arrest.

A. Failed phenotypic complementation of a transposon *eag* mutant, Tn:*rv1318c*. The mutant was complemented by introduction of an integrative plasmid containing an intact version of the disrupted gene, *rv1318c*, and its native promoter. WT, wild type Mtb.

B. Genetic complementation of Tn:*rv1318c*. Quantitative real time PCR revealed that the complementation strain (Comp) of Tn:*rv1318c* can restore the decreased expression of *rv1318c* transcript levels in Tn:*rv1318c* (Tn).

Strain	Position	Reference	Alternate	Quality Score	Depth Score	Mutation	Gene ID	Rv #	Comment
eag1	*338965*	*G*	*C*	*602*	*619*	Intergenic	MT0292	Rv0280	PPE family protein
	3497961	**C**	**A**	**7022**	**200**	**A228D**	MT3221	Rv3136	PPE family protein
eag2	**3497961**	C	A	2462	74	**A228D**	MT3221	Rv3136	PPE family protein
Tn: *lldD2*	**3497909**	**A**	**C**	**7553**	**205**	**S211G**	MT3221	Rv3136	PPE family protein
	3973579	G	T	7077	187	P131V	MT3646	Rv3542c	Essential for growth on cholesterol
Tn: *rv1318c*	563721	C	T	7272	195	R140S	MT0487	Rv0470A	Hypothetical protein
	3242629	A	C	74	79	H955P	MT3000	Rv2931	ppsA, involved in PDIM synthesis
	3497911	**C**	**G**	**6310**	**166**	**S211R**	MT3221	Rv3136	PPE family protein
Tn: *aao*	3337728	AGCTTTCTTC	A	1298.97	80	Del (27bp)	MT3061	Rv2983	Conserved Hypothetical
Tn: *papA5*	4297378	A	G	3861	107	Promoter	MT3938	Rv3830c	Possible TetR family

Table 4.2. Summary of variants identified by whole genome sequencing. Variants were identified using a GATK workflow as described in the experimental methods. 3 unique missense mutations were identified in *MT3221* at 2 unique sites in 4 different mutants. The spontaneous mutants are named *eag1* and *eag2*, whereas the four transposon mutants are named according to the location of the transposon insertion.

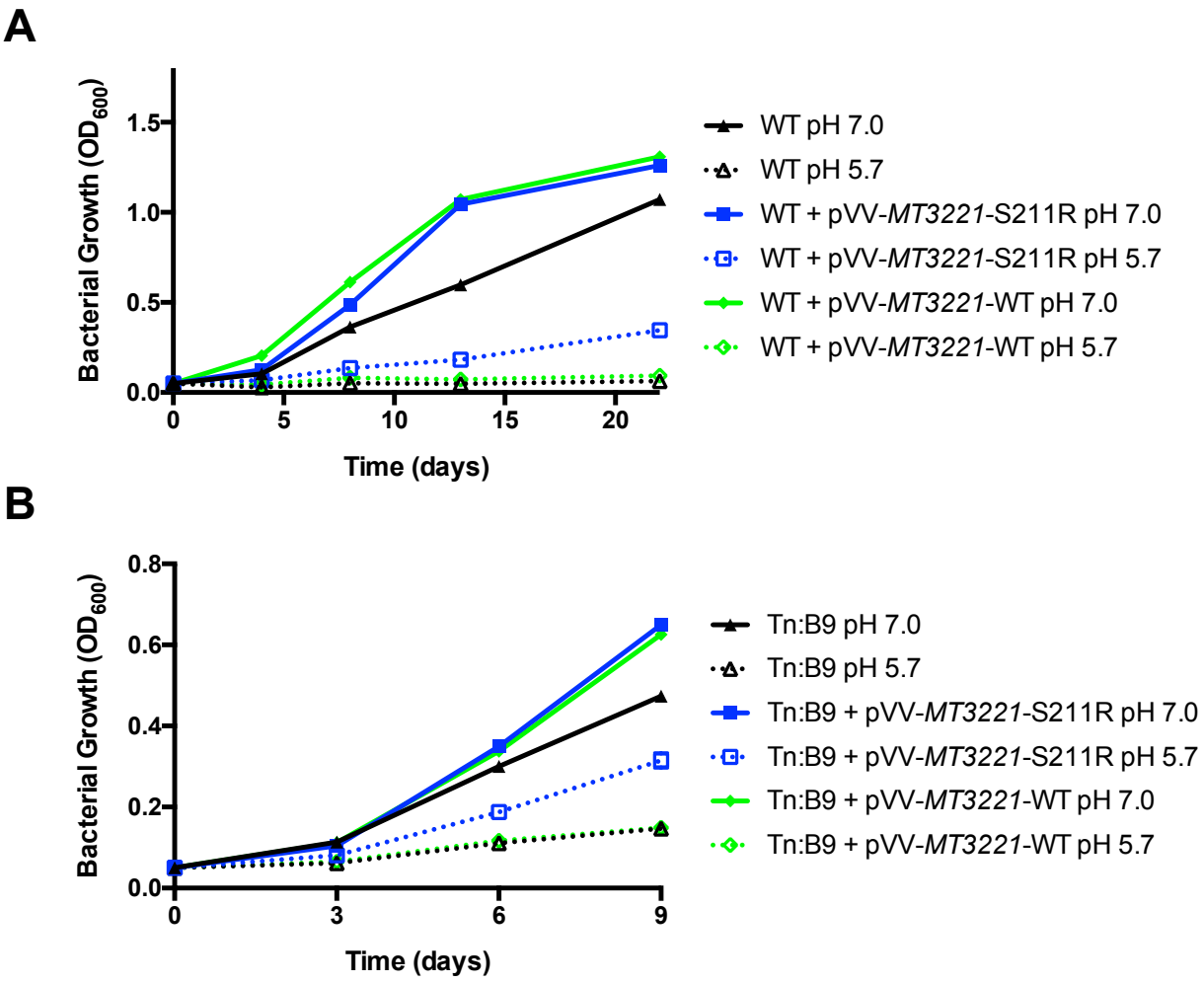

Figure 4.6. The S211R-encoding mutant allele of MT3221 enhances Mtb growth at acidic pH on glycerol. A) Growth curve of wild type Mtb (black) and wild type Mtb containing a plasmid overexpressing either the wild type or S211R-encoding mutant allele of *MT3221* (blue and green, respectively). Both overexpression constructs increase Mtb growth at pH 7.0, but only the mutant allele promotes Mtb growth at pH 5.7. B) Growth of the Mtb mutant containing spontaneous S211R-encoding mutation in *MT3221*. Overexpression of the wild type allele does not arrest growth at pH 5.7, and overexpression of the mutant MT3221 allele increases growth in the Tn:B9 mutant. Both overexpression constructs increase growth of the Tn:B9 strain at pH 7.0. Error bars represent the standard deviation.

Identification of polar effects in eag transposon mutants.

Of the 98 transposon mutants for which the transposon insertion site was identified, 7 independent insertions were found in the gene *fbpB* (*MT1934, rv1886c*; Figure 4.7A*)*. Given the unlikelihood of identifying 7 independent *fbpB* transposon mutants without disruption of *fbpB* being associated with enhanced acidic growth, I sought to characterize the genetic basis of these *eag* mutants. Introduction of an integrative plasmid containing *fbpB* and its native promoter was not able to restore growth arrest at acidic pH (Figure 4.7B). I hypothesized that polar effects caused by insertion of the transposon could be altering transcription of genes upstream or downstream of the *fbpB* gene*.* Indeed, measurement of mRNA transcript levels in wild type, two *fbpB* transposon mutants, and their complements revealed that while complementation of the *fbpB* mutants was sufficient to restore expression of *fbpB*, expression of the downstream gene, *rv1885c*, was $1/10^{th}$ of the wild type expression level in both the mutant and complemented strains (Figure 4.7D). The observation of polar effects in these *fbpB* transposon mutants suggests that the enhanced acidic growth phenotype could be due to repression of *rv1885c* expression rather than to disruption of *fpbB*.

A

Mutant ID	Insertion Site	Growth Ratio
Tn:*fbpB*-1	126	1.25
Tn:*fbpB*-2	146	1.93
Tn:*fbpB*-3	304	1.85
Tn:*fbpB*-4	404	1.56
Tn:*fbpB*-5	410	1.89
Tn:*fbpB*-6	449	1.25
Tn:*fbpB*-7	998	4.34

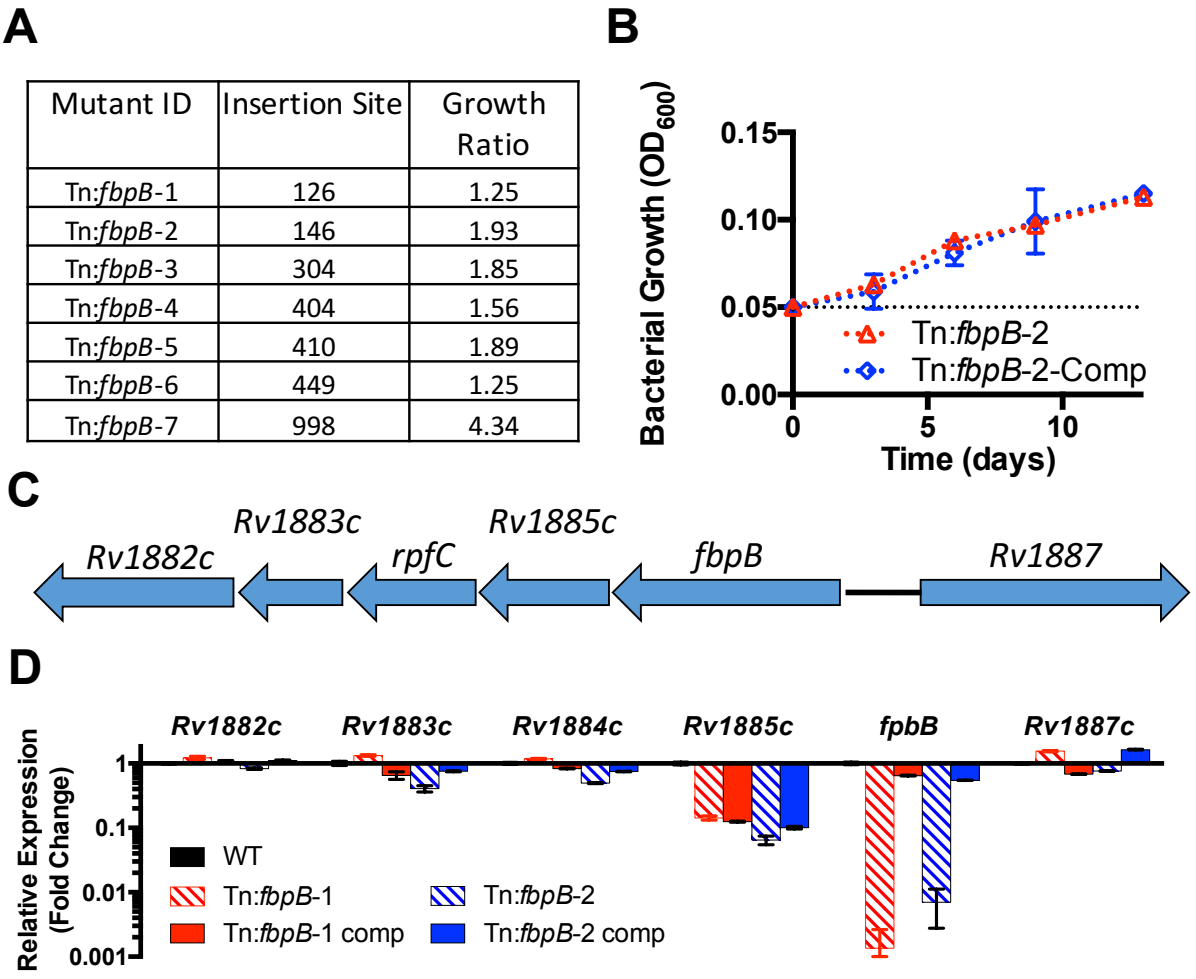

Figure 4.7. Identification of polar effects of transposon insertion in Tn:fbpB transposon mutants.

A. Table of seven isolated Tn:*fbpB* mutants with the insertion site and measured growth ratio (OD_{600} at Day 9 relative to the initial OD_{600}).

B. Growth curve of Tn:*fbpB* and its complement shows no restoration of acid growth arrest in the complemented strain.

C. Schematic diagram of *fbpB* genetic locus.

D. Quantitative real time PCR of the *fbpB* genetic locus. The gene rv1885c is expressed at $1/10^{th}$ of the wild type expression level in two unique Tn:*fbpB* transposon mutants. Complementation restores expression of *fbpB*. Error bars represent the standard deviation.

eag mutants have reduced phenotypic tolerance.

Given the increased tolerance of Mtb during acid growth arrest, I hypothesized that mutants with enhanced acidic pH growth would be more sensitive to both antibiotic and physiological stress. To test this hypothesis, wild type, a transposon *eag* mutant containing the S211R-encoding mutation in *MT3221* (Tn:B9), and WT Mtb containing a plasmid overexpressing either the wild type or mutant *MT3221* overexpression constructs were treated with isoniazid, rifampin, or the bicyclic nitroamidizole PA-824 after 3 days acclimation to minimal medium supplemented with glycerol as a single carbon source buffered to either pH 7.0 or pH 5.7. After exposure to each drug for 6 days, Mtb was plated for viability. Acid growth arrest was associated with 2-fold increased survival in wild type Mtb exposed to rifampin compared to Mtb grown at pH 7.0 (Figure 4.8A). Compared to wild type Mtb, the *eag* mutant exhibited a 1-log reduction in viability at acidic pH (Figure 4.8A), an even greater sensitivity to antibiotics than that of wild type Mtb at neutral pH. Similarly, the eag mutant and wild type Mtb overexpressing the *MT3221*-S211R allele exhibited increased sensitivity to isoniazid at pH 5.7 compared to wild type Mtb, with wild type Mtb overexpressing the wild type *MT3221* allele exhibiting sensitivity intermediate to wild type and mutant Mtb (Figure 4.8B). For both isoniazid and rifampicin, no significant difference in sensitivity was observed between strains at pH 7.0 (Figure 4.8A-B). The bicyclic nitroamidazole PA-824 was shown to be comparably effective at killing Mtb at both pH 7.0 and pH 5.7, demonstrating that Mtb growth arrest is not protective against all classes of antibiotics. The *eag* mutant and both *MT3221* overexpression strains exhibited decreased survival compared to wild type Mtb at pH 7.0 when treated with PA-824, but the slight decreases in survival in the *eag* mutant and *MT3221* overexpression strains were not statistically significant (Figure 4.8C). The increased sensitivity of mutants with enhanced growth at acidic pH to both rifampin and isoniazid supports the hypothesis that loss of growth arrest at acidic pH increases Mtb antibiotic sensitivity. Furthermore, the lack of tolerance to PA-824 at acidic pH demonstrates the potential of some antibiotics to be effective even during Mtb growth arrest.

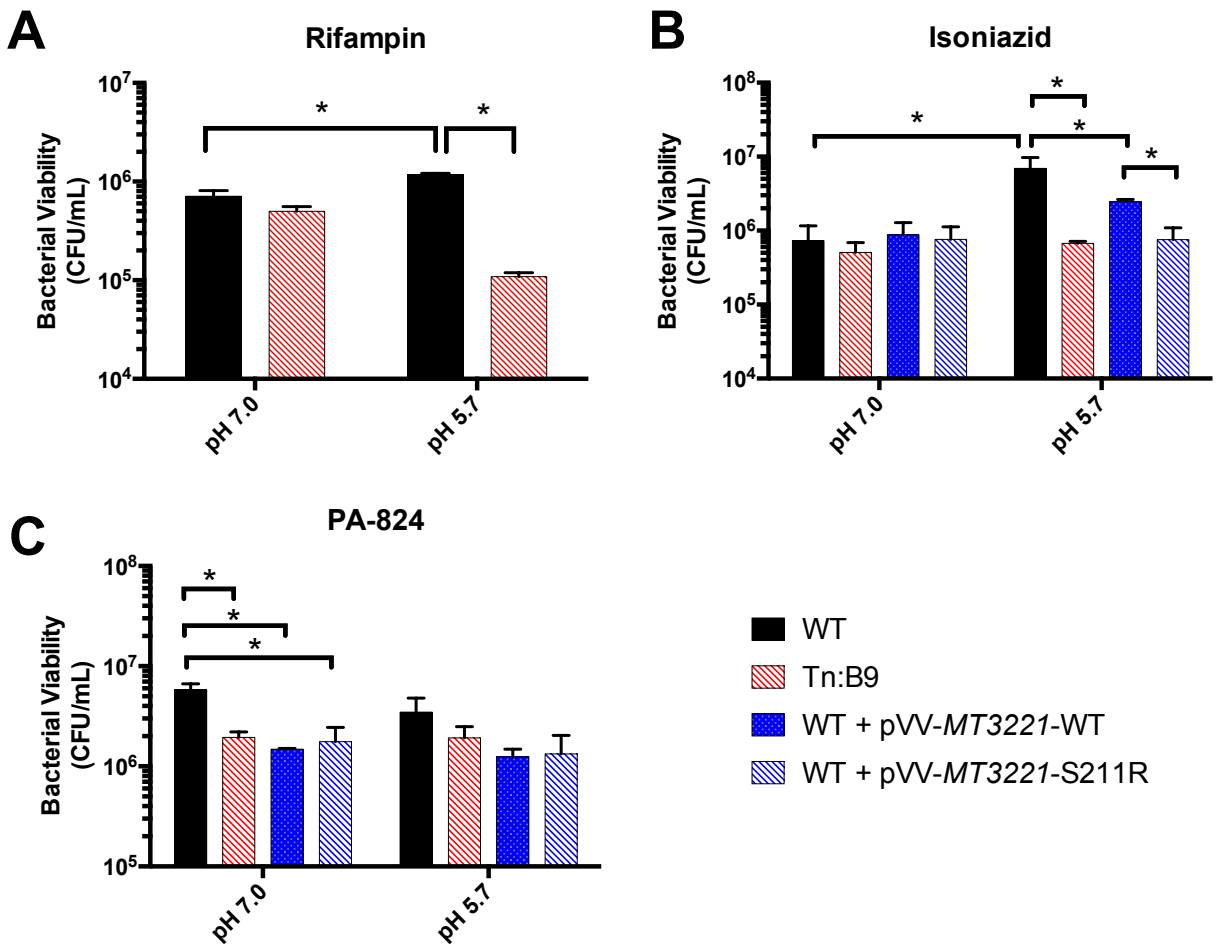

Figure 4.8. Increased sensitivity of enhanced acid growth mutants to antibiotics. Wild type Mtb (WT), an *eag* mutant (Tn:B9), and WT Mtb expressing either the wild type allele or S211R-encoding mutant allele of *MT3221* (WT + pVV-MT3221-WT and WT + pVV-MT3221-S211R, respectively) were acclimated to minimal medium containing glycerol as a single carbon source for 3 days before adding either rifampin (A), isoniazid (B), or PA-824 (C). The *eag* mutant exhibited increased sensitivity to both rifampin and isoniazid at pH 5.7 but not pH 7.0, and the strain overexpressing the S211R-encoding *MT3221* mutant allele also had increased sensitivity to isoniazid at pH 5.7. Both the mutant strain and the *MT3221* overexpression strains demonstrated increased sensitivity to PA-824 at pH 7.0. *$p < 0.05$ based on a student's t-test.

Discussion

The association between non-replicative persistence and phenotypic tolerance is well documented in the Mtb literature (50,56,60,118). The ability of so many distinct environmental conditions to produce a shared phenotype is particularly intriguing, and suggests that the response of Mtb to these environmental conditions may share common mechanisms of persistence. It is worth noting that specific differences in Mtb antibiotic tolerance do exist between the different *in vitro* persistent states. For example, while both hypoxic and nutrient starved non-replicating Mtb exhibit strong tolerance to isoniazid, the hypoxic non-replicating Mtb is less tolerant than starved Mtb to other antibiotics such as rifampin or streptomycin (56). Under conditions of acid growth arrest detailed in this chapter, Mtb exhibits increased tolerance to both isoniazid and rifampin, suggesting shared attributes with non-replicating persistence in response to hypoxia or starvation. Like hypoxia, acidic pH does not confer resistance to PA-824. Given that PA-824 is thought to poison the electron transport chain by acting as an NO donor (119), the lack of resistance to PA-824 during acid growth arrest suggests that under this condition Mtb still requires proper function of the electron transport chain.

In our screen for mutants that have enhanced growth at acidic pH, I identified and confirmed over 50 such mutants. The identification of these mutants supports the view that acid growth arrest is a genetically controlled phenotype in Mtb. Using whole genome sequencing, I identified single nucleotide variants in the gene *MT3221*, a gene that encodes the Mtb protein PPE51. Like many PE/PPE proteins, the function of PPE51 is not known, however; previous transcriptional profiling of Mtb by our lab shows that MT3221 is induced at acidic pH independent of growth arrest in a *phoP*-dependent manner (15,66). *MT3221* expression has also been shown to be reduced during starvation (57). The ability of point mutations in the gene *MT3221* to increase Mtb growth at acidic pH suggests that these mutations can change the activity of PPE51 during acid growth arrest. Given that PPE51 is a membrane-associated protein, I speculate that these point mutations may increase Mtb growth by changing the ability

of PPE51 to interact with other components of the Mtb cell wall. Two of the sequenced *eag* mutants did not contain mutations in MT3221, demonstrating that other mechanisms of enhanced acid growth exist at acidic pH. I anticipate that further whole genome sequencing of *eag* mutants will identify additional metabolic and regulatory mechanisms responsible for growth arrest at acidic pH.

Growth arrest in Mtb is often assumed to be a required outcome of the physiological limitations of Mtb. In the absence of oxygen as a terminal electron acceptor, the obligate aerobe Mtb requires non-replicating persistence to maintain redox homeostasis, and the disruption of this process leads to a short period of enhanced growth followed by increased cell death (50). Similarly, the growth arrest in the Loebel starvation model of persistence is readily attributable to the lack of adequate nutrients for energy generation. In these physiologically limited conditions, the fitness of Mtb is appreciated in its ability to remain viable until the situation improves. In the characterization of acid growth arrest in Mtb, I have demonstrated that growth arrest in this condition is not due to physiological limitation, as I have identified numerous mutants capable of growing where wild type Mtb does not. This suggests that Mtb has evolved to undergo acid growth arrest for reasons beyond specifically surviving the acidic pH environment. I propose that the fitness advantage of Mtb through acid growth arrest is in the ability of acid growth arrest to increase phenotypic tolerance. In this way, Mtb could use the host cue of acidic pH to prepare for the myriad other stresses encountered during infection.

Materials and Methods

Bacterial strains and growth conditions. All Mtb experiments, unless otherwise stated, were performed with Mtb strain CDC1551. Cultures were maintained in 7H9 Middlebrook medium supplemented with 10% OADC and 0.05% Tween-80. All single carbon source experiments were performed in a defined minimal medium as described by Lee *et al.* (36). The Medium was

buffered using 100 mM MOPS (pH 6.6-7.0) or MES (pH 5.7-6.5) (18). For growth experiments, Mtb was seeded in T-25 standing tissue culture flasks in 8 mL of minimal medium at an initial density of 0.05 OD_{600} and incubated at 37^{o}C and 500 µL samples were removed at each time point for optical density measurements. For viability assays, colony forming units were enumerated on 7H10 + 10% OADC agar plates following plating of serial dilutions in PBS + 0.05% Tween-80.

Measurement of ATP concentration. ATP concentration was measured using the commercially available Cell-Titer Glo kit (Promega) with Relative Luminescence Units (RLU) measured using a Perkin Elmer Envision plate reader. A standard curve of varying ATP concentrations was generated to calculate ATP concentrations of each sample based on RLU measurements, and these concentrations were normalized to bacterial CFU as assayed by viability plating.

Transposon library screen. A transposon mutant library of >100,000 mutants was generated using the phage Mycomar-T7 as described previously (120). The library was collected in 4 pools of ~25,000 mutants, and each pool was plated onto MMAT agar plates (1 g/L KH_2PO_4, 2.5 g/L Na_2PO_4, 0.5 g/L $(NH_4)_2SO_4$, 0.15 g/L asparagine, 10 mg/L $MgSO_4$, 50 mg/mL ferric ammonium citrate, 0.1 mg/L $ZnSO_4$, 0.5 mg $CaCl_2$, and 15 g/L agar) containing 10 mM glycerol as a single carbon source and buffered to pH 5.7 with 100 mM MES (18). Mutants capable of forming colonies on these plates were isolated and confirmed for acidic pH growth in liquid culture (MMAT + 10 mM glycerol buffered to pH 5.7 with 100 mM MES). The transposon insertion sites for confirmed mutants were identified using an established inverse PCR technique (121). In addition to the transposon-based screen, wild type Mtb was also plated in similar conditions and spontaneous mutants capable of forming colonies were also isolated.

Mutant Complementation. For confirmed mutants, complementation constructs were constructed by cloning the wild type version of each gene as well as its native promoter (~1000 bp upstream of gene start site) into an integrative plasmid containing a hygromycin resistance cassette, pMV306-Hyg. Efficacy of phenotypic complementation was determined by growth assays in MMAT pH 5.7 + 10 mM glycerol. Genetic complementation was verified by measuring transcript levels of the native gene using quantitative real-time PCR, as described previously (17), with amplification primers designed to flank the site of transposon insertion.

Whole Genome Sequencing. Genomic DNA of selected mutants as well as a wild type control was isolated, DNA libraries constructed, and a total of 12 samples were pooled in a single lane and sequenced using the Illumina MiSeq, in paired end, 250-bp read format (PE250). After the sequencing run, reads were demultiplexed and converted to FASTQ format using the Illumina bcl2 fastq (v1.8.4) script. The reads in the raw data files were then subjected to trimming of low-quality bases and removal of adapter sequences using Trimmomatic (v0.36) (98) with a 4-bp sliding window, cutting when the read quality dropped below 15 or read length was less than 36 bp. The trimmed reads were then aligned to the CDC1551 reference genome using the Burrow-Wheeler Aligner (BWA, (122). Genome Analysis ToolKit (GATK, (123)) base quality score recalibration, indel realignment, and duplicate removal were applied and SNP and INDEL discovery performed.

Determination of MBC90 and measurement of antibiotic tolerance. To measure Mtb antibiotic sensitivity in a variety of media, Mtb was seeded in 30 mL of the specified medium in a T75 flask at an initial density of OD_{600} 0.1 and incubated at 37C with 5% CO_2 for 3 days. After 3 days, cultures were spun down, resuspended in fresh medium of the same kind at OD_{600} 0.1, and 200 µL/well plated in a 96 well plate. 2 µL of antibiotics or SDS was added in 2.5-fold serial dilutions to the plates, and the Mtb incubated at 37°C in 5% CO_2 for 6 days. 10-fold serial

dilutions of the cultures were spot plated on 7H10 + 10% OADC agar plates on day 0 and day 6. The MBC_{90} was determined by the concentration of antibiotic or SDS that produced a one-log change in spot density at day 6 compared to day 0. Using the same experimental design, colony forming units were also measured after treatment with a single concentration of the following drugs: isoniazid (20 μM), rifampin (0.6 μM), and PA-824 (10 μM).

Statistical approaches and data replication.

For experiments measuring Mtb viability, Mtb was cultured in each treatment condition in biological triplicate. The spot plating assays to determine MBC_{90} were performed in biological duplicate and spot plating performed in technical duplicate and are representative data from 2 separate experiments. Bacterial growth curves were performed in biological duplicate except for Figure 4.4C, where two separate *eag* mutants were used for each treatment with similar levels of growth observed. For quantitative PCR experiments, Mtb RNA was isolated in biological duplicate for each treatment or strain and quantitative PCR performed in technical triplicate. Statistical significance of differences was determined based on a student's t-test with a cutoff of $p<0.05$.

Acknowledgements

I would like to acknowledge the assistance of Navanjeet Sahi, Hannah Bodnar, and Emily Juzwiak in the identification of transposon mutant insertion sites as well as the making of reagents and media used in this study.

CHAPTER 5 – Concluding Remarks

Mtb relies on its ability to sense and adapt to the host environment. Therefore, understanding both the environment encountered during infection as well as the response of Mtb to this environment should provide novel insights into how best to treat tuberculosis. To some extent, this work has already begun, as research of Mtb pathogenesis within host model systems such as macrophages, mice, or macaques has identified several genetic factors required for pathogenesis, including the anaplerotic node genes *pckA* (20,21) and *icl (25)*, the two component systems *phoPR* (64) and *dosRST* (5,116), and even global profiling of the genome to identify intracellular essentiality (124). This work has been vital in identifying the genetic basis of pathogenesis in Mtb, as well as emphasizing that the requirements for pathogenesis are often distinct from those necessary for growth *in vitro*. However, given the complexity and temporality of the *in vivo* environment, understanding the exact mechanism of individual genetic determinants is difficult within model systems of infection. To aid in this process, the reductionist approach of using *in vitro* culture to model individual facets of the *in vivo* environment, such as carbon source availability, oxygen tension, pH, nitric oxide, or reactive oxygen species/reactive nitrogen intermediates, has the potential to provide new insights into the mechanisms by which different genetic factors contribute to the pathogenesis of Mtb.

In minimal media culture conditions at acidic pH, Mtb exhibits carbon source specific growth arrest (Chapter 2), and this growth arrest increases Mtb phenotypic tolerance (Chapter 4). Within the *in vitro* context, this growth arrest appears almost unnecessary: Mtb is known to survive acidic conditions as low as pH 4.5 without loss in viability (3), and Mtb at acidic pH maintains a neutral cytoplasmic pH (Figure 2.2). Furthermore, *Mycobacterium smegmatis* has no such growth defect (Appendix Figure 4), indicating that *Mycobacteria* as a genus contains the capacity for growth at acidic pH. Based on these observations, a genetic screen was

performed to test whether acid growth arrest was a regulated process, and the identification of over 50 mutants with enhanced growth at acidic pH provides ample evidence to support that hypothesis (Chapter 4). The defect in phenotypic tolerance in these mutants provides a potential explanation as to why Mtb would evolve to exhibit such growth arrest in response to acidic pH; achieving acid growth arrest could be protective against the concomitant stresses encountered within the host. Investigating the pathogenesis of these mutants within an Mtb infection model, such as macrophage cell culture or a murine infection model, could provide a context in which to test this hypothesis.

One of the more difficult aspects of this research project was the process of phenotypic complementation of transposon mutants with enhanced growth at acidic pH. Indeed, to date only one point mutation within *MT3221* has been shown definitively as a genetic source of enhanced growth at acidic pH (Figure 4.6). The identification of spontaneous mutants within the transposon mutant background (Table 4.2) highlights one significant liability of performing a transposon screen, particularly for screens where spontaneous mutation can easily overcome the selective pressure. An approach to mitigate this liability that was attempted but not optimized is to utilize the next generation sequencing technique Tn-Seq (125) in tandem with a traditional transposon screen. Tn-Seq allows the simultaneous monitoring of all 100,000 transposon mutants simultaneously, with many mutants found within each Mtb gene. Thus, predicting which genes are relevant to a given phenotype can be done with a higher level of confidence. Generating a Tn-Seq dataset in conjunction with a traditional transposon screen allows for a more systematic approach to prioritizing which isolated mutants to study further, and has the added benefit of providing a broader genetic context in which to understand the basis of the phenotype in question. Alternatively, as is evident in the studies of enhanced acid growth mutants in Chapter 4, advances in accessibility and affordability of whole genome sequencing since the beginning of my Ph.D. studies have made it possible to perform genetic screens simply by isolating spontaneous mutants. Arguably, this whole genome sequencing

approach is becoming less resource and time consuming than traditional transposon library screening.

In addition to acid growth arrest, it is also instructive to discuss the conditions permissive for growth at acidic pH, as only 5 of all the carbon sources tested (oxaloacetate, acetate, pyruvate, phosphoenolpyruvate, and cholesterol) produce measureable Mtb growth at acidic pH (Figure 2.1). The specificity of these carbon sources is underscored by the inability of malate, hexanoic acid, or lactate to promote growth; carbon sources that are all a single enzymatic step away from oxaloacetate, acetate, and pyruvate, respectively. We have speculated that the differences in redox potential between these carbon sources could be responsible for their different outcomes on Mtb growth, with Mtb at acidic pH unable to utilize higher redox potential (*i.e.* high ΔE) compounds for growth (Chapter 2). The presence of a more reduced intracellular environment during pH 5.7 growth arrest provides some support for this hypothesis, as does the induction of several genes involved in redox homeostasis at acidic pH (Figures 2.4-5). Furthermore, the observation that Mtb grown on pyruvate at acidic pH secretes succinate provides another potential link between redox homeostasis and acidic pH (Chapter 3).

A notable exception to this redox potential hypothesis is the growth observed on cholesterol, a metabolite with a high redox potential. This exception is pertinent, as cholesterol has been shown to be an important carbon source during Mtb infection. The mechanisms by which Mtb metabolizes this high redox potential carbon source within an acidic environment are worth further characterization. One speculative possibility is that Mtb is capable of catabolizing cholesterol independent of redox-dependent enzymatic mechanisms such as dehydrogenases or oxygenases, and as such the hypothesized redox limitations of acidic pH would not restrict Mtb growth on cholesterol. This sort of redox-independent metabolic pathway for cholesterol catabolism was identified recently in the soil bacterium *Sterolibacterium denitrificans*, where cholesterol catabolism was shown to proceed via hydroxylation and hydrolysis reactions that degrade cholesterol regardless of oxygen availability (126,127). Given the importance of

cholesterol metabolism to Mtb pathogenesis, whether Mtb catabolizes cholesterol in a similar manner to *S. denitrificans,* or whether another explanation exists for Mtb growth on cholesterol at acidic pH is certainly an area worth further investigation.

Ultimately, one of the main host environments in which Mtb encounters acidic pH is the phagosome, an environment with ample cholesterol present, suggesting that the acidic environment encountered during infection ought to be growth permissive. Consistent with this hypothesis, *Mycobacterium marinum* within the zebrafish phagolysosome is observed to replicate, albeit at a slower rate, even in conditions as acidic as pH 4.5 (10). To properly interpret and apply the findings from the *in vitro* investigations of Mtb acid adaptation, this *in vivo* context in which Mtb encounters acidic pH must be considered. One aspect of this response worth considering is whether Mtb reduces the use of carbon sources such as glycerol for growth at acidic pH. It is reasonable to assume that catabolism of glycerol at acidic pH *in vivo* could lead to a markedly altered physiological state compared to catabolism of cholesterol or its catabolic products. Perhaps the carbon source specific growth observed *in vitro* is simply an unintended consequence of Mtb remodeling metabolism to a host-adaptive program. The mutants generated in Chapter 4 could be of use to test this hypothesis.

How Mtb adapts to the host environment is crucial to its success as a pathogen, and the ability of Mtb to slow its growth is necessary to tolerate both the host and antibiotic treatment. I have demonstrated that in response to the host cue of acidic pH, Mtb exhibits carbon source specific growth arrest that is associated with metabolic remodeling. Additionally, I have shown that growth arrest at acidic pH is a regulated process, and that dysregulation of acid growth arrest leads to decreased phenotypic tolerance. This work has furthered our understanding of the mechanisms of acid adaptation in Mtb, specifically via regulation of growth and metabolism. This foundation of *in vitro* characterization of acid adaptation provides an opportunity for future targeted investigation of the *in vivo* context of acid adaptation in Mtb, and contributes to our growing understanding of this pervasive and persistent pathogen.

APPENDIX

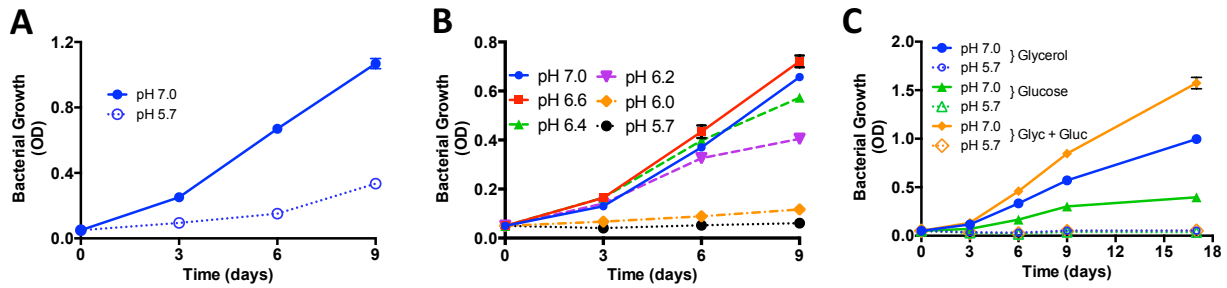

Appendix Figure 1. Mtb slows its growth in response to acidic pH. A. Mtb grown in the rich medium 7H9 slows growth at acidic pH, but does not arrest its growth. B. Mtb grown in minimal medium containing 10 mM glycerol arrests its growth at pH 5.7. The threshold for slowed growth is pH 6.4, the same pH at which the *phoP* pathway is induced by acidic pH. C. Mtb grown on minimal medium containing 10 mM glycerol or 10 mM glucose, or both carbon sources combined, exhibit arrested growth at pH 5.7. Error bars represent the standard deviation and the data are representative of three independent experiments.

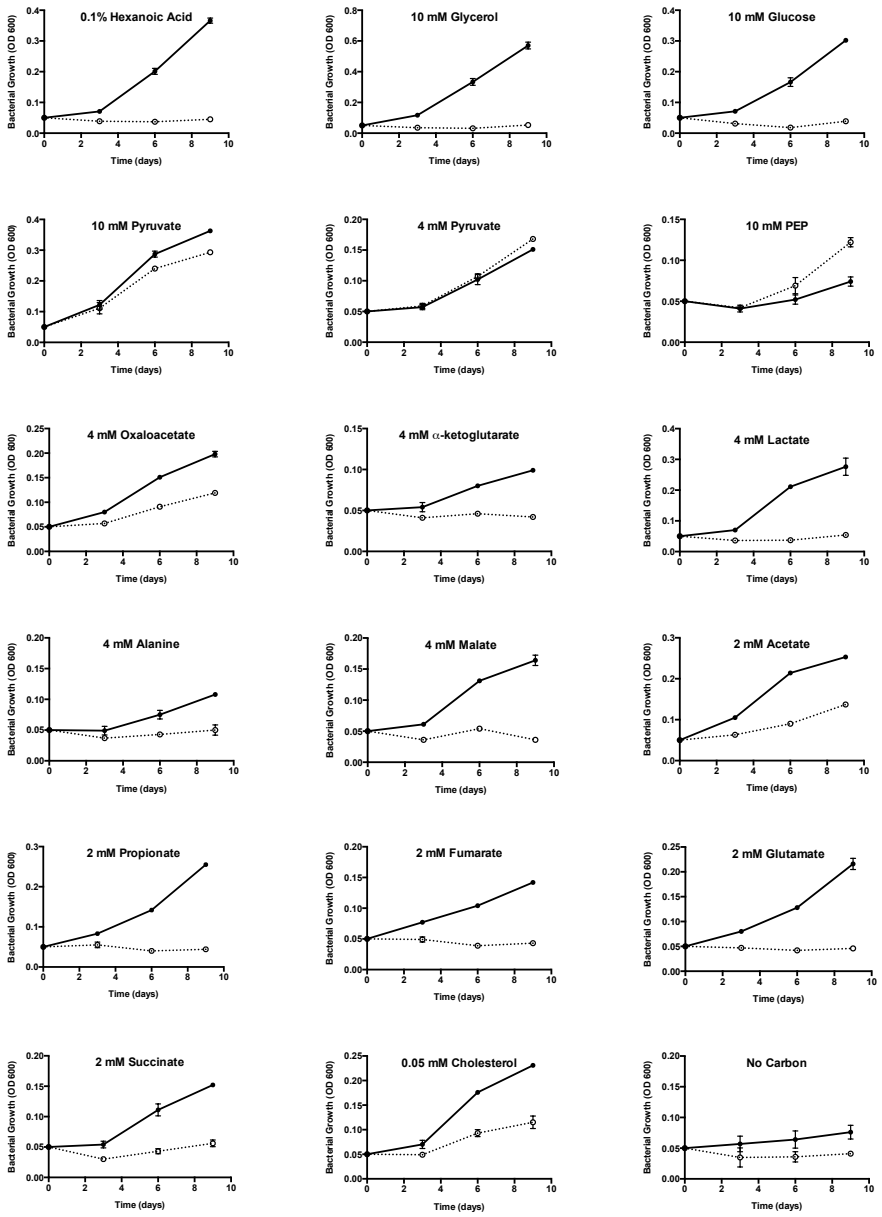

Appendix Figure 2. Nine day growth curves that correspond to the endpoint data summarized in Figure 2.1A.

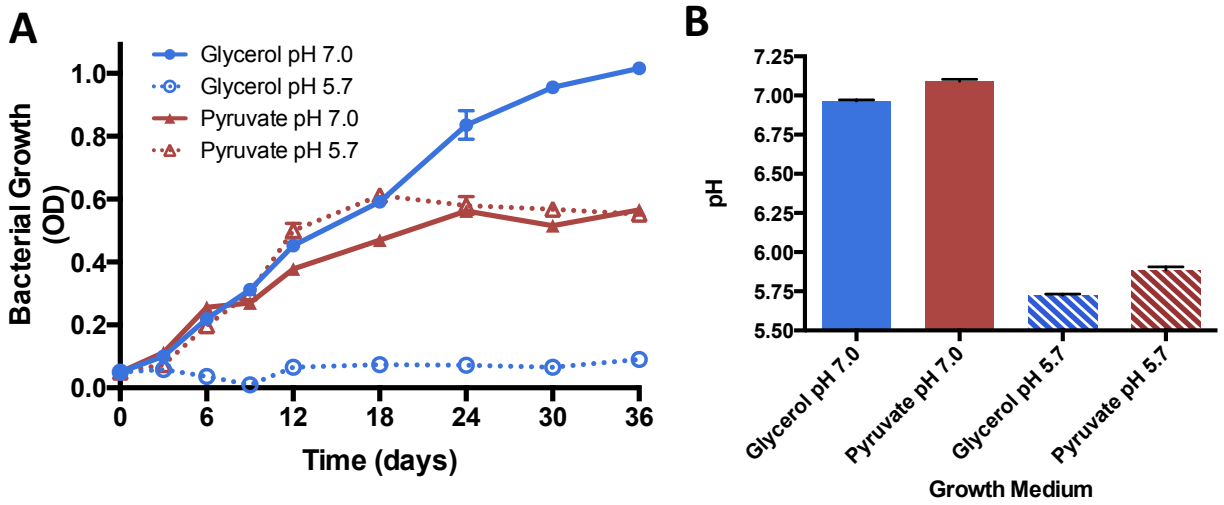

Appendix Figure 3. Long-term growth curves examining Mtb growth and medium pH. A. Growth of Mtb was examined over 36 days in 10 mM glycerol or 10 mM pyruvate at acidic and neutral pH. At stationary phase, Mtb accumulates a greater total biomass in glycerol at pH 7.0 as compared to pH 5.7, whereas, a similar total biomass is observed in pyruvate at both pH 7.0 and 5.7. B. pH of the culture supernatants was measured at the end of the time course. The media initially buffered at pH 7.0 with 100 mM MOPS or pH 5.7 with 100 mM MES maintained their pH through the course of the experiment.

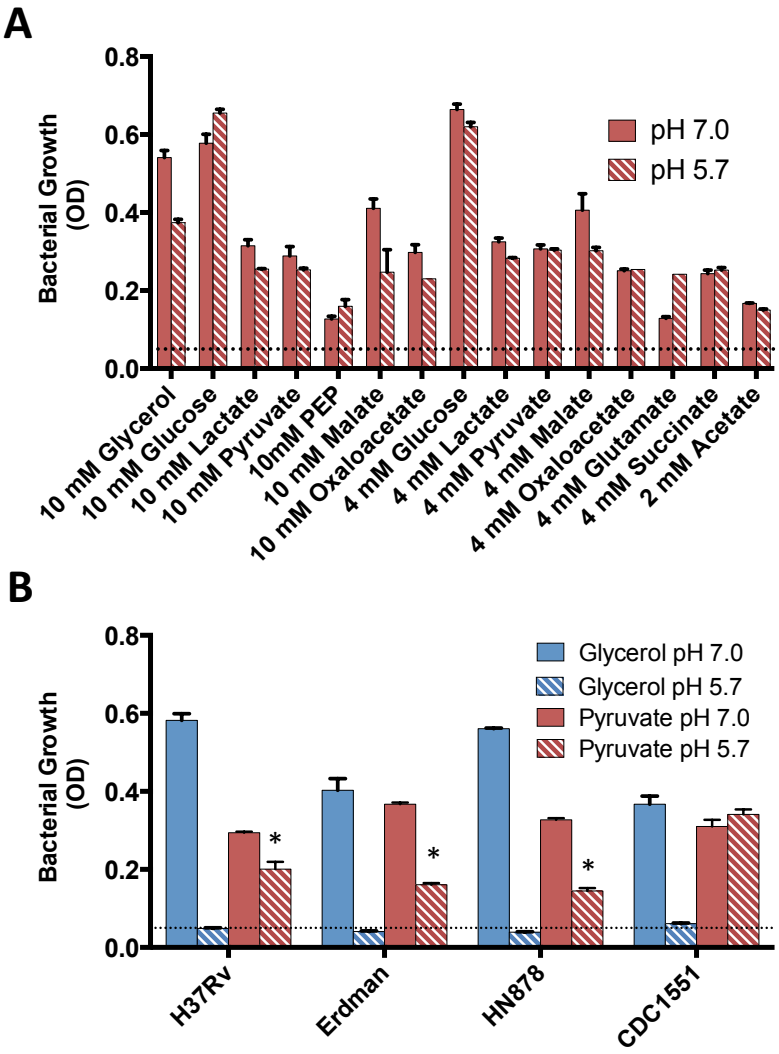

Appendix Figure 4. Carbon source specific growth arrest at acidic pH is species specific. A. *Mycobacterium smegmatis* does not arrest its growth at acidic pH on any of the tested carbon sources. Growth was initiated at a starting density of 0.05 OD_{600} (horizontal dotted line) and growth was measured at day 6. B. Growth arrest phenotypes at day 9 are generally conserved amongst diverse strains of Mtb. H37Rv, Erdman, HN878, and CDC1551 all exhibit carbon source specific growth arrest on glycerol and pyruvate enables growth. Error bars represent the standard deviation and the data are representative of three individual experiments. * shows that in pyruvate at acidic pH, H37Rv, Erdman and HN878 have significantly lower growth ($p<0.01$ using a student's t-test) as compared to CDC1551.

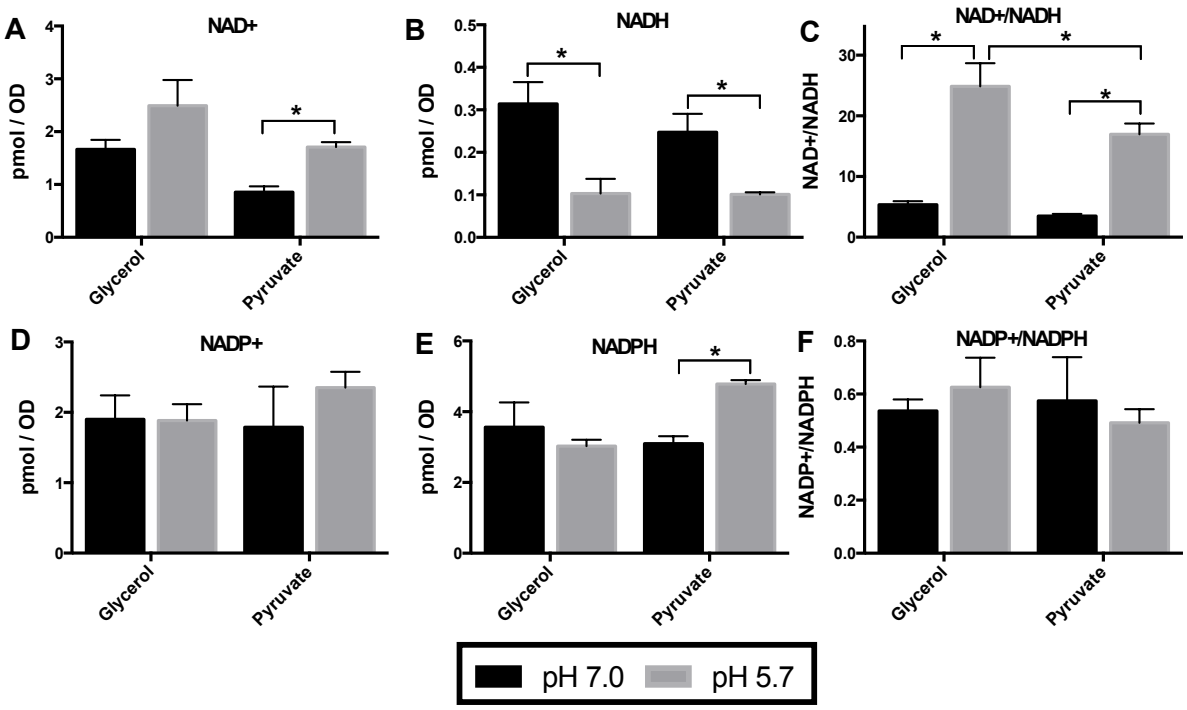

Appendix Figure 5. NAD(P)/NADPH ratios at acidic and neutral pH in 10 mM glycerol or 10 mM pyruvate. A. NAD^+ concentration. B. NADH concentration C. NAD^+/NADH ratio, D. $NADP^+$ concentration. E. NADPH concentration F. $NADP^+$/NADPH ratio. Error bars represent the standard deviation of three biological replicates and two technical replicates. Error bars represent the standard deviation of three biological replicates each calculated from the average of two technical replicates. The data are representative of three individual experiments. *$p<0.05$ using a student's t-test.

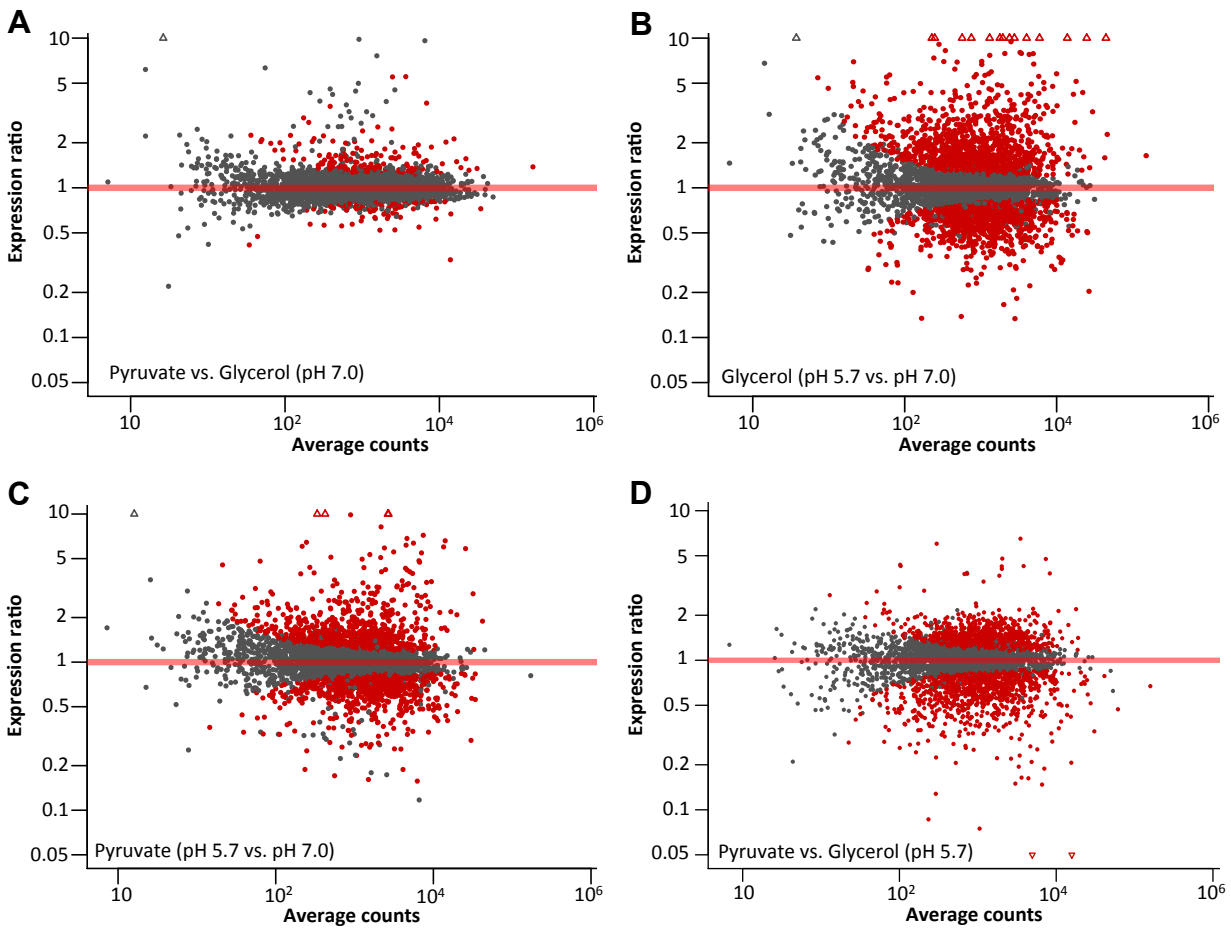

Appendix Figure 6. RNA-seq scatter plots demonstrate significant pH- and carbon-source specific transcriptional adaptations. A. Differential expression of genes at pH 7.0 in pyruvate as compared to glycerol (genes induced or repressed in the presence of pyruvate). B. Differential expression of genes in glycerol at pH 5.7 as compared to pH 7.0. (genes are induced or repressed at pH 5.7). C. Differential expression of genes in pyruvate at pH 5.7 as compared to pH 7.0. (genes are induced or repressed at pH 5.7). D. Differential expression of genes at pH 5.7 in pyruvate as compared to glycerol (genes induced or repressed in the presence of pyruvate). Scatter plots represent the average of 2 biological replicates. The red spots have a p-value <0.05. The triangles are beyond the scale of the axis.

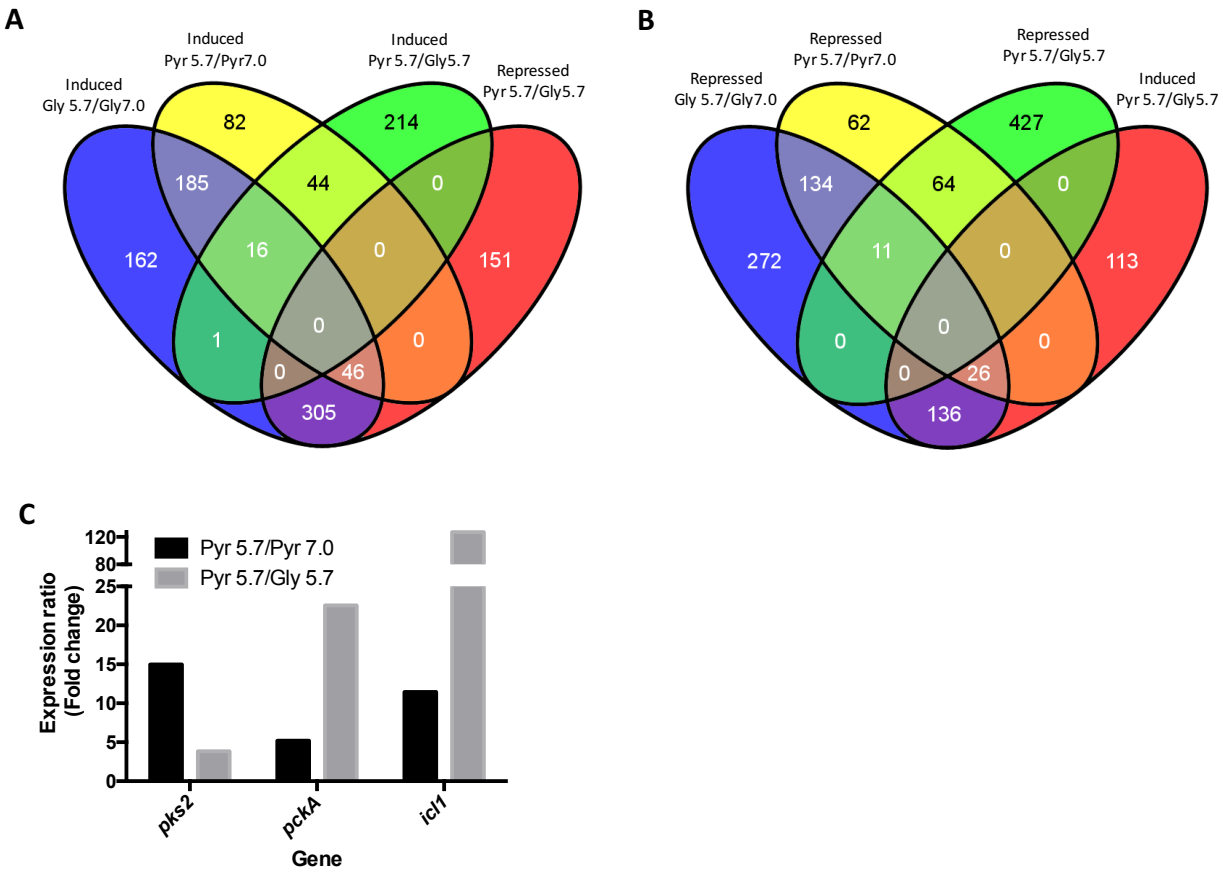

Appendix Figure 7. Genes that are induced or repressed by acidic pH in a carbon source independent and dependent manner. A. Venn diagram of genes that are induced at acidic pH by glycerol or pyruvate. B. Venn diagram of genes that are repressed at acidic pH by glycerol or pyruvate. These Venn diagrams correspond to the gene lists found on the GEO database. C. RNA-seq expression data for *pks2*, *icl1*, and *pckA* was confirmed using quantitative real-time PCR and previously described methods (17). The acidic pH induction of *pks2* was confirmed to be carbon source independent, and acidic pH induction of *icl1* and *pckA* was confirmed to be enhanced in pyruvate.

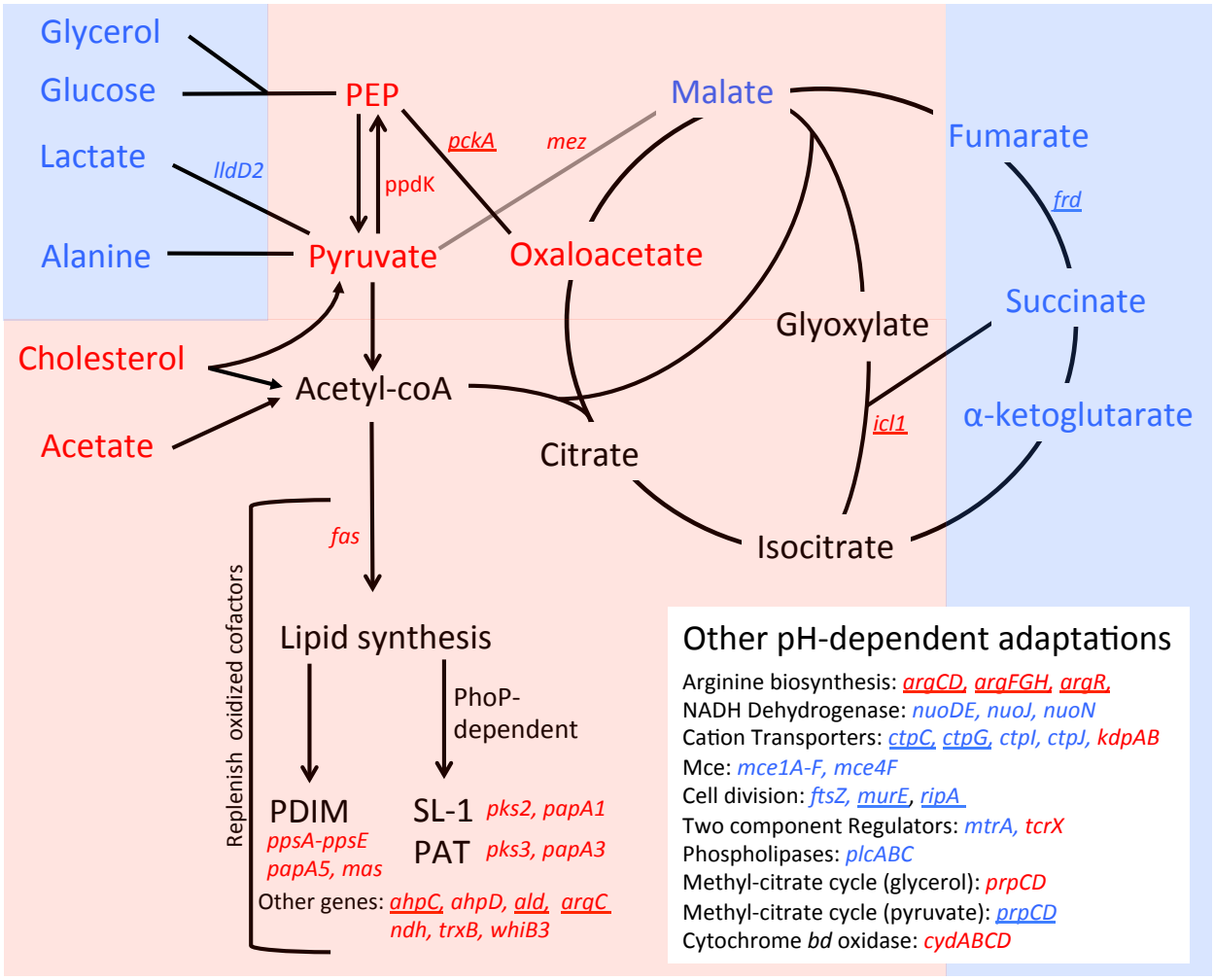

Appendix Figure 8. Summary model of growth and transcriptional profiling experiments examining pH-driven remodeling of physiology. Carbon sources in red or blue are permissive or non-permissive for growth at acidic pH, respectively. Genes in red or blue are induced or repressed at pH 5.7, respectively. Genes that are underlined are significantly more differentially regulated in pyruvate as compared to glycerol. Metabolic pathways shaded in red are favored at acidic pH. This figure was modeled after that by Muñoz-Elías and McKinney (88).

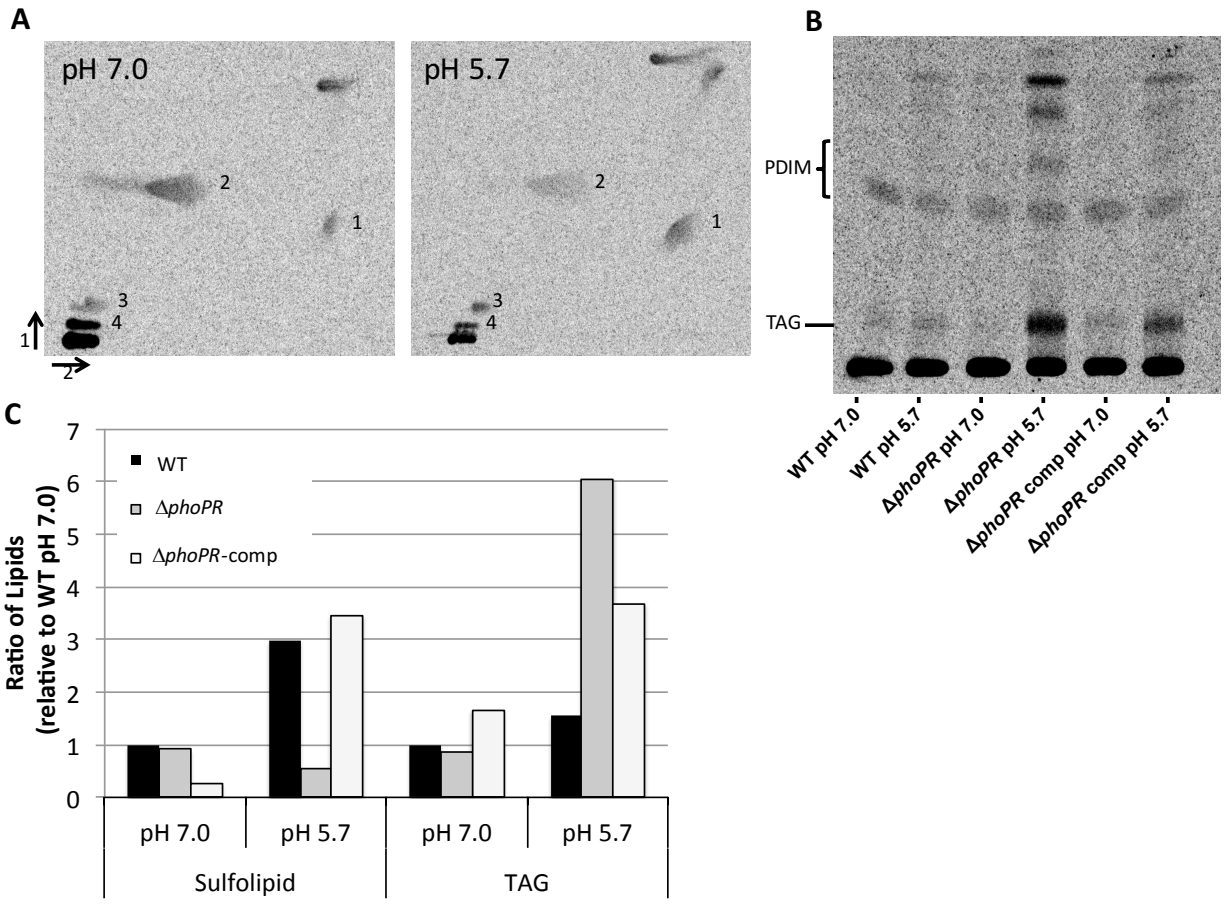

Appendix Figure 9. Acidic pH modulates Mtb lipid metabolism and carbon metabolism. A. 2D TLC to examine ^{14}C acylated trehaloses in WT Mtb at pH 7.0 and pH 5.7. The first dimension is chloroform:methanol:water (100:14:0.8 v/v/v) and in the second dimension chloroform:acetone:methanol:water (50:60:2.5:3, v/v/v/v). Bands 1, 2, 3 and 4 are predicted to be sulfolipid, trehalose dimycolate (TDM), di- or polyacyltrehaloses (DAT or PAT) or trehalose monomycolate (TMM), respectively, based on published studies (128). B. Analysis of PDIM accumulation at acidic pH. The TLC was developed in petroleum ether:acetone (98:2, v/v), and PDIM was identified based on the relative position on the TLC and previous mass spectrometry-based characterization (17). C. Relative ratios of lipids in Figure 2.6A-B relative to WT at pH 7.0. Quantification was performed using the ImageJ software.

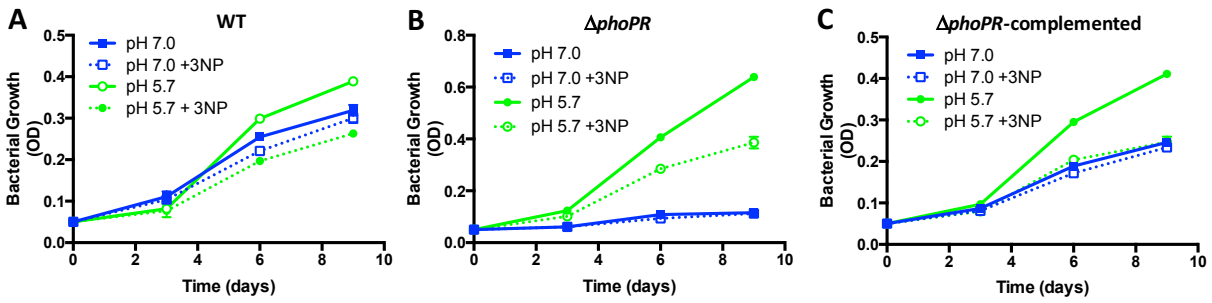

Appendix Figure 10. Nine day time course examining growth of Mtb in response to 3-NP. A. Wild type. B. Δ*phopPR*. C Δ*phopPR* complemented. The end-point data are presented in Figure 2.6C.

Dependent Variable				Mean Difference (I-J)		Sig. [b]		Difference [b]			
								Lower Bound		Upper Bound	
				Population		Population		Population		Population	
		Condition 1	Condition 2	Δ*icl1/2*	WT	Δ*icl1/2*	WT	Δ*icl1/2*	WT	Δ*icl1/2*	WT
2-Methylcitrate	Day 3	Gly pH 5.7	Gly pH 7.0	-11.419 *	-0.302	0.000	1.000	-17.883	-7.766	-4.955	7.161
			Pyr pH 5.7	-5.269	-0.033	0.162	1.000	-11.733	-7.496	1.195	7.431
			Pyr pH 7.0	2.746	-0.034	1.000	1.000	-3.718	-7.497	9.209	7.430
		Gly pH 7.0	Pyr pH 5.7	6.150	0.270	0.069	1.000	-0.314	-7.194	12.614	7.733
			Pyr pH 7.0	14.165 *	0.268	0.000	1.000	7.701	-7.195	20.628	7.732
		Pyr pH 5.7	Pyr pH 7.0	8.015 *	-0.001	0.010	1.000	1.551	-7.465	14.478	7.462
3-phosphoglycerate	Day 3	Gly pH 5.7	Gly pH 7.0	-0.284	-0.223	0.051	0.370	-0.569	-0.552	0.001	0.106
			Pyr pH 5.7	-0.042	-0.148	1.000	1.000	-0.327	-0.477	0.243	0.181
			Pyr pH 7.0	-.547 *	-0.064	0.000	1.000	-0.832	-0.393	-0.262	0.265
		Gly pH 7.0	Pyr pH 5.7	0.243	0.075	0.130	1.000	-0.042	-0.255	0.528	0.404
			Pyr pH 7.0	-0.263	0.159	0.082	1.000	-0.548	-0.170	0.022	0.488
		Pyr pH 5.7	Pyr pH 7.0	-.506 *	0.084	0.000	1.000	-0.791	-0.245	-0.221	0.414
Acetyl-CoA	Day 3	Gly pH 5.7	Gly pH 7.0	0.031	-0.024	1.000	1.000	-0.763	-0.941	0.825	0.893
			Pyr pH 5.7	-.825 *	-0.330	0.039	1.000	-1.620	-1.248	-0.031	0.587
			Pyr pH 7.0	-1.561 *	-0.103	0.000	1.000	-2.356	-1.020	-0.767	0.814
		Gly pH 7.0	Pyr pH 5.7	-.856 *	-0.306	0.030	1.000	-1.651	-1.224	-0.062	0.611
			Pyr pH 7.0	-1.592 *	-0.079	0.000	1.000	-2.387	-0.996	-0.798	0.838
		Pyr pH 5.7	Pyr pH 7.0	-0.736	0.227	0.081	1.000	-1.530	-0.690	0.059	1.145
Alpha-ketoglutarate	Day 3	Gly pH 5.7	Gly pH 7.0	-0.050	0.187	1.000	1.000	-1.174	-1.111	1.074	1.485
			Pyr pH 5.7	-0.259	-0.233	1.000	1.000	-1.383	-1.531	0.865	1.065
			Pyr pH 7.0	-0.204	-0.545	1.000	1.000	-1.328	-1.843	0.920	0.753
		Gly pH 7.0	Pyr pH 5.7	-0.209	-0.420	1.000	1.000	-1.333	-1.718	0.915	0.878
			Pyr pH 7.0	-0.154	-0.732	1.000	0.687	-1.278	-2.030	0.970	0.566
		Pyr pH 5.7	Pyr pH 7.0	0.055	-0.312	1.000	1.000	-1.070	-1.610	1.179	0.986
Citrate	Day 3	Gly pH 5.7	Gly pH 7.0	0.500	0.847	1.000	0.653	-0.779	-0.630	1.780	2.325
			Pyr pH 5.7	-1.981 *	-0.619	0.001	1.000	-3.260	-2.097	-0.701	0.858
			Pyr pH 7.0	-2.700 *	0.724	0.000	1.000	-3.980	-0.754	-1.420	2.201
		Gly pH 7.0	Pyr pH 5.7	-2.481 *	-1.466	0.000	0.053	-3.760	-2.944	-1.201	0.011
			Pyr pH 7.0	-3.200 *	-0.123	0.000	1.000	-4.480	-1.601	-1.921	1.354
		Pyr pH 5.7	Pyr pH 7.0	-0.720	1.343	0.692	0.090	-1.999	-0.135	0.560	2.821
Glutamate	Day 3	Gly pH 5.7	Gly pH 7.0	-.544 *	-.435 *	0.000	0.004	-0.818	-0.751	-0.270	-0.118
			Pyr pH 5.7	-0.014	-0.012	1.000	1.000	-0.288	-0.328	0.260	0.305
			Pyr pH 7.0	-.500 *	-.504 *	0.000	0.001	-0.774	-0.821	-0.226	-0.188
		Gly pH 7.0	Pyr pH 5.7	.530 *	.423 *	0.000	0.005	0.256	0.107	0.804	0.740
			Pyr pH 7.0	0.044	-0.070	1.000	1.000	-0.230	-0.386	0.318	0.247
		Pyr pH 5.7	Pyr pH 7.0	-.486 *	-.493 *	0.000	0.001	-0.760	-0.809	-0.212	-0.176
Glyceraldehyde-3-Phosphate	Day 3	Gly pH 5.7	Gly pH 7.0	-0.342	0.707	1.000	1.000	-3.161	-2.548	2.477	3.963
			Pyr pH 5.7	0.784	-0.447	1.000	1.000	-2.035	-3.703	3.603	2.808
			Pyr pH 7.0	-1.140	0.999	1.000	1.000	-3.959	-2.256	1.679	4.254
		Gly pH 7.0	Pyr pH 5.7	1.127	-1.155	1.000	1.000	-1.692	-4.410	3.946	2.100
			Pyr pH 7.0	-0.798	0.291	1.000	1.000	-3.617	-2.964	2.021	3.546
		Pyr pH 5.7	Pyr pH 7.0	-1.924	1.446	0.357	1.000	-4.743	-1.809	0.895	4.701
Glycerol-3-Phosphate	Day 3	Gly pH 5.7	Gly pH 7.0	-0.089	0.222	1.000	0.417	-0.383	-0.117	0.204	0.561
			Pyr pH 5.7	.474 *	.698 *	0.001	0.000	0.181	0.359	0.768	1.037
			Pyr pH 7.0	.465 *	.715 *	0.001	0.000	0.172	0.376	0.759	1.054
		Gly pH 7.0	Pyr pH 5.7	.563 *	.475 *	0.000	0.003	0.270	0.137	0.857	0.814
			Pyr pH 7.0	.555 *	.493 *	0.000	0.002	0.261	0.154	0.848	0.832
		Pyr pH 5.7	Pyr pH 7.0	-0.009	0.017	1.000	1.000	-0.302	-0.322	0.285	0.356
Malate	Day 3	Gly pH 5.7	Gly pH 7.0	-0.111	0.129	1.000	1.000	-0.672	-0.519	0.451	0.777
			Pyr pH 5.7	-.923 *	-1.340 *	0.001	0.000	-1.484	-1.988	-0.362	-0.692
			Pyr pH 7.0	-0.185	0.048	1.000	1.000	-0.746	-0.600	0.377	0.696
		Gly pH 7.0	Pyr pH 5.7	-.813 *	-1.470 *	0.002	0.000	-1.374	-2.118	-0.251	-0.822
			Pyr pH 7.0	-0.074	-0.081	1.000	1.000	-0.635	-0.729	0.487	0.567
		Pyr pH 5.7	Pyr pH 7.0	.739 *	1.388 *	0.006	0.000	0.177	0.740	1.300	2.036
Phosphoenolpyruvate	Day 3	Gly pH 5.7	Gly pH 7.0	-0.227	-0.070	0.301	1.000	-0.545	-0.438	0.092	0.298
			Pyr pH 5.7	0.098	0.135	1.000	1.000	-0.221	-0.233	0.416	0.503
			Pyr pH 7.0	-0.263	-0.021	0.151	1.000	-0.582	-0.389	0.055	0.347
		Gly pH 7.0	Pyr pH 5.7	.324 *	0.205	0.044	0.710	0.006	-0.163	0.643	0.573
			Pyr pH 7.0	-0.037	0.049	1.000	1.000	-0.355	-0.318	0.282	0.417
		Pyr pH 5.7	Pyr pH 7.0	-.361 *	-0.156	0.021	1.000	-0.679	-0.523	-0.042	0.212
Propionyl-CoA	Day 3	Gly pH 5.7	Gly pH 7.0	-.323 *	-.339 *	0.001	0.002	-0.521	-0.567	-0.125	-0.110
			Pyr pH 5.7	-0.044	0.048	1.000	1.000	-0.242	-0.181	0.154	0.276
			Pyr pH 7.0	0.039	-0.228	1.000	0.051	-0.159	-0.456	0.237	0.001
		Gly pH 7.0	Pyr pH 5.7	.279 *	.386 *	0.003	0.000	0.081	0.158	0.477	0.615
			Pyr pH 7.0	.362 *	0.111	0.000	1.000	0.164	-0.118	0.560	0.340
		Pyr pH 5.7	Pyr pH 7.0	0.083	-.276 *	1.000	0.013	-0.115	-0.504	0.281	-0.047
Succinate	Day 3	Gly pH 5.7	Gly pH 7.0	-0.071	-0.004	1.000	1.000	-0.415	-0.401	0.272	0.393
			Pyr pH 5.7	-0.109	-0.278	1.000	0.320	-0.453	-0.675	0.235	0.118
			Pyr pH 7.0	0.089	0.266	1.000	0.385	-0.255	-0.131	0.433	0.663
		Gly pH 7.0	Pyr pH 5.7	-0.037	-0.274	1.000	0.340	-0.381	-0.671	0.306	0.123
			Pyr pH 7.0	0.160	0.270	1.000	0.363	-0.183	-0.127	0.504	0.667
		Pyr pH 5.7	Pyr pH 7.0	0.198	.544 *	0.646	0.004	-0.146	0.147	0.542	0.941
Succinyl-CoA	Day 3	Gly pH 5.7	Gly pH 7.0	-0.323	-0.360	0.105	0.128	-0.688	-0.781	0.042	0.062
			Pyr pH 5.7	-0.078	0.025	1.000	1.000	-0.442	-0.396	0.287	0.446
			Pyr pH 7.0	0.014	-0.139	1.000	1.000	-0.351	-0.560	0.378	0.282
		Gly pH 7.0	Pyr pH 5.7	0.245	0.385	0.380	0.088	-0.120	-0.037	0.610	0.806
			Pyr pH 7.0	0.336	0.221	0.083	0.844	-0.028	-0.200	0.701	0.642
		Pyr pH 5.7	Pyr pH 7.0	0.091	-0.164	1.000	1.000	-0.273	-0.585	0.456	0.257

Based on estimated marginal means

*. The mean difference is significant at the .05 level.

b. Adjustment for multiple comparisons: Bonferroni.

Appendix Table 1. Pairwise comparison of metabolite concentrations between different treatments for WT and Δ*icl1/2* mutant strains on day 3. For each measured metabolite, the mean difference in concentration, statistical significance of difference, and the lower and upper bounds of the 95% confidence interval were calculated based on estimated marginal means using the statistical analysis software SPSS. Mean difference is the relative peak area per µg protein of the WT or Δ*icl1/2* mutant strain cultured in "Condition 1" minus the relative peak area per µg protein of the same strain cultured in "Condition 2". Gly, glycerol; Pyr, pyuvate.

Dependent Variable				Mean Difference (I-J)		Sig.[b]		95% Confidence Interval for Difference[b]			
								Lower Bound		Upper Bound	
				Population		Population		Population		Population	
		Condition 1	Condition 2	*Δicl1/2*	WT	*Δicl1/2*	WT	*Δicl1/2*	WT	*Δicl1/2*	WT
2-Methylcitrate	Day 6	Gly pH 5.7	Gly pH 7.0	-15.594*	-0.480	0.005	1.000	-27.547	-12.433	-3.641	11.473
			Pyr pH 5.7	-1.797	0.346	1.000	1.000	-13.750	-11.607	10.156	12.299
			Pyr pH 7.0	4.517	0.206	1.000	1.000	-7.436	-11.747	16.470	12.159
		Gly pH 7.0	Pyr pH 5.7	13.797*	0.826	0.016	1.000	1.844	-11.127	25.750	12.779
			Pyr pH 7.0	20.111*	0.686	0.000	1.000	8.158	-11.267	32.064	12.639
		Pyr pH 5.7	Pyr pH 7.0	6.314	-0.140	0.883	1.000	-5.639	-12.093	18.267	11.813
3-phosphoglycerate	Day 6	Gly pH 5.7	Gly pH 7.0	-0.027	-.207*	1.000	0.022	-0.212	-0.392	0.159	-0.021
			Pyr pH 5.7	-0.003	0.020	1.000	1.000	-0.188	-0.165	0.183	0.206
			Pyr pH 7.0	-0.021	-0.087	1.000	1.000	-0.206	-0.273	0.165	0.098
		Gly pH 7.0	Pyr pH 5.7	0.024	.227*	1.000	0.010	-0.161	0.041	0.210	0.412
			Pyr pH 7.0	0.006	0.119	1.000	0.477	-0.179	-0.066	0.192	0.305
		Pyr pH 5.7	Pyr pH 7.0	-0.018	-0.107	1.000	0.686	-0.203	-0.293	0.168	0.078
Acetyl-CoA	Day 6	Gly pH 5.7	Gly pH 7.0	0.137	-0.317*	1.000	0.606	-0.392	-0.846	0.665	0.211
			Pyr pH 5.7	-.687*	-.941*	0.005	0.000	-1.215	-1.470	-0.159	-0.413
			Pyr pH 7.0	-.636*	-0.516	0.011	0.059	-1.164	-1.044	-0.108	0.012
		Gly pH 7.0	Pyr pH 5.7	-.824*	-.624*	0.001	0.013	-1.352	-1.152	-0.295	-0.096
			Pyr pH 7.0	-.773*	-0.199	0.002	1.000	-1.301	-0.727	-0.244	0.329
		Pyr pH 5.7	Pyr pH 7.0	0.051	0.425	1.000	0.183	-0.477	-0.103	0.579	0.954
Alpha-ketoglutarate	Day 6	Gly pH 5.7	Gly pH 7.0	-0.337	-0.285	1.000	1.000	-1.635	-1.584	0.962	1.013
			Pyr pH 5.7	-2.313*	-2.148*	0.000	0.000	-3.611	-3.447	-1.014	-0.850
			Pyr pH 7.0	-0.547	-1.405*	1.000	0.028	-1.846	-2.704	0.751	-0.107
		Gly pH 7.0	Pyr pH 5.7	-1.976*	-1.863*	0.001	0.002	-3.274	-3.161	-0.677	-0.565
			Pyr pH 7.0	-0.210	-1.120	1.000	0.126	-1.509	-2.419	1.088	0.178
		Pyr pH 5.7	Pyr pH 7.0	1.766*	0.743	0.003	0.705	0.467	-0.556	3.064	2.041
Citrate	Day 6	Gly pH 5.7	Gly pH 7.0	0.279	0.519	1.000	1.000	-0.946	-0.706	1.505	1.745
			Pyr pH 5.7	-3.753*	-0.199	0.000	1.000	-4.979	-1.424	-2.528	1.027
			Pyr pH 7.0	-2.259*	0.284	0.000	1.000	-3.484	-0.942	-1.033	1.509
		Gly pH 7.0	Pyr pH 5.7	-4.033*	-0.718	0.000	0.655	-5.258	-1.944	-2.807	0.507
			Pyr pH 7.0	-2.538*	-0.236	0.000	1.000	-3.764	-1.461	-1.312	0.990
		Pyr pH 5.7	Pyr pH 7.0	1.495*	0.482	0.010	1.000	0.269	-0.743	2.720	1.708
Glutamate	Day 6	Gly pH 5.7	Gly pH 7.0	-.643*	-.512*	0.000	0.000	-0.803	-0.672	-0.484	-0.353
			Pyr pH 5.7	-0.003	-0.067	1.000	1.000	-0.163	-0.226	0.156	0.093
			Pyr pH 7.0	-.706*	-.904*	0.000	0.000	-0.866	-1.063	-0.547	-0.744
		Gly pH 7.0	Pyr pH 5.7	.640*	.446*	0.000	0.000	0.481	0.286	0.799	0.605
			Pyr pH 7.0	-0.063	-.391*	1.000	0.000	-0.222	-0.551	0.096	-0.232
		Pyr pH 5.7	Pyr pH 7.0	-.703*	-.837*	0.000	0.000	-0.862	-0.996	-0.544	-0.678
Glyceraldehyde-3-Phosphate	Day 6	Gly pH 5.7	Gly pH 7.0	-0.611	-0.502	1.000	1.000	-2.426	-2.317	1.204	1.313
			Pyr pH 5.7	1.299	0.984	0.316	0.823	-0.516	-0.831	3.113	2.799
			Pyr pH 7.0	-0.351	2.441*	1.000	0.004	-2.166	0.626	1.464	4.255
		Gly pH 7.0	Pyr pH 5.7	1.909*	1.486	0.035	0.168	0.095	-0.329	3.724	3.301
			Pyr pH 7.0	0.260	2.943*	1.000	0.000	-1.555	1.128	2.075	4.758
		Pyr pH 5.7	Pyr pH 7.0	-1.649	1.457*	0.093	0.186	-3.464	-0.358	0.165	3.272
Glycerol-3-Phosphate	Day 6	Gly pH 5.7	Gly pH 7.0	-0.016	0.073	1.000	0.318	-0.118	-0.029	0.085	0.174
			Pyr pH 5.7	.415*	.496*	0.000	0.000	0.313	0.395	0.516	0.598
			Pyr pH 7.0	.421*	.509*	0.000	0.000	0.320	0.407	0.523	0.610
		Gly pH 7.0	Pyr pH 5.7	.431*	.424*	0.000	0.000	0.329	0.322	0.532	0.525
			Pyr pH 7.0	.437*	.436*	0.000	0.000	0.336	0.335	0.539	0.538
		Pyr pH 5.7	Pyr pH 7.0	0.007	0.012	1.000	1.000	-0.095	-0.089	0.108	0.114
Malate	Day 6	Gly pH 5.7	Gly pH 7.0	0.013	0.287	1.000	1.000	-1.220	-0.947	1.247	1.520
			Pyr pH 5.7	-2.902*	-1.272*	0.000	0.040	-4.135	-2.506	-1.668	-0.039
			Pyr pH 7.0	-0.200	-0.264	1.000	1.000	-1.434	-1.498	1.033	0.969
		Gly pH 7.0	Pyr pH 5.7	-2.915*	-1.559*	0.000	0.007	-4.149	-2.793	-1.682	-0.326
			Pyr pH 7.0	-0.213	-0.551	1.000	1.000	-1.447	-1.785	1.020	0.683
		Pyr pH 5.7	Pyr pH 7.0	2.702*	1.008	0.000	0.169	1.468	-0.225	3.935	2.242
Phosphoenolpyruvate	Day 6	Gly pH 5.7	Gly pH 7.0	0.000	-0.383	1.000	1.000	-1.036	-1.419	1.036	0.653
			Pyr pH 5.7	-0.350	-1.192*	1.000	0.017	-1.386	-2.228	0.687	-0.156
			Pyr pH 7.0	-0.561	-0.901	0.825	0.121	-1.597	-1.937	0.475	0.135
		Gly pH 7.0	Pyr pH 5.7	-0.350	-0.809	1.000	0.213	-1.386	-1.845	0.687	0.228
			Pyr pH 7.0	-0.561	-0.518	0.825	1.000	-1.597	-1.554	0.475	0.518
		Pyr pH 5.7	Pyr pH 7.0	-0.212	0.290	1.000	1.000	-1.248	-0.746	0.825	1.327
Propionyl-CoA	Day 6	Gly pH 5.7	Gly pH 7.0	-0.156	-0.268	1.000	0.143	-0.474	-0.585	0.161	0.050
			Pyr pH 5.7	0.288	0.203	0.093	0.487	-0.029	-0.114	0.606	0.521
			Pyr pH 7.0	0.254	-0.165	0.189	0.919	-0.064	-0.483	0.571	0.152
		Gly pH 7.0	Pyr pH 5.7	.445*	.471*	0.002	0.001	0.127	0.153	0.762	0.788
			Pyr pH 7.0	.410*	0.102	0.006	1.000	0.093	-0.215	0.727	0.420
		Pyr pH 5.7	Pyr pH 7.0	-0.035	-.368*	1.000	0.016	-0.352	-0.686	0.283	-0.051
Succinate	Day 6	Gly pH 5.7	Gly pH 7.0	-0.258	-0.094	0.400	1.000	-0.641	-0.476	0.124	0.289
			Pyr pH 5.7	-.796*	-0.234	0.000	0.572	-1.179	-0.616	-0.414	0.149
			Pyr pH 7.0	-0.082	-0.088	1.000	1.000	-0.464	-0.470	0.300	0.294
		Gly pH 7.0	Pyr pH 5.7	-.538*	-0.140	0.002	1.000	-0.921	-0.522	-0.156	0.242
			Pyr pH 7.0	0.176	0.006	1.000	1.000	-0.206	-0.377	0.559	0.388
		Pyr pH 5.7	Pyr pH 7.0	.714*	0.146	0.000	1.000	0.332	-0.237	1.097	0.528
Succinyl-CoA	Day 6	Gly pH 5.7	Gly pH 7.0	-0.093	-.535*	1.000	0.000	-0.351	-0.793	0.165	-0.277
			Pyr pH 5.7	0.172	0.045	0.424	1.000	-0.087	-0.214	0.430	0.303
			Pyr pH 7.0	0.137	-.313*	0.879	0.011	-0.122	-0.571	0.395	-0.055
		Gly pH 7.0	Pyr pH 5.7	.265*	.580*	0.042	0.000	0.006	0.321	0.523	0.838
			Pyr pH 7.0	0.230	0.222	0.106	0.130	-0.029	-0.036	0.488	0.480
		Pyr pH 5.7	Pyr pH 7.0	-0.035	-.358*	1.000	0.003	-0.294	-0.616	0.223	-0.099

Based on estimated marginal means

*. The mean difference is significant at the .05 level.

b. Adjustment for multiple comparisons: Bonferroni.

Appendix Table 2. Pairwise comparison of metabolite concentrations between different treatments for WT and Δ*icl1/2* mutant strains on day 6. For each measured metabolite, the mean difference in concentration, statistical significance of difference, and the lower and upper bounds of the 95% confidence interval were calculated based on estimated marginal means using the statistical analysis software SPSS. Mean difference is the relative peak area per µg protein of the WT or Δ*icl1/2* mutant strain cultured in "Condition 1" minus the relative peak area per µg protein of the same strain cultured in "Condition 2". Gly, glycerol; Pyr, pyruvate.

Dependent Variable				Mean Difference (I-J)		Sig.[b]		95% Confidence Interval for Difference [b]			
								Lower Bound		Upper Bound	
				Population		Population		Population		Population	
		Condition 1	Condition 2	*ΔpckA*	WT	*ΔpckA*	WT	*ΔpckA*	WT	*ΔpckA*	WT
2-Methylcitrate	Day 3	Gly pH 5.7	Gly pH 7.0	-0.636	-0.487	0.757	1.000	-1.776	-1.627	0.503	0.652
			Pyr pH 5.7	-0.618	-0.731	0.823	0.483	-1.757	-1.871	0.522	0.408
			Pyr pH 7.0	-1.458 *	-1.781 *	0.006	0.001	-2.597	-2.920	-0.318	-0.641
		Gly pH 7.0	Pyr pH 5.7	0.019	-0.244	1.000	1.000	-1.121	-1.384	1.158	0.895
			Pyr pH 7.0	-0.821	-1.294 *	0.306	0.019	-1.961	-2.433	0.318	-0.154
		Pyr pH 5.7	Pyr pH 7.0	-0.840	-1.050	0.278	0.086	-1.979	-2.189	0.300	0.090
3-phosphoglycerate	Day 3	Gly pH 5.7	Gly pH 7.0	0.793	0.297	0.569	1.000	-0.502	-0.999	2.089	1.593
			Pyr pH 5.7	0.135	0.537	1.000	1.000	-1.161	-0.759	1.431	1.832
			Pyr pH 7.0	0.578	0.640	1.000	1.000	-0.717	-0.655	1.874	1.936
		Gly pH 7.0	Pyr pH 5.7	-0.658	0.240	0.978	1.000	-1.954	-1.056	0.638	1.536
			Pyr pH 7.0	-0.215	0.344	1.000	1.000	-1.511	-0.952	1.081	1.640
		Pyr pH 5.7	Pyr pH 7.0	0.443	0.104	1.000	1.000	-0.853	-1.192	1.739	1.400
Acetyl-CoA	Day 3	Gly pH 5.7	Gly pH 7.0	-0.011	0.575	1.000	0.474	-0.901	-0.316	0.880	1.465
			Pyr pH 5.7	-0.093	1.026 *	1.000	0.017	-0.984	0.135	0.797	1.917
			Pyr pH 7.0	-0.092	1.387 *	1.000	0.001	-0.982	0.496	0.799	2.278
		Gly pH 7.0	Pyr pH 5.7	-0.083	0.451	1.000	0.984	-0.973	-0.440	0.808	1.342
			Pyr pH 7.0	-0.081	0.812	1.000	0.091	-0.972	-0.078	0.810	1.703
		Pyr pH 5.7	Pyr pH 7.0	0.002	0.361	1.000	1.000	-0.889	-0.530	0.892	1.252
Alpha-ketoglutarate	Day 3	Gly pH 5.7	Gly pH 7.0	0.319	1.033 *	1.000	0.008	-0.502	0.211	1.141	1.854
			Pyr pH 5.7	-0.361	.835 *	1.000	0.045	-1.182	0.013	0.460	1.656
			Pyr pH 7.0	-0.055	1.821 *	1.000	0.000	-0.876	1.000	0.767	2.643
		Gly pH 7.0	Pyr pH 5.7	-0.680	-0.198	0.158	1.000	-1.502	-1.019	0.141	0.624
			Pyr pH 7.0	-0.374	0.789	1.000	0.066	-1.195	-0.033	0.447	1.610
		Pyr pH 5.7	Pyr pH 7.0	0.306	.987 *	1.000	0.012	-0.515	0.165	1.128	1.808
Citrate	Day 3	Gly pH 5.7	Gly pH 7.0	0.097	0.599	1.000	0.313	-0.738	-0.236	0.933	1.435
			Pyr pH 5.7	-0.295	0.615	1.000	0.279	-1.131	-0.220	0.540	1.451
			Pyr pH 7.0	-0.358	.852 *	1.000	0.044	-1.194	0.016	0.477	1.687
		Gly pH 7.0	Pyr pH 5.7	-0.393	0.016	1.000	1.000	-1.228	-0.820	0.443	0.852
			Pyr pH 7.0	-0.456	0.253	0.811	1.000	-1.291	-0.583	0.380	1.088
		Pyr pH 5.7	Pyr pH 7.0	-0.063	0.237	1.000	1.000	-0.899	-0.599	0.773	1.072
Glutamate	Day 3	Gly pH 5.7	Gly pH 7.0	-0.451	0.089	0.573	1.000	-1.190	-0.649	0.288	0.828
			Pyr pH 5.7	-0.069	0.630	1.000	0.134	-0.808	-0.108	0.669	1.369
			Pyr pH 7.0	-0.626	0.695	0.140	0.075	-1.364	-0.043	0.113	1.434
		Gly pH 7.0	Pyr pH 5.7	0.382	0.541	0.934	0.286	-0.357	-0.198	1.121	1.280
			Pyr pH 7.0	-0.175	0.606	1.000	0.166	-0.913	-0.133	0.564	1.345
		Pyr pH 5.7	Pyr pH 7.0	-0.556	0.065	0.252	1.000	-1.295	-0.674	0.182	0.804
Glyceraldehyde-3-Phosphate	Day 3	Gly pH 5.7	Gly pH 7.0	0.221	.884 *	1.000	0.036	-0.623	0.040	1.065	1.728
			Pyr pH 5.7	0.121	0.781	1.000	0.084	-0.723	-0.063	0.965	1.625
			Pyr pH 7.0	-0.212	1.271 *	1.000	0.001	-1.056	0.427	0.632	2.115
		Gly pH 7.0	Pyr pH 5.7	-0.100	-0.103	1.000	1.000	-0.944	-0.947	0.744	0.741
			Pyr pH 7.0	-0.433	0.387	0.954	1.000	-1.277	-0.457	0.411	1.231
		Pyr pH 5.7	Pyr pH 7.0	-0.333	0.490	1.000	0.674	-1.177	-0.354	0.511	1.334
Glycerol-3-Phosphate	Day 3	Gly pH 5.7	Gly pH 7.0	-0.183	0.174	1.000	1.000	-0.796	-0.439	0.430	0.787
			Pyr pH 5.7	0.351	1.162 *	0.704	0.000	-0.262	0.549	0.964	1.775
			Pyr pH 7.0	0.244	1.056 *	1.000	0.000	-0.369	0.443	0.858	1.669
		Gly pH 7.0	Pyr pH 5.7	0.534	.988 *	0.120	0.000	-0.079	0.375	1.147	1.602
			Pyr pH 7.0	0.427	.882 *	0.352	0.002	-0.186	0.269	1.040	1.495
		Pyr pH 5.7	Pyr pH 7.0	-0.106	-0.106	1.000	1.000	-0.719	-0.719	0.507	0.507
Malate	Day 3	Gly pH 5.7	Gly pH 7.0	0.115	0.110	1.000	1.000	-2.945	-2.950	3.175	3.170
			Pyr pH 5.7	-1.865	-2.793	0.577	0.091	-4.925	-5.853	1.194	0.267
			Pyr pH 7.0	-2.437	-6.082 *	0.193	0.000	-5.497	-9.142	0.623	-3.022
		Gly pH 7.0	Pyr pH 5.7	-1.980	-2.903	0.469	0.071	-5.040	-5.963	1.080	0.157
			Pyr pH 7.0	-2.552	-6.191 *	0.152	0.000	-5.612	-9.251	0.508	-3.132
		Pyr pH 5.7	Pyr pH 7.0	-0.572	-3.288 *	1.000	0.029	-3.632	-6.348	2.488	-0.229
Phosphoenolpyruvate	Day 3	Gly pH 5.7	Gly pH 7.0	0.723	0.227	0.870	1.000	-0.638	-1.133	2.084	1.588
			Pyr pH 5.7	1.263	1.270	0.082	0.079	-0.098	-0.091	2.624	2.631
			Pyr pH 7.0	0.789	0.989	0.678	0.296	-0.572	-0.372	2.149	2.350
		Gly pH 7.0	Pyr pH 5.7	0.540	1.042	1.000	0.233	-0.821	-0.319	1.901	2.403
			Pyr pH 7.0	0.066	0.761	1.000	0.753	-1.295	-0.600	1.427	2.122
		Pyr pH 5.7	Pyr pH 7.0	-0.474	-0.281	1.000	1.000	-1.835	-1.642	0.886	1.080
Propionyl-CoA	Day 3	Gly pH 5.7	Gly pH 7.0	-0.400	0.365	1.000	1.000	-1.325	-0.560	0.525	1.290
			Pyr pH 5.7	-0.447	0.218	1.000	1.000	-1.372	-0.707	0.478	1.143
			Pyr pH 7.0	-1.277 *	0.571	0.003	0.553	-2.202	-0.354	-0.352	1.496
		Gly pH 7.0	Pyr pH 5.7	-0.047	-0.147	1.000	1.000	-0.972	-1.072	0.878	0.778
			Pyr pH 7.0	-0.877	0.206	0.072	1.000	-1.802	-0.719	0.048	1.131
		Pyr pH 5.7	Pyr pH 7.0	-0.830	0.353	0.101	1.000	-1.755	-0.572	0.095	1.278
Succinate	Day 3	Gly pH 5.7	Gly pH 7.0	-0.190	0.104	1.000	1.000	-1.057	-0.764	0.678	0.971
			Pyr pH 5.7	-0.557	-0.247	0.484	1.000	-1.424	-1.115	0.311	0.620
			Pyr pH 7.0	-1.102 *	-0.374	0.007	1.000	-1.969	-1.242	-0.234	0.493
		Gly pH 7.0	Pyr pH 5.7	-0.367	-0.351	1.000	1.000	-1.235	-1.219	0.501	0.516
			Pyr pH 7.0	-.912 *	-0.478	0.035	0.786	-1.780	-1.346	-0.044	0.389
		Pyr pH 5.7	Pyr pH 7.0	-0.545	-0.127	0.521	1.000	-1.413	-0.994	0.323	0.741
Succinyl-CoA	Day 3	Gly pH 5.7	Gly pH 7.0	-0.581	0.521	0.891	1.000	-1.684	-0.582	0.522	1.625
			Pyr pH 5.7	-0.416	0.299	1.000	1.000	-1.519	-0.804	0.687	1.403
			Pyr pH 7.0	-1.481 *	0.624	0.004	0.730	-2.584	-0.479	-0.378	1.727
		Gly pH 7.0	Pyr pH 5.7	0.165	-0.222	1.000	1.000	-0.938	-1.325	1.268	0.881
			Pyr pH 7.0	-0.900	0.102	0.171	1.000	-2.003	-1.001	0.203	1.206
		Pyr pH 5.7	Pyr pH 7.0	-1.065	0.324	0.064	1.000	-2.168	-0.779	0.038	1.428

Based on estimated marginal means

*. The mean difference is significant at the .05 level.

b. Adjustment for multiple comparisons: Bonferroni.

Appendix Table 3. Pairwise comparison of metabolite concentrations between different treatments for WT and Δ*pckA* mutant strains on day 3. For each measured metabolite, the mean difference in concentration, statistical significance of difference, and the lower and upper bounds of the 95% confidence interval were calculated based on estimated marginal means using the statistical analysis software SPSS. Mean difference is the relative peak area per µg protein of the WT or Δ*pckA* mutant strain cultured in "Condition 1" minus the relative peak area per µg protein of the same strain cultured in "Condition 2". Gly, glycerol; Pyr, pyruvate + glycerol.

Dependent Variable				Mean Difference (I-J)		Sig. [b]		95% Confidence Interval for Difference [b]			
								Lower Bound		Upper Bound	
				Population		Population		Population		Population	
		Condition 1	Condition 2	ΔpckA	WT	ΔpckA	WT	ΔpckA	WT	ΔpckA	WT
2-Methylcitrate	Day 6	Gly pH 5.7	Gly pH 7.0	-0.486	-0.212	1.000	1.000	-1.494	-1.219	0.521	0.796
			Pyr pH 5.7	-0.753	-2.953 *	0.262	0.000	-1.761	-3.960	0.255	-1.945
			Pyr pH 7.0	-1.408 *	-1.967 *	0.003	0.000	-2.416	-2.975	-0.401	-0.960
		Gly pH 7.0	Pyr pH 5.7	-0.266	-2.741 *	1.000	0.000	-1.274	-3.749	0.741	-1.733
			Pyr pH 7.0	-0.922	-1.755 *	0.090	0.000	-1.929	-2.763	0.086	-0.748
		Pyr pH 5.7	Pyr pH 7.0	-0.655	0.986	0.460	0.058	-1.663	-0.022	0.352	1.993
3-phosphoglycerate	Day 6	Gly pH 5.7	Gly pH 7.0	0.335	0.193	1.000	1.000	-0.468	-0.610	1.137	0.996
			Pyr pH 5.7	0.256	-0.013	1.000	1.000	-0.546	-0.816	1.059	0.790
			Pyr pH 7.0	-0.403	-0.640	1.000	0.193	-1.206	-1.443	0.399	0.163
		Gly pH 7.0	Pyr pH 5.7	-0.078	-0.206	1.000	1.000	-0.881	-1.009	0.725	0.597
			Pyr pH 7.0	-0.738	-.833 *	0.087	0.038	-1.541	-1.635	0.065	-0.030
		Pyr pH 5.7	Pyr pH 7.0	-0.660	-0.627	0.164	0.213	-1.463	-1.429	0.143	0.176
Acetyl-CoA	Day 6	Gly pH 5.7	Gly pH 7.0	.847 *	0.631	0.023	0.159	0.084	-0.132	1.610	1.394
			Pyr pH 5.7	-0.091	0.673	1.000	0.112	-0.854	-0.091	0.672	1.436
			Pyr pH 7.0	0.637	0.315	0.151	1.000	-0.126	-0.448	1.400	1.078
		Gly pH 7.0	Pyr pH 5.7	-.938 *	0.042	0.009	1.000	-1.701	-0.721	-0.175	0.805
			Pyr pH 7.0	-0.210	-0.316	1.000	1.000	-0.973	-1.079	0.553	0.447
		Pyr pH 5.7	Pyr pH 7.0	0.728	-0.358	0.069	1.000	-0.035	-1.121	1.491	0.406
Alpha-ketoglutarate	Day 6	Gly pH 5.7	Gly pH 7.0	2.981	5.537 *	0.400	0.008	-1.435	1.121	7.396	9.952
			Pyr pH 5.7	-8.756 *	-13.214 *	0.000	0.000	-13.172	-17.629	-4.341	-8.798
			Pyr pH 7.0	2.199	4.509 *	1.000	0.043	-2.217	0.093	6.614	8.924
		Gly pH 7.0	Pyr pH 5.7	-11.737 *	-18.750 *	0.000	0.000	-16.153	-23.166	-7.322	-14.335
			Pyr pH 7.0	-0.782	-1.028	1.000	1.000	-5.198	-5.443	3.633	3.388
		Pyr pH 5.7	Pyr pH 7.0	10.955 *	17.723 *	0.000	0.000	6.539	13.307	15.370	22.138
Citrate	Day 6	Gly pH 5.7	Gly pH 7.0	-0.617	-0.609	0.625	0.653	-1.655	-1.647	0.421	0.429
			Pyr pH 5.7	-0.804	-3.371 *	0.222	0.000	-1.842	-4.409	0.234	-2.333
			Pyr pH 7.0	-1.667 *	-3.412 *	0.000	0.000	-2.705	-4.450	-0.629	-2.374
		Gly pH 7.0	Pyr pH 5.7	-0.186	-2.762 *	1.000	0.000	-1.224	-3.800	0.852	-1.724
			Pyr pH 7.0	-1.050 *	-2.803 *	0.046	0.000	-2.088	-3.841	-0.012	-1.765
		Pyr pH 5.7	Pyr pH 7.0	-0.863	-0.042	0.155	1.000	-1.901	-1.080	0.175	0.996
Glutamate	Day 6	Gly pH 5.7	Gly pH 7.0	-0.669	-1.986 *	0.870	0.001	-1.928	-3.246	0.590	-0.727
			Pyr pH 5.7	-0.050	0.002	1.000	1.000	-1.309	-1.258	1.209	1.261
			Pyr pH 7.0	-1.591 *	-3.421 *	0.007	0.000	-2.850	-4.680	-0.332	-2.162
		Gly pH 7.0	Pyr pH 5.7	0.619	1.988 *	1.000	0.001	-0.640	0.729	1.878	3.247
			Pyr pH 7.0	-0.922	-1.434 *	0.286	0.018	-2.181	-2.694	0.337	-0.175
		Pyr pH 5.7	Pyr pH 7.0	-1.541 *	-3.422 *	0.010	0.000	-2.800	-4.682	-0.282	-2.163
Glyceraldehyde-3-Phosphate	Day 6	Gly pH 5.7	Gly pH 7.0	0.546	-0.065	1.000	1.000	-0.625	-1.237	1.717	1.106
			Pyr pH 5.7	-0.063	-0.714	1.000	0.577	-1.234	-1.885	1.108	0.457
			Pyr pH 7.0	-0.380	-1.537 *	1.000	0.005	-1.551	-2.709	0.791	-0.366
		Gly pH 7.0	Pyr pH 5.7	-0.609	-0.648	0.919	0.776	-1.780	-1.820	0.562	0.523
			Pyr pH 7.0	-0.927	-1.472 *	0.199	0.008	-2.098	-2.643	0.245	-0.301
		Pyr pH 5.7	Pyr pH 7.0	-0.317	-0.824	1.000	0.340	-1.488	-1.995	0.854	0.348
Glycerol-3-Phosphate	Day 6	Gly pH 5.7	Gly pH 7.0	0.147	-1.021 *	1.000	0.000	-0.373	-1.541	0.667	-0.501
			Pyr pH 5.7	.715 *	0.385	0.003	0.272	0.195	-0.135	1.236	0.906
			Pyr pH 7.0	0.387	-0.038	0.268	1.000	-0.134	-0.558	0.907	0.483
		Gly pH 7.0	Pyr pH 5.7	.568 *	1.406 *	0.026	0.000	0.048	0.886	1.089	1.927
			Pyr pH 7.0	0.239	.983 *	1.000	0.000	-0.281	0.463	0.760	1.504
		Pyr pH 5.7	Pyr pH 7.0	-0.329	-0.423	0.510	0.174	-0.849	-0.943	0.191	0.097
Malate	Day 6	Gly pH 5.7	Gly pH 7.0	-0.040	-0.060	1.000	1.000	-4.728	-4.747	4.647	4.628
			Pyr pH 5.7	-9.060 *	-21.454 *	0.000	0.000	-13.747	-26.141	-4.372	-16.766
			Pyr pH 7.0	-3.918	-9.594 *	0.150	0.000	-8.606	-14.282	0.769	-4.907
		Gly pH 7.0	Pyr pH 5.7	-9.019 *	-21.394 *	0.000	0.000	-13.707	-26.081	-4.332	-16.706
			Pyr pH 7.0	-3.878	-9.535 *	0.159	0.000	-8.565	-14.222	0.810	-4.847
		Pyr pH 5.7	Pyr pH 7.0	5.141 *	11.859 *	0.025	0.000	0.454	7.172	9.829	16.547
Phosphoenolpyruvate	Day 6	Gly pH 5.7	Gly pH 7.0	-0.017	-0.528	1.000	0.722	-0.947	-1.458	0.914	0.403
			Pyr pH 5.7	0.288	0.595	1.000	0.490	-0.643	-0.336	1.218	1.525
			Pyr pH 7.0	-0.195	-0.654	1.000	0.341	-1.125	-1.584	0.736	0.277
		Gly pH 7.0	Pyr pH 5.7	0.304	1.123 *	1.000	0.011	-0.626	0.192	1.235	2.053
			Pyr pH 7.0	-0.178	-0.126	1.000	1.000	-1.108	-1.056	0.753	0.805
		Pyr pH 5.7	Pyr pH 7.0	-0.482	-1.248 *	0.928	0.004	-1.413	-2.179	0.448	-0.318
Propionyl-CoA	Day 6	Gly pH 5.7	Gly pH 7.0	-0.146	-0.152	1.000	1.000	-0.594	-0.599	0.301	0.295
			Pyr pH 5.7	-.458 *	-.640 *	0.042	0.002	-0.906	-1.087	-0.011	-0.193
			Pyr pH 7.0	-.665 *	-1.082 *	0.001	0.000	-1.112	-1.529	-0.218	-0.635
		Gly pH 7.0	Pyr pH 5.7	-0.312	-.488 *	0.351	0.026	-0.759	-0.935	0.135	-0.041
			Pyr pH 7.0	-.519 *	-.930 *	0.016	0.000	-0.966	-1.377	-0.072	-0.483
		Pyr pH 5.7	Pyr pH 7.0	-0.207	-0.442	1.000	0.054	-0.654	-0.889	0.240	0.005
Succinate	Day 6	Gly pH 5.7	Gly pH 7.0	-0.196	-0.220	1.000	1.000	-2.204	-2.228	1.811	1.788
			Pyr pH 5.7	-1.798	-7.737 *	0.102	0.000	-3.806	-9.745	0.209	-5.729
			Pyr pH 7.0	-1.250	-2.629 *	0.538	0.005	-3.258	-4.637	0.758	-0.621
		Gly pH 7.0	Pyr pH 5.7	-1.602	-7.517 *	0.191	0.000	-3.610	-9.525	0.406	-5.509
			Pyr pH 7.0	-1.053	-2.409 *	0.899	0.012	-3.061	-4.416	0.955	-0.401
		Pyr pH 5.7	Pyr pH 7.0	0.549	5.108 *	1.000	0.000	-1.459	3.100	2.557	7.116
Succinyl-CoA	Day 6	Gly pH 5.7	Gly pH 7.0	-0.163	-0.228	1.000	1.000	-0.621	-0.686	0.295	0.230
			Pyr pH 5.7	-0.433	-.568 *	0.073	0.009	-0.891	-1.026	0.026	-0.109
			Pyr pH 7.0	-.618 *	-1.080 *	0.004	0.000	-1.076	-1.538	-0.160	-0.622
		Gly pH 7.0	Pyr pH 5.7	-0.270	-0.339	0.647	0.272	-0.728	-0.798	0.189	0.119
			Pyr pH 7.0	-0.455	-.852 *	0.053	0.000	-0.913	-1.310	0.004	-0.393
		Pyr pH 5.7	Pyr pH 7.0	-0.185	-.512 *	1.000	0.022	-0.643	-0.970	0.273	-0.054

Based on estimated marginal means

*. The mean difference is significant at the .05 level.

b. Adjustment for multiple comparisons: Bonferroni.

Appendix Table 4. Pairwise comparison of metabolite concentrations between different treatments for WT and Δ*pckA* mutant strains on day 6. For each measured metabolite, the mean difference in concentration, statistical significance of difference, and the lower and upper bounds of the 95% confidence interval were calculated based on estimated marginal means using the statistical analysis software SPSS. Mean difference is the relative peak area per µg protein of the WT or Δ*pckA* mutant strain cultured in "Condition 1" minus the relative peak area per µg protein of the same strain cultured in "Condition 2". Gly, glycerol; Pyr, pyruvate + glycerol.

Dependent Variable				Mean Difference (I-J)				Sig.[b]				95% Confidence Interval for Difference[b]							
												Lower Bound				Upper Bound			
				Treatment				Treatment				Treatment				Treatment			
				Gly pH 5.7	Gly pH 7.0	Pyr pH 5.7	Pyr pH 7.0	Gly pH 5.7	Gly pH 7.0	Pyr pH 5.7	Pyr pH 7.0	Gly pH 5.7	Gly pH 7.0	Pyr pH 5.7	Pyr pH 7.0	Gly pH 5.7	Gly pH 7.0	Pyr pH 5.7	Pyr pH 7.0
2-Methylcitrate	Day 3	WT	*Δicl1/2*	-3.934	-15.050*	-9.170*	-1.154	.115	.000	.001	.634	-8.909	-20.025	-14.145	-6.129	1.042	-10.075	-4.195	3.821
3-phosphoglycerate	Day 3	WT	*Δicl1/2*	.086	.024	.192	-.398*	.422	.818	.082	.001	-.133	-.195	-.027	-.617	.306	.244	.412	-.178
Acetyl-CoA	Day 3	WT	*Δicl1/2*	-.036	.019	-.531	-1.494*	.904	.948	.085	.000	-.647	-.592	-1.142	-2.105	.576	.631	.081	-.882
Alpha-ketoglutarate	Day 3	WT	*Δicl1/2*	.156	-.081	.130	.496	.711	.847	.757	.246	-.710	-.947	-.735	-.369	1.021	.784	.995	1.362
Citrate	Day 3	WT	*Δicl1/2*	.106	-.240	-1.255*	-3.317*	.824	.616	.015	.000	-.879	-1.225	-2.240	-4.302	1.091	.745	-.270	-2.332
Glutamate	Day 3	WT	*Δicl1/2*	.016	-.093	.014	.021	.875	.369	.892	.840	-.195	-.304	-.197	-.190	.227	.118	.225	.232
Glyceraldehyde-3-Phosphate	Day 3	WT	*Δicl1/2*	-.305	-1.355	.926	-2.444*	.772	.207	.384	.029	-2.475	-3.525	-1.243	-4.614	1.865	.815	3.096	-.274
Glycerol-3-Phosphate	Day 3	WT	*Δicl1/2*	.230*	-.081	.007	-.019	.046	.463	.950	.864	.005	-.307	-.219	-.245	.456	.145	.233	.207
Malate	Day 3	WT	*Δicl1/2*	.208	-.032	.625*	-.025	.328	.878	.007	.906	-.224	-.464	.193	-.457	.640	.400	1.057	.407
Phosphoenolpyruvate	Day 3	WT	*Δicl1/2*	.140	-.016	.103	-.102	.247	.890	.393	.394	-.105	-.262	-.142	-.348	.385	.229	.348	.143
Propionyl-CoA	Day 3	WT	*Δicl1/2*	.083	.099	-.008	.350*	.269	.192	.910	.000	-.069	-.054	-.161	.197	.235	.251	.144	.502
Succinate	Day 3	WT	*Δicl1/2*	.071	.003	.240	-.106	.584	.980	.073	.412	-.194	-.261	-.024	-.371	.335	.268	.505	.158
Succinyl-CoA	Day 3	WT	*Δicl1/2*	.092	.129	-.011	.245	.502	.350	.937	.084	-.189	-.152	-.292	-.036	.373	.410	.270	.525

Based on estimated marginal means

*. The mean difference is significant at the .05 level.

b. Adjustment for multiple comparisons: Bonferroni.

Appendix Table 5. Pairwise comparison of metabolite concentrations within WT and Δ*icl1/2* mutant strains under different culture conditions on day 3. For each measured metabolite, the mean difference in concentration, statistical significance of difference, and the lower and upper bounds of the 95% confidence interval were calculated based on estimated marginal means using the statistical analysis software SPSS. Mean difference is the relative peak area per µg protein of the WT strain minus the relative peak area per µg protein of the Δ*icl1/2* mutant strain. Gly, glycerol; Pyr, pyruvate.

Dependent Variable				Mean Difference (I-J)				Sig. [b]				95% Confidence Interval for Difference [b]							
												Lower Bound				Upper Bound			
				Treatment				Treatment				Treatment				Treatment			
				Gly pH 5.7	Gly pH 7.0	Pyr pH 5.7	Pyr pH 7.0	Gly pH 5.7	Gly pH 7.0	Pyr pH 5.7	Pyr pH 7.0	Gly pH 5.7	Gly pH 7.0	Pyr pH 5.7	Pyr pH 7.0	Gly pH 5.7	Gly pH 7.0	Pyr pH 5.7	Pyr pH 7.0
2-Methylcitrate	Day 6	WT	Δ*icl1/*	-23.653 *	-38.767 *	-25.796 *	-19.342 *	.000	.000	.000	.000	-32.311	-47.425	-34.453	-28.000	-14.996	-30.110	-17.138	-10.685
3-phosphoglycerate	Day 6	WT	Δ*icl1/*	.052	.232 *	.029	.118	.436	.001	.662	.082	-.082	.097	-.105	-.016	.186	.366	.163	.253
Acetyl-CoA	Day 6	WT	Δ*icl1/*	-.324	.130	-.070	-.444 *	.094	.495	.713	.024	-.707	-.253	-.452	-.827	.058	.512	.313	-.062
Alpha-ketoglutarate	Day 6	WT	Δ*icl1/*	-.133	-.185	-.297	.725	.775	.692	.524	.126	-1.073	-1.125	-1.238	-.215	.808	.756	.643	1.666
Citrate	Day 6	WT	Δ*icl1/*	-.067	-.307	-3.622 *	-2.609 *	.879	.486	.000	.000	-.954	-1.195	-4.509	-3.497	.821	.581	-2.734	-1.722
Glutamate	Day 6	WT	Δ*icl1/*	.022	-.109	.085	.219 *	.701	.063	.141	.001	-.093	-.225	-.030	.104	.137	.006	.201	.335
Glyceraldehyde-3-Phosphate	Day 6	WT	Δ*icl1/*	.776	.667	1.091	-2.015 *	.238	.309	.101	.004	-.538	-.647	-.224	-3.330	2.091	1.982	2.405	-.701
Glycerol-3-Phosphate	Day 6	WT	Δ*icl1/*	.081 *	-.008	-.001	-.007	.033	.823	.971	.846	.007	-.082	-.075	-.081	.154	.065	.072	.066
Malate	Day 6	WT	Δ*icl1/*	.146	-.127	-1.483 *	.210	.741	.774	.002	.635	-.747	-1.020	-2.376	-.683	1.040	.766	-.589	1.104
Phosphoenolpyruvate	Day 6	WT	Δ*icl1/*	1.425 *	1.808 *	2.267 *	1.765 *	.001	.000	.000	.000	.675	1.058	1.517	1.015	2.175	2.559	3.018	2.516
Propionyl-CoA	Day 6	WT	Δ*icl1/*	-.212	-.101	-.127	.207	.069	.379	.270	.076	-.442	-.331	-.357	-.023	.018	.129	.103	.437
Succinate	Day 6	WT	Δ*icl1/*	-.010	-.174	-.573 *	-.004	.942	.209	.000	.976	-.287	-.451	-.850	-.281	.267	.102	-.296	.273
Succinyl-CoA	Day 6	WT	Δ*icl1/*	-.205 *	.237 *	-.078	.244 *	.033	.015	.401	.012	-.393	.049	-.265	.057	-.018	.424	.109	.432

Based on estimated marginal means

*. The mean difference is significant at the .05 level.

b. Adjustment for multiple comparisons: Bonferroni.

Appendix Table 6. Pairwise comparison of metabolite concentrations within WT and Δ*icl1/2* mutant strains under different culture conditions on day 6. For each measured metabolite, the mean difference in concentration, statistical significance of difference, and the lower and upper bounds of the 95% confidence interval were calculated based on estimated marginal means using the statistical analysis software SPSS. Mean difference is the relative peak area per µg protein of the WT strain minus the relative peak area per µg protein of the Δ*icl1/2* mutant strain. Gly, glycerol; Pyr, pyruvate.

Dependent Variable				Mean Difference (I-J) Treatment				Sig. [b] Treatment				95% Confidence Interval for Difference [b] Lower Bound Treatment				95% Confidence Interval for Difference [b] Upper Bound Treatment			
				Gly pH 5.7	Gly pH 7.0	GP pH 5.7	GP pH 7.0	Gly pH 5.7	Gly pH 7.0	GP pH 5.7	GP pH 7.0	Gly pH 5.7	Gly pH 7.0	GP pH 5.7	GP pH 7.0	Gly pH 5.7	Gly pH 7.0	GP pH 5.7	GP pH 7.0
2-Methylcitrate	Day 3	WT	Δ*pckA*	-.043	-.192	.070	.280	.915	.638	.864	.495	-.869	-1.018	-.755	-.545	.782	.633	.895	1.105
3-phosphoglycerate	Day 3	WT	Δ*pckA*	-.733	-.236	-1.134 *	-.795	.122	.612	.019	.094	-1.671	-1.175	-2.073	-1.734	.206	.702	-.196	.144
Acetyl-CoA	Day 3	WT	Δ*pckA*	.691 *	.105	-.429	-.788 *	.037	.742	.185	.018	.046	-.540	-1.074	-1.433	1.336	.750	.216	-.143
Alpha-ketoglutarate	Day 3	WT	Δ*pckA*	.910 *	.197	-.286	-.966 *	.004	.505	.335	.002	.315	-.398	-.881	-1.561	1.505	.792	.309	-.371
Citrate	Day 3	WT	Δ*pckA*	1.339 *	.837 *	.428	.129	.000	.008	.159	.667	.734	.232	-.177	-.476	1.944	1.442	1.034	.734
Glutamate	Day 3	WT	Δ*pckA*	.725 *	.184	.025	-.596 *	.010	.488	.924	.030	.190	-.351	-.510	-1.131	1.260	.719	.560	-.061
Glyceraldehyde-3-Phosphate	Day 3	WT	Δ*pckA*	.977 *	.314	.317	-.506	.003	.304	.299	.101	.365	-.298	-.294	-1.117	1.588	.925	.928	.105
Glycerol-3-Phosphate	Day 3	WT	Δ*pckA*	.843 *	.486 *	.031	.031	.001	.033	.887	.887	.399	.042	-.413	-.413	1.287	.930	.475	.475
Malate	Day 3	WT	Δ*pckA*	.836	.841	1.763	4.480 *	.448	.445	.115	.000	-1.381	-1.376	-.453	2.264	3.052	3.057	3.980	6.696
Phosphoenolpyruvate	Day 3	WT	Δ*pckA*	-.962	-.466	-.968	-1.162 *	.055	.342	.054	.022	-1.947	-1.452	-1.954	-2.147	.024	.519	.017	-.176
Propionyl-CoA	Day 3	WT	Δ*pckA*	.414	-.351	-.250	-1.433 *	.217	.294	.452	.000	-.256	-1.021	-.920	-2.103	1.084	.319	.420	-.763
Succinate	Day 3	WT	Δ*pckA*	.798 *	.505	.489	.071	.014	.111	.123	.819	.170	-.123	-.139	-.557	1.427	1.133	1.118	.699
Succinyl-CoA	Day 3	WT	Δ*pckA*	.350	-.753	-.366	-1.755 *	.380	.064	.358	.000	-.450	-1.552	-1.165	-2.554	1.149	.046	.433	-.956

Based on estimated marginal means

*. The mean difference is significant at the .05 level.

b. Adjustment for multiple comparisons: Bonferroni.

Appendix Table 7. Pairwise comparison of metabolite concentrations within WT and Δ*pckA* mutant strains under different culture conditions on day 3. For each measured metabolite, the mean difference in concentration, statistical significance of difference, and the lower and upper bounds of the 95% confidence interval were calculated based on estimated marginal means using the statistical analysis software SPSS. Mean difference is the relative peak area per µg protein of the WT strain minus the relative peak area per µg protein of the Δ*pckA* mutant strain. Gly, glycerol; GP, glycerol + pyruvate.

Dependent Variable				Mean Difference (I-J)				Sig.[b]				95% Confidence Interval for Difference [b]							
												Lower Bound				Upper Bound			
				Treatment				Treatment				Treatment				Treatment			
				Gly pH 5.7	Gly pH 7.0	GP pH 5.7	GP pH 7.0	Gly pH 5.7	Gly pH 7.0	GP pH 5.7	GP pH 7.0	Gly pH 5.7	Gly pH 7.0	GP pH 5.7	GP pH 7.0	Gly pH 5.7	Gly pH 7.0	GP pH 5.7	GP pH 7.0
2-Methylcitrate	Day 6	WT	Δ*pckA*	.160	-.115	2.360 *	.719	.658	.751	.000	.053	-.570	-.844	1.630	-.011	.890	.615	3.090	1.449
3-phosphoglycerate	Day 6	WT	Δ*pckA*	.019	.161	.288	.255	.948	.578	.320	.378	-.563	-.421	-.293	-.326	.600	.742	.870	.837
Acetyl-CoA	Day 6	WT	Δ*pckA*	.166	.383	-.597 *	.489	.544	.168	.035	.081	-.386	-.170	-1.150	-.064	.719	.935	-.044	1.041
Alpha-ketoglutarate	Day 6	WT	Δ*pckA*	3.275 *	.719	7.732 *	.965	.045	.650	.000	.543	.077	-2.479	4.534	-2.233	6.473	3.918	10.931	4.163
Citrate	Day 6	WT	Δ*pckA*	.761 *	.753 *	3.328 *	2.507 *	.047	.050	.000	.000	.010	.001	2.577	1.755	1.513	1.505	4.080	3.259
Glutamate	Day 6	WT	Δ*pckA*	.101	1.419 *	.050	1.931 *	.822	.003	.911	.000	-.811	.507	-.862	1.019	1.013	2.331	.962	2.843
Glyceraldehyde-3-Phosphate	Day 6	WT	Δ*pckA*	.652	1.264 *	1.303 *	1.809 *	.127	.005	.004	.000	-.196	.416	.455	.961	1.501	2.112	2.151	2.658
Glycerol-3-Phosphate	Day 6	WT	Δ*pckA*	.072	1.240 *	.402 *	.496 *	.699	.000	.037	.011	-.305	.864	.025	.120	.449	1.617	.779	.873
Malate	Day 6	WT	Δ*pckA*	.771	.790	13.165 *	6.447 *	.647	.639	.000	.001	-2.624	-2.605	9.770	3.052	4.166	4.185	16.560	9.842
Phosphoenolpyruvate	Day 6	WT	Δ*pckA*	.194	.705 *	-.113	.653	.562	.041	.735	.057	-.480	.031	-.787	-.021	.868	1.379	.561	1.327
Propionyl-CoA	Day 6	WT	Δ*pckA*	.269	.275	.451 *	.686 *	.100	.093	.008	.000	-.054	-.049	.127	.362	.593	.599	.775	1.010
Succinate	Day 6	WT	Δ*pckA*	.593	.617	6.532 *	1.972 *	.412	.394	.000	.009	-.861	-.838	5.077	.518	2.047	2.071	7.986	3.426
Succinyl-CoA	Day 6	WT	Δ*pckA*	.251	.316	.386 *	.713 *	.134	.062	.024	.000	-.081	-.016	.054	.381	.583	.648	.718	1.045

Based on estimated marginal means

*. The mean difference is significant at the .05 level.

b. Adjustment for multiple comparisons: Bonferroni.

Appendix Table 8. Pairwise comparison of metabolite concentrations within WT and Δ*pckA* mutant strains under different culture conditions on day 6. For each measured metabolite, the mean difference in concentration, statistical significance of difference, and the lower and upper bounds of the 95% confidence interval were calculated based on estimated marginal means using the statistical analysis software SPSS. Mean difference is the relative peak area per μg protein of the WT strain minus the relative peak area per μg protein of the Δ*pckA* mutant strain. Gly, glycerol; GP, glycerol + pyruvate.

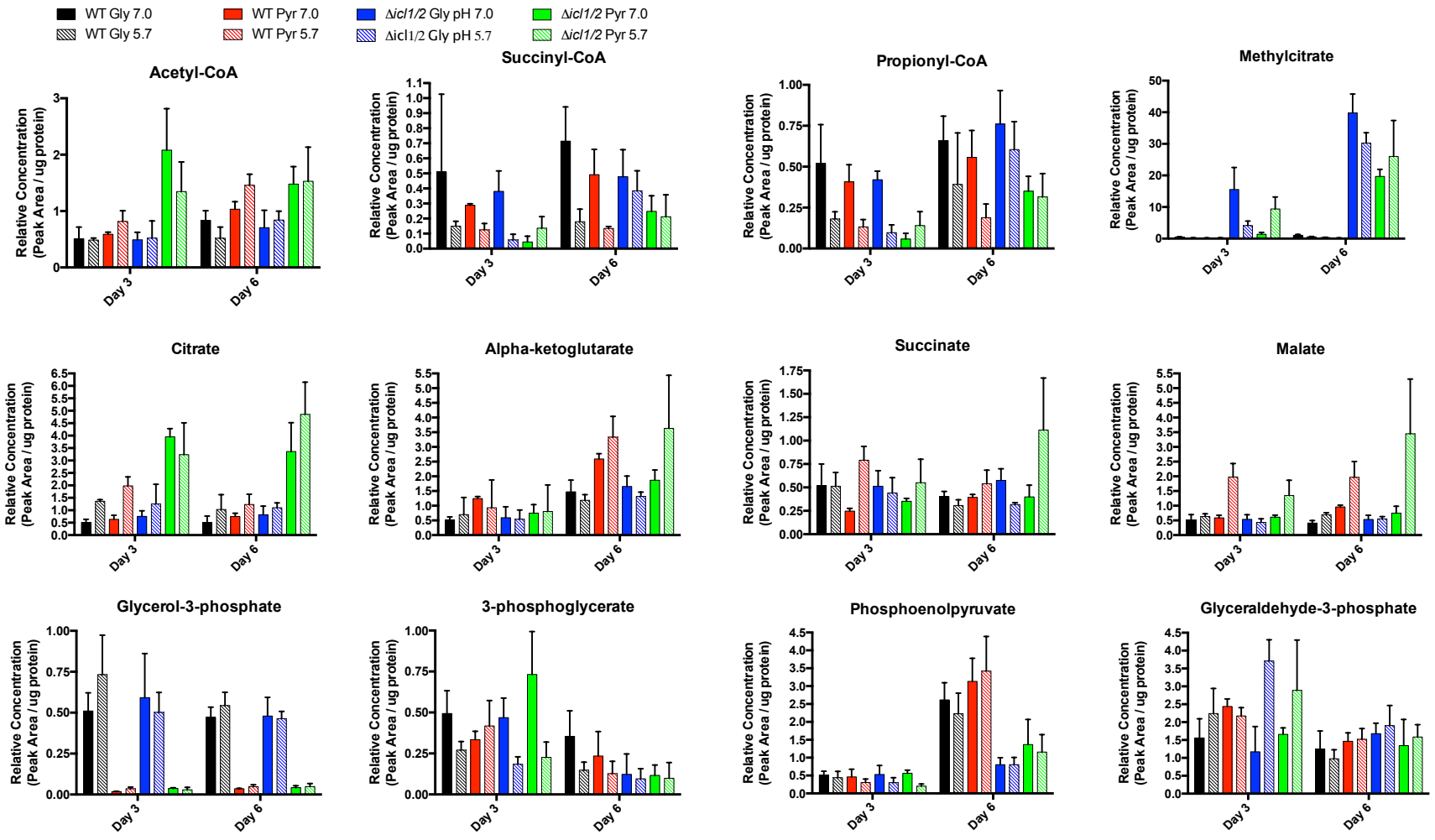

Appendix Figure 11. Metabolic profiling of Mtb Erdman wildtype and Δ*icl1/2* mutant strains on minimal media agar plates buffered to pH 7.0 or pH 5.7 and containing either glycerol or pyruvate as a single carbon source. Metabolite concentration is reported as the relative peak area per µg of protein for each treatment. Error bars represent the standard deviation.

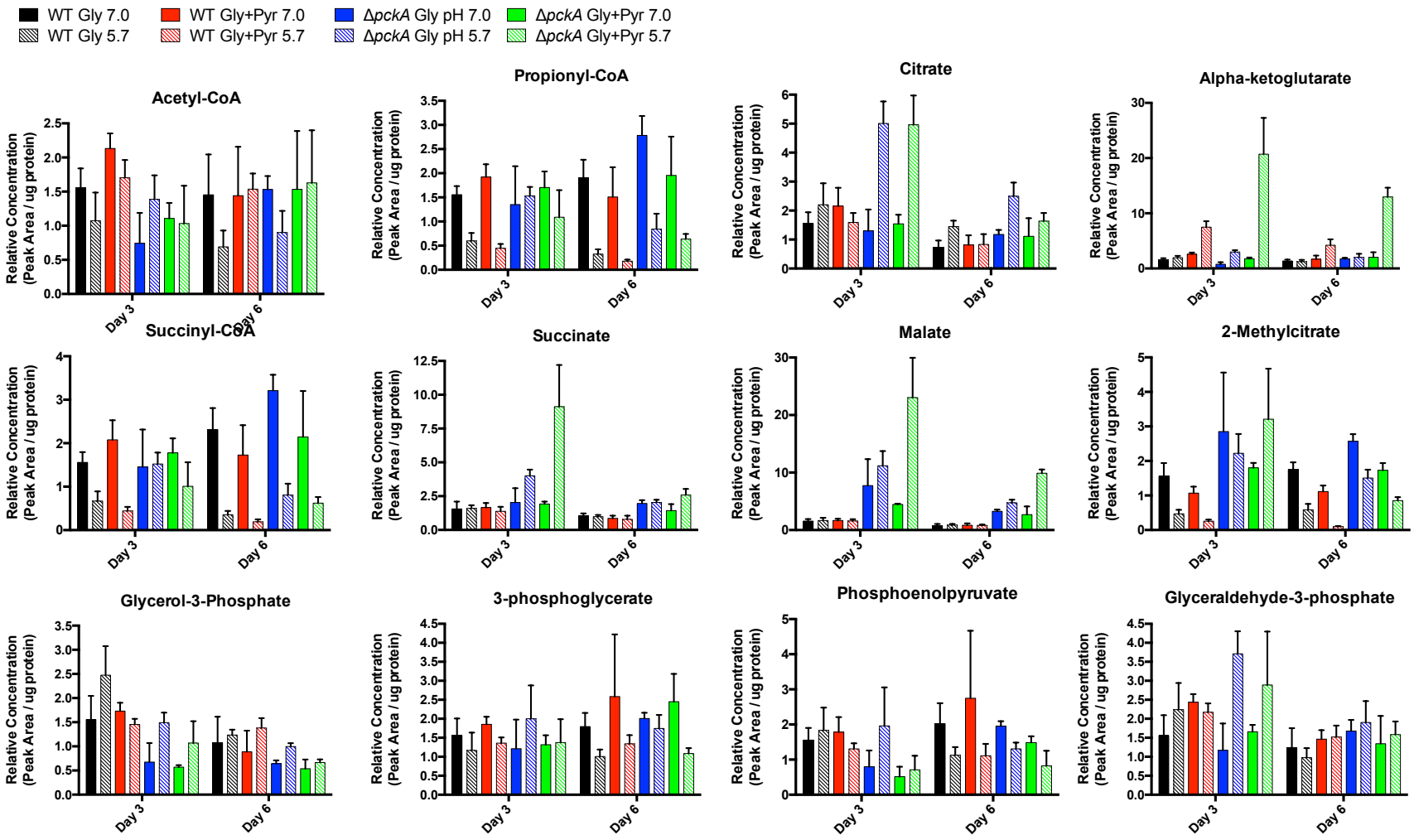

Appendix Figure 12. Metabolic profiling of Mtb Erdman wildtype and Δ*pckA* mutant strains on minimal media agar plates buffered to pH 7.0 or pH 5.7 and containing either glycerol or glycerol and pyruvate. Metabolite concentration is reported as the relative peak area per µg of protein for each treatment. Error bars represent the standard deviation.

REFERENCES

REFERENCES

1. WHO. (2016) Global Tuberculosis Report.

2. Barry, C. E., 3rd, Boshoff, H. I., Dartois, V., Dick, T., Ehrt, S., Flynn, J., Schnappinger, D., Wilkinson, R. J., and Young, D. (2009) The spectrum of latent tuberculosis: rethinking the biology and intervention strategies. *Nat Rev Microbiol* **7**, 845-855

3. Vandal, O. H., Nathan, C. F., and Ehrt, S. (2009) Acid resistance in *Mycobacterium tuberculosis*. *J Bacteriol* **191**, 4714-4721

4. Wolschendorf, F., Ackart, D., Shrestha, T. B., Hascall-Dove, L., Nolan, S., Lamichhane, G., Wang, Y., Bossmann, S. H., Basaraba, R. J., and Niederweis, M. (2011) Copper resistance is essential for virulence of *Mycobacterium tuberculosis*. *PNAS* **108**, 1621-1626

5. Converse, P. J., Karakousis, P. C., Klinkenberg, L. G., Kesavan, A. K., Ly, L. H., Allen, S. S., Grosset, J. H., Jain, S. K., Lamichhane, G., Manabe, Y. C., McMurray, D. N., Nuermberger, E. L., and Bishai, W. R. (2009) Role of the DosR-DosS two-component regulatory system in *Mycobacterium tuberculosis* virulence in three animal models. *Infect Immun* **77**, 1230-1237

6. Weiss, G., and Schaible, U. E. (2015) Macrophage defense mechanisms against intracellular bacteria. *Immunological Reviews* **264**, 182-203

7. Voskuil, M. I., Bartek, I. L., Visconti, K., and Schoolnik, G. K. (2011) The response of *Mycobacterium tuberculosis* to reactive oxygen and nitrogen species. *Front Microbiol* **2**, 105

8. Vandal, O. H., Roberts, J. A., Odaira, T., Schnappinger, D., Nathan, C. F., and Ehrt, S. (2009) Acid-susceptible mutants of *Mycobacterium tuberculosis* share hypersusceptibility to cell wall and oxidative stress and to the host environment. *J Bacteriol* **191**, 625-631

9. Vandal, O. H., Pierini, L. M., Schnappinger, D., Nathan, C. F., and Ehrt, S. (2008) A membrane protein preserves intrabacterial pH in intraphagosomal *Mycobacterium tuberculosis*. *Nat Med* **14**, 849-854

10. Levitte, S., Adams, Kristin N., Berg, Russell D., Cosma, Christine L., Urdahl, Kevin B., and Ramakrishnan, L. (2016) Mycobacterial acid tolerance enables phagolysosomal survival and establishment of tuberculous infection *in vivo*. *Cell Host & Microbe* **20**, 250-258

11. Rohde, K. H., Abramovitch, R. B., and Russell, D. G. (2007) *Mycobacterium tuberculosis* invasion of macrophages: linking bacterial gene expression to environmental cues. *Cell Host Microbe* **2**, 352-364

12. Perez, E., Samper, S., Bordas, Y., Guilhot, C., Gicquel, B., and Martin, C. (2001) An essential role for *phoP* in *Mycobacterium tuberculosis* virulence. *Mol Microbiol* **41**, 179-187

13. Arbues, A., Aguilo, J. I., Gonzalo-Asensio, J., Marinova, D., Uranga, S., Puentes, E., Fernandez, C., Parra, A., Cardona, P. J., Vilaplana, C., Ausina, V., Williams, A., Clark, S., Malaga, W., Guilhot, C., Gicquel, B., and Martin, C. (2013) Construction, characterization and preclinical evaluation of MTBVAC, the first live-attenuated *M. tuberculosis*-based vaccine to enter clinical trials. *Vaccine* **31**, 4867-4873

14. Spertini, F., Audran, R., Chakour, R., Karoui, O., Steiner-Monard, V., Thierry, A., Mayor, C., Rettby, N., Jaton, K., Vallotton, L., Lazor-Blanchet, C., Doce, J., Puentes, E., Marinova, D., Aguilo, N., and Martin, C. Safety of human immunisation with a live-attenuated *Mycobacterium tuberculosis* vaccine: a randomised, double-blind, controlled phase I trial. *Lancet Respir Med* **3**, 953-962

15. Baker, J. J., Johnson, B. K., and Abramovitch, R. B. (2014) Slow growth of *Mycobacterium tuberculosis* at acidic pH is regulated by *phoPR* and host-associated carbon sources. *Mol Microbiol* **94**, 56-69

16. Bansal, R., Kumar, V., Sevalkar, R., Singh, P., and Sarkar, D. (2017) *Mycobacterium tuberculosis* virulence ‐ regulator PhoP interacts with alternative sigma factor SigE during acid ‐ stress response. *Mol Microbiol*

17. Abramovitch, R. B., Rohde, K. H., Hsu, F. F., and Russell, D. G. (2011) *aprABC*: a *Mycobacterium tuberculosis* complex-specific locus that modulates pH-driven adaptation to the macrophage phagosome. *Mol Microbiol* **80**, 678-694

18. Piddington, D. L., Kashkouli, A., and Buchmeier, N. A. (2000) Growth of *Mycobacterium tuberculosis* in a defined medium is very restricted by acid pH and Mg2+ levels. *Infect Immun* **68**, 4518-4522

19. Zhang, Y., Wade, M., Scorpio, A., Zhang, H., and Sun, Z. (2003) Mode of action of pyrazinamide: disruption of *Mycobacterium tuberculosis* membrane transport and energetics by pyrazinoic acid. *J. Antimicrob. Chemother.* **52**, 790-795

20. Marrero, J., Rhee, K. Y., Schnappinger, D., Pethe, K., and Ehrt, S. (2010) Gluconeogenic carbon flow of tricarboxylic acid cycle intermediates is critical for *Mycobacterium*

tuberculosis to establish and maintain infection. *Proc of the National Academy of Sciences of the United States of America* **107**, 9819-9824

21. Liu, K., Yu, J., and Russell, D. G. (2003) *pckA*-deficient *Mycobacterium bovis* BCG shows attenuated virulence in mice and in macrophages. *Microbiology* **149**, 1829-1835

22. Venugopal, A., Bryk, R., Shi, S., Rhee, K., Rath, P., Schnappinger, D., Ehrt, S., and Nathan, C. (2011) Virulence of *Mycobacterium tuberculosis* depends on lipoamide dehydrogenase, a member of three multienzyme complexes. *Cell Host Microbe* **9**, 21-31

23. Shi, S., and Ehrt, S. (2005) Dihydrolipoamide acyltransferase is critical for *Mycobacterium tuberculosis* pathogenesis. *Infect Immun* **74**, 56-63

24. Maksymiuk, C., Balakrishnan, A., Bryk, R., Rhee, K. Y., and Nathan, C. F. (2015) E1 of α-ketoglutarate dehydrogenase defends *Mycobacterium tuberculosis* against glutamate anaplerosis and nitroxidative stress. *Proc Natl Acad Sci USA* **112**

25. McKinney, J. D., Honer zu Bentrup, K., Munoz-Elias, E. J., Miczak, A., Chen, B., Chan, W. T., Swenson, D., Sacchettini, J. C., Jacobs, W. R., Jr., and Russell, D. G. (2000) Persistence of *Mycobacterium tuberculosis* in macrophages and mice requires the glyoxylate shunt enzyme isocitrate lyase. *Nature* **406**, 735-738

26. Munoz-Elias, E. J., and McKinney, J. D. (2005) *Mycobacterium tuberculosis* isocitrate lyases 1 and 2 are jointly required for in vivo growth and virulence. *Nat Med* **11**, 638-644

27. Griffin, J. E., Pandey, A. K., Gilmore, S. A., Mizrahi, V., McKinney, J. D., Bertozzi, C. R., and Sassetti, C. M. (2012) Cholesterol catabolism by *Mycobacterium tuberculosis* requires transcriptional and metabolic adaptations. *Chem Biol* **19**, 218-227

28. Griffin, J. E., Gawronski, J. D., Dejesus, M. A., Ioerger, T. R., Akerley, B. J., and Sassetti, C. M. (2011) High-resolution phenotypic profiling defines genes essential for mycobacterial growth and cholesterol catabolism. *PLoS Pathog* **7**, e1002251

29. Miner, M. D., Chang, J. C., Pandey, A. K., Sassetti, C. M., and Sherman, D. R. (2009) Role of cholesterol in *Mycobacterium tuberculosis* infection. *Indian J Exp Biol* **47**, 407-411

30. Pandey, A. K., and Sassetti, C. M. (2008) Mycobacterial persistence requires the utilization of host cholesterol. *Proc Natl Acad Sci U S A* **105**, 4376-4380

31. Van der Geize, R., Yam, K., Heuser, T., Wilbrink, M. H., Hara, H., Anderton, M. C., Sim, E., Dijkhuizen, L., Davies, J. E., Mohn, W. W., and Eltis, L. D. (2007) A gene cluster encoding cholesterol catabolism in a soil actinomycete provides insight into *Mycobacterium tuberculosis* survival in macrophages. *Proc Natl Acad Sci U S A* **104**, 1947-1952

32. Russell, D. G. (2003) Phagosomes, fatty acids and tuberculosis. *Nat Cell Biol* **5**, 776-778

33. Eoh, H., and Rhee, K. Y. (2014) Methylcitrate cycle defines the bactericidal essentiality of isocitrate lyase for survival of *Mycobacterium tuberculosis* on fatty acids. *Proc Natl Acad Sci U S A* **111**, 4976-4981

34. VanderVen, B. C., Fahey, R. J., Lee, W., Liu, Y., Abramovitch, R. B., Memmott, C., Crowe, A. M., Eltis, L. D., Perola, E., Deininger, D. D., Wang, T., Locher, C. P., and Russell, D. G. (2015) Novel inhibitors of cholesterol degradation in *Mycobacterium tuberculosis* reveal how the bacterium's metabolism is constrained by the intracellular environment. *PLoS Pathog* **11**, e1004679

35. Savvi, S., Warner, D. F., Kana, B. D., McKinney, J. D., Mizrahi, V., and Dawes, S. S. (2008) Functional characterization of a vitamin B-12-dependent methylmalonyl pathway in *Mycobacterium tuberculosis*: Implications for propionate metabolism during growth on fatty acids. *J Bacteriol* **190**, 3886-3895

36. Lee, W., Vanderven, B. C., Fahey, R. J., and Russell, D. G. (2013) Intracellular *Mycobacterium tuberculosis* exploits host-derived fatty acids to limit metabolic stress. *J Biol Chem*

37. Watanabe, S., Zimmermann, M., Goodwin, M. B., Sauer, U., Barry, C. E., 3rd, and Boshoff, H. I. (2011) Fumarate reductase activity maintains an energized membrane in anaerobic *Mycobacterium tuberculosis*. *PLoS Pathog* **7**, e1002287

38. Eoh, H., and Rhee, K. Y. (2013) Multifunctional essentiality of succinate metabolism in adaptation to hypoxia in *Mycobacterium tuberculosis*. *Proc Natl Acad Sci U S A* **110**, 6554-6559

39. Nandakumar, M., Nathan, C., and Rhee, K. Y. (2014) Isocitrate lyase mediates broad antibiotic tolerance in *Mycobacterium tuberculosis*. *Nat Commun* **5**, 4306

40. Beste, D. J. V., Bonde, B., Hawkins, N., Ward, J. L., Beale, M. H., Noack, S., Noh, K., Kruger, N. J., Ratcliffe, R. G., and McFadden, J. (2011) C-13 metabolic flux analysis identifies an unusual route for pyruvate dissimilation in *Mycobacteria* which requires isocitrate lyase and carbon dioxide fixation. *Plos Pathog* **7**

41. Fischer, E., and Sauer, U. (2003) A novel metabolic cycle catalyzes glucose oxidation and anaplerosis in hungry *Escherichia coli*. *J Biol Chem* **278**, 46446-46451

42. Corper, H. J., and Cohn, M. L. (1951) The viability and virulence of old cultures of tubercle bacilli (Studies on 30-year-old broth cultures maintained at 37° C.). *Tubercle* **32**, 232-237

43. Gill, W. P., Harik, N. S., Whiddon, M. R., Liao, R. P., Mittler, J. E., and Sherman, D. R. (2009) A replication clock for *Mycobacterium tuberculosis*. *Nat Med* **15**, 211-214

44. Rohde, K. H., Veiga, D. F., Caldwell, S., Balazsi, G., and Russell, D. G. (2012) Linking the transcriptional profiles and the physiological states of *Mycobacterium tuberculosis* during an extended intracellular infection. *PLoS Pathog* **8**, e1002769

45. Munoz-Elias, E. J., Timm, J., Botha, T., Chan, W. T., Gomez, J. E., and McKinney, J. D. (2005) Replication dynamics of *Mycobacterium tuberculosis* in chronically infected mice. *Infect Immun* **73**, 546-551

46. Beste, D. J. V., Laing, E., Bonde, B., Avignone-Rossa, C., Bushell, M. E., and McFadden, J. J. (2007) Transcriptomic analysis identifies growth rate modulation as a component of the adaptation of mycobacteria to survival inside the macrophage. *J Bacteriol* **189**, 3969-3976

47. Wayne, L. G., and Sohaskey, C. D. (2001) Nonreplicating persistence of *Mycobacterium tuberculosis*. *Annu Rev Microbiol* **55**, 139-163

48. Rustad, T. R., Sherrid, A. M., Minch, K. J., and Sherman, D. R. (2009) Hypoxia: a window into *Mycobacterium tuberculosis* latency. *Cell Microbiol* **11**, 1151-1159

49. Voskuil, M. I., Schnappinger, D., Visconti, K. C., Harrell, M. I., Dolganov, G. M., Sherman, D. R., and Schoolnik, G. K. (2003) Inhibition of respiration by nitric oxide induces a *Mycobacterium tuberculosis* dormancy program. *J Exp Med* **198**, 705-713

50. Baek, S. H., Li, A. H., and Sassetti, C. M. (2011) Metabolic regulation of mycobacterial growth and antibiotic sensitivity. *PLoS Biol* **9**, e1001065

51. Loebel, R. O., Shorr, E., and Richardson, H. B. (1933) The influence of adverse conditions upon the respiratory metabolism and growth of human tubercle bacilli. *J Bacteriol* **26**, 167-200

52. Rifat, D., Bishai, W. R., and Karakousis, P. C. (2009) Phosphate Depletion: A novel trigger for *Mycobacterium tuberculosis* persistence. *J. Infect. Dis.* **200**, 1126-1135

53. Deb, C., Lee, C. M., Dubey, V. S., Daniel, J., Abomoelak, B., Sirakova, T. D., Pawar, S., Rogers, L., and Kolattukudy, P. E. (2009) A novel in vitro multiple-stress dormancy model for *Mycobacterium tuberculosis* generates a lipid-loaded, drug-tolerant, dormant pathogen. *Plos One* **4**, e6077

54. Wayne, L. G., and Hayes, L. G. (1996) An in vitro model for sequential study of shiftdown of *Mycobacterium tuberculosis* through two stages of nonreplicating persistence. *Infect Immun* **64**, 2062-2069

55. Shleeva, M. O., Bagramyan, K., Telkov, M. V., Mukamolova, G. V., Young, M., Kell, D. B., and Kaprelyants, A. S. (2002) Formation and resuscitation of "non-culturable" cells of *Rhodococcus rhodochrous* and *Mycobacterium tuberculosis* in prolonged stationary phase. *Microbiology (Reading, England)* **148**, 1581-1591

56. Gengenbacher, M., Rao, S. P., Pethe, K., and Dick, T. (2010) Nutrient-starved, non-replicating *Mycobacterium tuberculosis* requires respiration, ATP synthase and isocitrate lyase for maintenance of ATP homeostasis and viability. *Microbiology* **156**, 81-87

57. Betts, J. C., Lukey, P. T., Robb, L. C., McAdam, R. A., and Duncan, K. (2002) Evaluation of a nutrient starvation model of *Mycobacterium tuberculosis* persistence by gene and protein expression profiling. *Mol Microbiol* **43**, 717-731

58. Rao, S. P., Alonso, S., Rand, L., Dick, T., and Pethe, K. (2008) The protonmotive force is required for maintaining ATP homeostasis and viability of hypoxic, nonreplicating *Mycobacterium tuberculosis*. *Proc Natl Acad Sci U S A* **105**, 11945-11950

59. Liu, Y., Tan, S., Huang, L., Abramovitch, R. B., Rohde, K. H., Zimmerman, M. D., Chen, C., Dartois, V., VanderVen, B. C., and Russell, D. G. (2016) Immune activation of the host cell induces drug tolerance in *Mycobacterium tuberculosis* both in vitro and in vivo. *The Journal of experimental medicine* **213**, 809-825

60. Zheng, H., Colvin, C. J., Johnson, B. K., Kirchhoff, P. D., Wilson, M., Jorgensen-Muga, K., Larsen, S. D., and Abramovitch, R. B. (2016) Inhibitors of *Mycobacterium tuberculosis* DosRST signaling and persistence. *Nat Chem Biol*

61. Pandey, A. K., and Sassetti, C. M. (2008) Mycobacterial persistence requires the utilization of host cholesterol. *Proc Natl Acad Sci U S A* **105**, 4376-4380

62. Sauer, U., and Eikmanns, B. J. (2005) The PEP-pyruvate-oxaloacetate node as the switch point for carbon flux distribution in bacteria. *FEMS Microbiol Rev* **29**, 765-794

63. Beste, D. J., Noh, K., Niedenfuhr, S., Mendum, T. A., Hawkins, N. D., Ward, J. L., Beale, M. H., Wiechert, W., and McFadden, J. (2013) (13)C-Flux spectral analysis of host-pathogen metabolism reveals a mixed diet for intracellular *Mycobacterium tuberculosis*. *Chem Biol* **20**, 1012-1021

64. Walters, S. B., Dubnau, E., Kolesnikova, I., Laval, F., Daffe, M., and Smith, I. (2006) The *Mycobacterium tuberculosis* PhoPR two-component system regulates genes essential for virulence and complex lipid biosynthesis. *Mol Microbiol* **60**, 312-330

65. Gonzalo-Asensio, J., Mostowy, S., Harders-Westerveen, J., Huygen, K., Hernandez-Pando, R., Thole, J., Behr, M., Gicquel, B., and Martin, C. (2008) PhoP: a missing piece in the intricate puzzle of *Mycobacterium tuberculosis* virulence. *Plos One* **3**, e3496

66. Johnson, B. K., Colvin, C. J., Needle, D. B., Mba Medie, F., Champion, P. A., and Abramovitch, R. B. (2015) The carbonic anhydrase inhibitor ethoxzolamide inhibits the *Mycobacterium tuberculosis* PhoPR regulon and Esx-1 secretion and attenuates virulence. *Antimicrob Agents Chemother* **59**, 4436-4445

67. Asensio, J. G., Maia, C., Ferrer, N. L., Barilone, N., Laval, F., Soto, C. Y., Winter, N., Daffe, M., Gicquel, B., Martin, C., and Jackson, M. (2006) The virulence-associated two component PhoP-PhoR system controls the biosynthesis of polyketide-derived lipids in *Mycobacterium tuberculosis*. *J Biol Chem* **281**, 1313-1316

68. Singh, A., Crossman, D. K., Mai, D., Guidry, L., Voskuil, M. I., Renfrow, M. B., and Steyn, A. J. C. (2009) *Mycobacterium tuberculosis* WhiB3 maintains redox homeostasis by regulating virulence lipid anabolism to modulate macrophage response. *Plos Pathog* **5**, e1000545

69. Fisher, M. A., Plikaytis, B. B., and Shinnick, T. M. (2002) Microarray analysis of the *Mycobacterium tuberculosis* transcriptional response to the acidic conditions found in phagosomes. *J Bacteriol* **184**, 4025-4032

70. Galagan, J. E., Minch, K., Peterson, M., Lyubetskaya, A., Azizi, E., Sweet, L., Gomes, A., Rustad, T., Dolganov, G., Glotova, I., Abeel, T., Mahwinney, C., Kennedy, A. D., Allard, R., Brabant, W., Krueger, A., Jaini, S., Honda, B., Yu, W. H., Hickey, M. J., Zucker, J., Garay, C., Weiner, B., Sisk, P., Stolte, C., Winkler, J. K., Van de Peer, Y., Iazzetti, P., Camacho, D., Dreyfuss, J., Liu, Y., Dorhoi, A., Mollenkopf, H. J., Drogaris, P., Lamontagne, J., Zhou, Y., Piquenot, J., Park, S. T., Raman, S., Kaufmann, S. H., Mohney, R. P., Chelsky, D., Moody, D. B., Sherman, D. R., and Schoolnik, G. K. (2013) The *Mycobacterium tuberculosis* regulatory network and hypoxia. *Nature* **499**, 178-183

71. Martin, C., Williams, A., Hernandez-Pando, R., Cardona, P. J., Gormley, E., Bordat, Y., Soto, C. Y., Clark, S. O., Hatch, G. J., Aguilar, D., Ausina, V., and Gicquel, B. (2006) The live *Mycobacterium tuberculosis phoP* mutant strain is more attenuated than BCG and confers protective immunity against tuberculosis in mice and guinea pigs. *Vaccine* **24**, 3408-3419

72. Upton, A. M., and McKinney, J. D. (2007) Role of the methylcitrate cycle in propionate metabolism and detoxification in *Mycobacterium smegmatis*. *Microbiology* **153**, 3973-3982

73. Russell, D. G., Cardona, P. J., Kim, M. J., Allain, S., and Altare, F. (2009) Foamy macrophages and the progression of the human tuberculosis granuloma. *Nat Immunol* **10**, 943-948

74. Kim, M. J., Wainwright, H. C., Locketz, M., Bekker, L. G., Walther, G. B., Dittrich, C., Visser, A., Wang, W., Hsu, F. F., Wiehart, U., Tsenova, L., Kaplan, G., and Russell, D. G. (2010) Caseation of human tuberculosis granulomas correlates with elevated host lipid metabolism. *EMBO Mol Med* **2**, 258-274

75. Chang, J. C., Miner, M. D., Pandey, A. K., Gill, W. P., Harik, N. S., Sassetti, C. M., and Sherman, D. R. (2009) *igr* genes and *Mycobacterium tuberculosis* cholesterol metabolism. *J Bacteriol* **191**, 5232-5239

76. Dannenberg, A. M. (2006) *Pathogenesis of Human Pulmonary Tuberculosis: Insights from the Rabbit Model*, ASM Press

77. Tian, J., Bryk, R., Itoh, M., Suematsu, M., and Nathan, C. (2005) Variant tricarboxylic acid cycle in *Mycobacterium tuberculosis*: identification of alpha-ketoglutarate decarboxylase. *Proc Natl Acad Sci U S A* **102**, 10670-10675

78. Homolka, S., Niemann, S., Russell, D. G., and Rohde, K. H. (2010) Functional genetic diversity among Mycobacterium tuberculosis complex clinical isolates: delineation of conserved core and lineage-specific transcriptomes during intracellular survival. *PLoS Pathog* **6**, e1000988

79. Purdy, G. E., Niederweis, M., and Russell, D. G. (2009) Decreased outer membrane permeability protects mycobacteria from killing by ubiquitin-derived peptides. *Mol Microbiol* **73**, 844-857

80. Tan, S., Sukumar, N., Abramovitch, R. B., Parish, T., and Russell, D. G. (2013) *Mycobacterium tuberculosis* responds to chloride and pH as synergistic cues to the immune status of its host cell. *PLoS Pathog* **9**, e1003282

81. Farhana, A., Guidry, L., Srivastava, A., Singh, A., Hondalus, M. K., and Steyn, A. (2010) Reductive stress in microbes: implications for understanding *Mycobacterium tuberculosis* disease and persistence. *Advances in microbial physiology* **57**, 43-117

82. Hanson, G. T., Aggeler, R., Oglesbee, D., Cannon, M., Capaldi, R. A., Tsien, R. Y., and Remington, S. J. (2004) Investigating mitochondrial redox potential with redox-sensitive green fluorescent protein indicators. *J Biol Chem* **279**, 13044-13053

83. Cannon, M. B., and Remington, S. J. (2006) Re-engineering redox-sensitive green fluorescent protein for improved response rate. *Protein Sci* **15**, 45-57

84. Bhaskar, A., Chawla, M., Mehta, M., Parikh, P., Chandra, P., Bhave, D., Kumar, D., Carroll, K. S., and Singh, A. (2014) Reengineering redox sensitive GFP to measure mycothiol redox potential of *Mycobacterium tuberculosis* during infection. *PLoS Pathog* **10**, e1003902

85. Sirakova, T. D., Thirumala, A. K., Dubey, V. S., Sprecher, H., and Kolattukudy, P. E. (2001) The *Mycobacterium tuberculosis pks2* gene encodes the synthase for the hepta- and octamethyl-branched fatty acids required for sulfolipid synthesis. *J Biol Chem* **276**, 16833-16839

86. Jain, M., Petzold, C. J., Schelle, M. W., Leavell, M. D., Mougous, J. D., Bertozzi, C. R., Leary, J. A., and Cox, J. S. (2007) Lipidomics reveals control of *Mycobacterium tuberculosis v*irulence lipids via metabolic coupling. *Proc Natl Acad Sci U S A* **104**, 5133-5138

87. Schloss, J. V., and Cleland, W. W. (1982) Inhibition of isocitrate lyase by 3-nitropropionate, a reaction-intermediate analogue. *Biochemistry* **21**, 4420-4427

88. Munoz-Elias, E. J., and McKinney, J. D. (2006) Carbon metabolism of intracellular bacteria. *Cell Microbiol* **8**, 10-22

89. Shi, L., Sohaskey, C. D., Pfeiffer, C., Datta, P., Parks, M., McFadden, J., North, R. J., and Gennaro, M. L. (2010) Carbon flux rerouting during *Mycobacterium tuberculosis* growth arrest. *Mol Microbiol* **78**, 1199-1215

90. Timm, J., Post, F. A., Bekker, L. G., Walther, G. B., Wainwright, H. C., Manganelli, R., Chan, W. T., Tsenova, L., Gold, B., Smith, I., Kaplan, G., and McKinney, J. D. (2003) Differential expression of iron-, carbon-, and oxygen-responsive mycobacterial genes in the lungs of chronically infected mice and tuberculosis patients. *Proc Natl Acad Sci USA* **100**, 14321-14326

91. Boshoff, H. I., and Barry, C. E., 3rd. (2005) Tuberculosis - metabolism and respiration in the absence of growth. *Nat Rev Microbiol* **3**, 70-80

92. Bryk, R., Lima, C. D., Erdjument-Bromage, H., Tempst, P., and Nathan, C. (2002) Metabolic enzymes of mycobacteria linked to antioxidant defense by a thioredoxin-like protein. *Science* **295**, 1073-1077

93. Vilcheze, C., Weisbrod, T. R., Chen, B., Kremer, L., Hazbon, M. H., Wang, F., Alland, D., Sacchettini, J. C., and Jacobs, W. R., Jr. (2005) Altered NADH/NAD+ ratio mediates coresistance to isoniazid and ethionamide in mycobacteria. *Antimicrob Agents Chemother* **49**, 708-720

94. Akif, M., Khare, G., Tyagi, A. K., Mande, S. C., and Sardesai, A. A. (2008) Functional studies of multiple thioredoxins from *Mycobacterium tuberculosis*. *J Bacteriol* **190**, 7087-7095

95. Vilcheze, C., Av-Gay, Y., Attarian, R., Liu, Z., Hazbon, M. H., Colangeli, R., Chen, B., Liu, W., Alland, D., Sacchettini, J. C., and Jacobs, W. R., Jr. (2008) Mycothiol biosynthesis is essential for ethionamide susceptibility in *Mycobacterium tuberculosis*. *Mol Microbiol* **69**, 1316-1329

96. Frigui, W., Bottai, D., Majlessi, L., Monot, M., Josselin, E., Brodin, P., Garnier, T., Gicquel, B., Martin, C., Leclerc, C., Cole, S. T., and Brosch, R. (2008) Control of *M. tuberculosis* ESAT-6 secretion and specific T cell recognition by PhoP. *PLoS Pathog* **4**, e33

97. Passemar, C., Arbues, A., Malaga, W., Mercier, I., Moreau, F., Lepourry, L., Neyrolles, O., Guilhot, C., and Astarie-Dequeker, C. (2013) Multiple deletions in the polyketide synthase gene repertoire of *Mycobacterium tuberculosis* reveal functional overlap of cell envelope lipids in host-pathogen interactions. *Cell Microbiol*

98. Lohse, M., Bolger, A. M., Nagel, A., Fernie, A. R., Lunn, J. E., Stitt, M., and Usadel, B. (2012) RobiNA: a user-friendly, integrated software solution for RNA-Seq-based transcriptomics. *Nucleic Acids Res* **40**, W622-627

99. Langmead, B., Trapnell, C., Pop, M., and Salzberg, S. L. (2009) Ultrafast and memory-efficient alignment of short DNA sequences to the human genome. *Genome Biol* **10**, R25

100. Li, H., Handsaker, B., Wysoker, A., Fennell, T., Ruan, J., Homer, N., Marth, G., Abecasis, G., and Durbin, R. (2009) The Sequence Alignment/Map format and SAMtools. *Bioinformatics* **25**, 2078-2079

101. Anders, S., and Huber, W. (2010) Differential expression analysis for sequence count data. *Genome Biol* **11**, R106

102. Garcia-Alcalde, F., Okonechnikov, K., Carbonell, J., Cruz, L. M., Gotz, S., Tarazona, S., Dopazo, J., Meyer, T. F., and Conesa, A. (2012) Qualimap: evaluating next-generation sequencing alignment data. *Bioinformatics* **28**, 2678-2679

103. Schneider, C. A., Rasband, W. S., and Eliceiri, K. W. (2012) NIH Image to ImageJ: 25 years of image analysis. *Nat Methods* **9**, 671-675

104. Pethe, K., Sequeira, P. C., Agarwalla, S., Rhee, K., Kuhen, K., Phong, W. Y., Patel, V., Beer, D., Walker, J. R., Duraiswamy, J., Jiricek, J., Keller, T. H., Chatterjee, A., Tan, M. P., Ujjini, M., Rao, S. P., Camacho, L., Bifani, P., Mak, P. A., Ma, I., Barnes, S. W., Chen, Z., Plouffe, D., Thayalan, P., Ng, S. H., Au, M., Lee, B. H., Tan, B. H., Ravindran, S., Nanjundappa, M., Lin, X., Goh, A., Lakshminarayana, S. B., Shoen, C., Cynamon, M., Kreiswirth, B., Dartois,

V., Peters, E. C., Glynne, R., Brenner, S., and Dick, T. (2009) A chemical genetic screen in *Mycobacterium tuberculosis* identifies carbon-source-dependent growth inhibitors devoid of in vivo efficacy. *Nature communications* **1**, 57

105. VanderVen, B. C., Hermetter, A., Huang, A., Maxfield, F. R., Russell, D. G., and Yates, R. M. (2010) Development of a novel, cell-based chemical screen to identify inhibitors of intraphagosomal lipolysis in macrophages. *Cytometry A* **77**, 751-760

106. Tan, M. P., Sequeira, P., Lin, W. W., Phong, W. Y., Cliff, P., Ng, S. H., Lee, B. H., Camacho, L., Schnappinger, D., Ehrt, S., Dick, T., Pethe, K., and Alonso, S. (2010) Nitrate respiration protects hypoxic *Mycobacterium tuberculosis* against acid- and reactive nitrogen species stresses. *Plos One* **5**, e13356

107. Gould, T. A., van de Langemheen, H., Munoz-Elias, E. J., McKinney, J. D., and Sacchettini, J. C. (2006) Dual role of isocitrate lyase 1 in the glyoxylate and methylcitrate cycles in *Mycobacterium tuberculosis*. *Mol Microbiol* **61**, 940-947

108. Reichardt, N., Duncan, S. H., Young, P., Belenguer, A., Leitch, C., Scott, K. P., Flint, H. J., and Louis, P. (2014) Phylogenetic distribution of three pathways for propionate production within the human gut microbiota. *The ISME Journal* **8**, 1323-1335

109. Saxena, R. K., Anand, P., Saran, S., Isar, J., and Agarwal, L. (2010) Microbial production and applications of 1,2-propanediol. *Indian Journal of Microbiology* **50**, 2-11

110. Flynn, J. L., and Chan, J. (2001) Tuberculosis: latency and reactivation. *Infect Immun* **69**, 4195-4201

111. WHO. (2010) *Treatment of tuberculosis: guidelines*, World Health Organization

112. McKinney, J. D. (2000) In vivo veritas: the search for TB drug targets goes live. *Nat Med* **6**, 1330-1333

113. Turapov, O., O'Connor, B. D., Sarybaeva, A. A., Williams, C., Patel, H., Kadyrov, A. S., Sarybaev, A. S., Woltmann, G., Barer, M. R., and Mukamolova, G. V. (2016) Phenotypically adapted *Mycobacterium tuberculosis* populations from sputum are tolerant to first-line drugs. *Antimicrobial Agents and Chemotherapy* **60**, 2476-2483

114. Leistikow, R. L., Morton, R. A., Bartek, I. L., Frimpong, I., Wagner, K., and Voskuil, M. I. (2010) The *Mycobacterium tuberculosis* DosR regulon assists in metabolic homeostasis and enables rapid recovery from nonrespiring dormancy. *J Bacteriol* **192**, 1662-1670

115. Gautam, U. S., McGillivray, A., Mehra, S., Didier, P. J., Midkiff, C. C., Kissee, R. S., Golden, N. A., Alvarez, X., Niu, T., Rengarajan, J., Sherman, D. R., and Kaushal, D. (2015) DosS Is

required for the complete virulence of *Mycobacterium tuberculosis* in mice with classical granulomatous lesions. *Am J Respir Cell Mol Biol* **52**, 708-716

116. Mehra, S., Foreman, T. W., Didier, P. J., Ahsan, M. H., Hudock, T. A., Kissee, R., Golden, N. A., Gautam, U. S., Johnson, A. M., Alvarez, X., Russell-Lodrigue, K. E., Doyle, L. A., Roy, C. J., Niu, T., Blanchard, J. L., Khader, S. A., Lackner, A. A., Sherman, D. R., and Kaushal, D. (2015) The DosR regulon modulates adaptive immunity and Is essential for *Mycobacterium tuberculosis* persistence. *Am J Respir Crit Care Med* **191**, 1185-1196

117. Bartek, I. L., Reichlen, M. J., Honaker, R. W., Leistikow, R. L., Clambey, E. T., Scobey, M. S., Hinds, A. B., Born, S. E., Covey, C. R., Schurr, M. J., Lenaerts, A. J., and Voskuil, M. I. (2016) Antibiotic Bactericidal Activity Is Countered by Maintaining pH Homeostasis in *Mycobacterium smegmatis*. *mSphere* **1**, 16

118. Gomez, J. E., and McKinney, J. D. (2004) *M. tuberculosis* persistence, latency, and drug tolerance. *Tuberculosis (Edinburgh, Scotland)* **84**, 29-44

119. Manjunatha, U., Boshoff, H. I., and Barry, C. E. (2009) The mechanism of action of PA-824: Novel insights from transcriptional profiling. *Commun Integr Biol* **2**, 215-218

120. Bardarov, S., Kriakov, J., Carriere, C., Yu, S., Vaamonde, C., McAdam, R. A., Bloom, B. R., Hatfull, G. F., and Jacobs, W. R. (1997) Conditionally replicating mycobacteriophages: A system for transposon delivery to *Mycobacterium tuberculosis*. *Proceedings of the National Academy of Sciences* **94**, 10961-10966

121. Ochman, H., Gerber, A. S., and Hartl, D. L. (1988) Genetic applications of an inverse polymerase chain reaction. *Genetics* **120**, 621-623

122. Li, H. (2013) Aligning sequence reads, clone sequences and assembly contigs with BWA-MEM. *arXiv* **1303.3997v1 [q-bio.GN]**

123. McKenna, A., Hanna, M., Banks, E., Sivachenko, A., Cibulskis, K., Kernytsky, A., Garimella, K., Altshuler, D., Gabriel, S., Daly, M., and DePristo, M. A. (2010) The Genome Analysis Toolkit: a MapReduce framework for analyzing next-generation DNA sequencing data. *Genome Res* **20**, 1297-1303

124. Rengarajan, J., Bloom, B. R., and Rubin, E. J. (2005) Genome-wide requirements for *Mycobacterium tuberculosis* adaptation and survival in macrophages. *Proc Natl Acad Sci U S A* **102**, 8327-8332

125. van Opijnen, T., and Camilli, A. (2013) Transposon insertion sequencing: a new tool for systems-level analysis of microorganisms. *Nature Reviews Microbiology* **11**, 435-442

126. Wang, P.-H., Lee, T.-H., Ismail, W., Tsai, C.-Y., Lin, C.-W., Tsai, Y.-W., and Chiang, Y.-R. (2013) An oxygenase-independent cholesterol catabolic pathway operates under oxic conditions. *PLoS ONE* **8**

127. Lin, C.-W., Wang, P.-H., Ismail, W., Tsai, Y.-W., El Nayal, A., Yang, C.-Y., Yang, F.-C., Wang, C.-H., and Chiang, Y.-R. (2015) Substrate Uptake and Subcellular Compartmentation of Anoxic Cholesterol Catabolism in Sterolibacterium denitrificans. *J Biol Chem* **290**, 1155-1169

128. Bhatt, K., Gurcha, S. S., Bhatt, A., Besra, G. S., and Jacobs, W. R. (2007) Two polyketide-synthase-associated acyltransferases are required for sulfolipid biosynthesis in *Mycobacterium tuberculosis*. *Microbiology* **153**, 513-520